COHESIVE PROPERTIES OF TRANSITION METAL ALLOYS

BY YOSHIRO KAKEHASHI

MAY 1980

Contents

Abstract

A method to treat cohesive properties of transition metal alloys such as the lattice parameter and the bulk modulus and so on is devoloped. It is based on the virial theorem which has been used in the studies of the cohesive properties of pure metals by Liberman and Pettifor. The merit of this method lies in the fact that the ambiguity in the double counting term can be avoided in the pressure expression, and that the volume dependence of parameters can be easily determined from the results of the first principle calculation for the pure metal, which enable us to discuss the cohesive properties of the real transition metal alloys semi-quantitatively. This method is applied to the calculation of the lattice parameters of the Nb-Zr alloy and the Pd base 4d transition metal alloys in Part I, and its usefulness is verified. It is also found that the origins of the deviation from Vegard's law lie in the gain of the bond energy of the d electron and in the s-d charge transfer effect. In Part II, the cohesive properties of 3d transition metal alloys are elucidated qualitatively on the basis of the electronic structure. The formation energy, the deviation from Vegard's law and the change of the bulk modulus of the Cu-Mn alloy, the αFe base 3d transition metal alloys and the Ni base 3d transition metal alloys are calculated on the basis of the virial theorem with the two-band tight binding model. The results agree well with the experimental trends. It is shown that the magnetic pressure can be

expressed approximately by a linear combination of the squares of the local magnetic moment and that the changes of the lattice parameters with the concentration in the 3d transition metal alloys are determined mainly by the change of the magnitudes of the local magnetic moment. This conclusion gives a justification of the empirical expression for the magnetic alloys which is found by Shiga and Schlosser. The importance of the magnetic effect is also pointed out in the formation energy and the bulk modulus. In Part III, the theory is extended to finite temperatures. Liberman-Pettifor's expression is given from the most general point of view. Then, the expressions for the spontaneous volume magnetostriction, the electronic contribution to the thermal expansion coefficient, the forced volume magnetostriction and the bulk modulus at finite temperature are obtained with use of the static approximation in the functional integral formulation. On the basis of these expressions, it is deduced that the origins of the so-called invar effect do not lie in the vanishing of the spontaneous magnetization nor in the directional change of the local moments but in the change of the amplitude of the local magnetic moments and the charge transfer effect between s and d orbitals. Furthermore, it is shown that the empirical formula for the magnetic pressure and the Weiss model can be derived from our point of view. A preliminary result of the calculation for the spontaneous magnetostriction and for the magnetic contribution to the thermal expansion coefficient in αFe is also outlined and discussed.

Introduction

Cohesive properties of pure transition metals in the ground state have been investigated in last few years in detail, and many calculations for their cohesive properties have been performed. At present, it is known well that the energy band theory can explain their properties quantitatively except for the 3d transition metal. It has been shown by Moruzzi, Janak and Williams[1] in the most detail. They have calculated the cohesive energy, the lattice parameter and the bulk modulus for all metals from Li to In on the basis of the selfconsistent local spin density functional theory and have obtained a remarkably good agreement with the observed value.

On the other hand, the respective roles of sp electron and d electron in transition metals have been also elucidated by Pettifor[2],[3] and Gelatt et al.[4]. They have shown that s electrons cause the repulsive force and d electrons cause the attractive force at the equilibrium volume. They have also verified that there is the cancellation between the shift of the d level and the change in the double counting energy and so Friedel's bonding energy picture is correct.

The purpose of this paper is to propose a method of treating the cohesive properties of alloys on the basis of these recent results for the pure transition metals and to elucidate cohesive properties of all transition metal alloys and the mechanisms underlying these properties.

Cohesive properties of transition metal alloys are not sufficiently studied either experimentally or theoretically. Only the theoretical comparison of the ordering energies for

simple structures is made qualitatively. For example, Haydock et al.[5], assuming a common d band, have verified a correlation between the structual stability of Laves phases and the d electron number per atom. Gautier et al.[6], Cyrot and Cyrot-Lackman[7] have calculated the formation energy of disordered transition metal alloys and explained the trends across the periodic table due to d electrons.

However, the lattice parameters, bulk moduli of transition metal alloys and the roles of s and d electrons in these quantities have not been explained at all in the microscopic theory. The lattice parameters of many alloys deviate from the concentration-linear Vegard law. Thirty years ago, Friedel[8] discussed this phenomenon on the basis of the classical elastic theory. He has shown that the sign of the deviation is determined by both the difference in the atomic volumes and that in the bulk moduli of the two components. His expression explains the sign of the observed deviation well, but not its magnitude , particularly for the transition metal alloys. Furthermore, th the microscopic mechanisms underlying the deviation are not clarified because of being the phenomenological theory.

The reason why the lattice constant of alloys has not been discussed yet on the basis of the electronic theory seems to be as follows. Firstly, the volume dependence of s and d bands (especially, the centers of gravity of these bands) had not been known in detail. So, the origin of the repulsive force was not clear and it was difficult to make up a simplified model. Secondly, the effect of charge transfer from site to site or from s orbital to d orbital and the Madelung energy effect could not be estimated

accurately because the estimation of these quantities needs to perform the first principle calculation. Finally, since we consider energies of the order of 0.001 Ry (or 0.001 Å) resulting from the subtraction of a large energy value of the alloy from that of the pure metal, we must calculate the energy and lattice prameter very carefully.

At the present stage that Pettifor has elucidated the first problem for pure metals, it is not so difficult to overcome the second and third problems making up a correct model. Especially, the Madelung energy is not important in the completely disordered alloy. In Part I, we propose a simple model for the pressure $3P\Omega$ of alloys which relates closely to the first principle calculation. The formulation is based on a method of expressing the Liberman-Pettifor formula for the virial theorem in terms of the atomic orbital. The L.C.A.O. method is a useful method not only for the calculation of the electronic structure in alloys but also for understanding the role of the constituent atoms in alloys.

We need some approximations to calculate the pressure in alloys with use of Liberman-Pettifor's formula although the formula can be applied in principle, for any crystal structures and any configurations of atoms. We consider the ideal substitutional alloy that can be divided into the geometrically equivalent unit cells with one atom at the center. Such a restriction becomes important in the estimation of parameters.

Pettifor's expression in the pure metal becomes a help

to derive the pressure expression in alloys in terms of the L.C.A.O.. He has shown that the pressure in the pure metal can be approximately expressed as a sum of the core part which is proportional to the electron number n and the bond part proportional to the bond energy $\int^{EF} (\epsilon_0 - \omega)\rho(\omega)d\omega$:

$$3P\Omega = A(\Omega)n + B\int^{EF}(\omega - \epsilon_0)\rho(\omega)d\omega , \qquad (1)$$

where ϵ_0 is the center of the band, $A(\Omega)$ is a volume dependent coefficient and B is a volume independent factor. A single band is assumed here for brevity. An expression similar to eq.(1) should be also derived in the L.C.A.O. method.

The pressure in the L.C.A.O. method is given as follows:

$$3P\Omega = \frac{(-1)}{2\pi}\int^{EF}\sum_{\alpha\beta\gamma} Im\, D^{\alpha}_{\beta\gamma}\cdot G_{\gamma\beta}\, d\omega , \qquad (2)$$

where $D^{\alpha}_{\beta\gamma}$ is a matrix element in the pressure expression (see eq.(I.1.3).). $G_{\gamma\beta}$ is the one electron Green function in the atomic-orbital representation. The diagonal terms of the Green function, $G_{\beta\beta}$, in eq.(2) correspond to the first term in eq.(1). The second term in eq.(1) results from the overlaps of atomic orbitals. Therefore, it should correspond to the off-diagonal part in eq.(2). As a matter of fact, we can show that the off-diagonal part is proportional to the bond energy if we make the two center approximation for the matrix $D^{\alpha}_{\beta\gamma}$ and make another approximation that the ratio of $D^{\alpha}_{\alpha\beta}$ to the transfer matrix $t_{\alpha\beta}$ is independent of the sites. Thus we have a one-to-one correspondence between eqs.(1) and (2).

These considerations can be extended directly in the case of alloy if we approximate $D^{\alpha}_{\alpha\beta}/t_{\alpha\beta}$ with a constant which is independent of the type of atoms on the sites α and β. We will show in Part I that the pressure in alloys which is obtained in terms of the L.C.A.O. also consists of a core part and a bonding energy part, each of the same form as for pure metals.

We should emphasize that our expression for the pressure agrees with Pettifor's expression in the pure limit. Therefore, we can determine the parameters in alloys from Pettifor's parameters for the pressure in the pure metals after some reasonable approximations, and so there are scarcely ambiguities in parameters for the pressure in alloys and their volume dependences. This enables us to calculate the lattice parameter and the bulk modulus definitely.

If we started from an expression for the energy with the usual Hubbard type Hamiltonian $H = \sum_{i\sigma} \epsilon^0_i n_{i\sigma} + \sum'_{ij\sigma} t_{ij} a^{\dagger}_{i\sigma} a_{j\sigma} + \sum_i U^0_i n_{i\uparrow} n_{i\downarrow}$ (where ϵ^0_i is the atomic level at the site i, t_{ij} is the transfer integral, $a^{\dagger}_{i\sigma}$ and $a_{j\sigma}$ are respectively the creation and annihilation operators, $n_{i\sigma} = a^{\dagger}_{i\sigma} a_{i\sigma}$ and U^0_i is the intra-atomic coulomb integral at the site i.), we would get the pressure:

$$3P\Omega \equiv -3\Omega \frac{d\langle H\rangle}{d\Omega}$$

$$= \sum_{i\sigma} \left(-3\Omega \frac{\partial \epsilon_i^o}{\partial \Omega}\right) \langle n_{i\sigma} \rangle$$

$$+ \sum_{ij\sigma}{}' \left(-3\Omega \frac{\partial t_{ij}}{\partial \Omega}\right) \langle a_{i\sigma}^{+} a_{i\sigma} \rangle + \sum_{i} \left(-3\Omega \frac{\partial v_i^o}{\partial \Omega}\right) \langle n_{i\uparrow} n_{i\downarrow} \rangle$$

However, it would be difficult to determine the value and the volume dependence of $-3\Omega \partial \epsilon_i^0 / \partial \Omega$ without a phenomenological assumption. Therefore the alloying effect in the lattice constant and the bulk modulus would not be easily taken into account theoretically. It would also be difficult to estimate the volume dependence of the coulomb integral, $-3\Omega \partial U_i^0 / \partial \Omega$. An approximation which can be adopted is $\partial U_i^0 / \partial \Omega \approx 0$. However, such an approximation corresponds to the neglect of Coulomb energy in the virial theorem which comes from the volume dependence of the coulomb energy in the total energy. The coulomb energy is important when we determine the equilibrium volume as stressed by Pettifor. The above mentioned difficulties also appear when we start from an expression for the energy with the two-band tight binding model. On the other hand, such difficulties due to the coulomb energy can be avoided in our approach.

Further merit in our approach is that it clarifies the role of s and d electron as shown by Pettifor. Therefore, we can easily get a physical picture.

We will show first of all that our model explains the pressure-volume relation and the change of the lattice

parameter of 4d transition metal alloys in Part I. The calculation of the electronic structure in the disordered alloy is performed with use of the off-diagonal CPA and the charge neutrality condition at each site through Part I and Part II.

It may be verified from the calculation in Part I that our model for transition metal alloys describes the change of the lattice constant and the bulk modulus semi-quantitatively. Part II will be devoted to elucidate cohesive properties of 3d transition metal alloys from our point of view.

Cohesive properties of 3d transition metal alloys are different from those of 4d alloys in many points. These anomalous properties of 3d alloys are related to the complex magnetic properties in most cases. These ground-state properties in pure metals have been elucidated just a few years ago.[9]~[14] The cohesive properties of magnetic alloys, which show more interesting behaviors than the pure metals, have been discussed merely on the basis of a semiphenomenological theory considering the band energy only, in connection with the invar anomaly.

We will calculate and elucidate the most fundamental cohesive quantities, that is the formation energy, the deviation of the lattice parameter from Vegard's law and the bulk modulus of 3d metal alloy in Part II. The elucidation of these properties gives a base understanding more complex and interesting phenomena such as the invar anomalies[15] and

the pressure-induced ferromagnetic -antiferromagnetic transition in Au_2Mn and FeRh[16].

It has been known for a long time that the lattice parameters of 3d transition metal alloys make large changes with their magnetic states. According to the theory of the magnetovolume effect based on the ferromagnetic Stoner model[15], it is roughly expected that the volume expansion is in proportion to the square of the spontaneous magnetization. However, this theoretical expression is obviously not enough to explain the magnetovolume effect in all 3d ferromagnetic transition metal alloys. For example, the lattice parameter of Ni-Mn alloy does not show any change at the critical concentration (30at% Mn) where the spontaneous magnetization vanishes.[17]

On the other hand, Shiga[18] and Schlosser[19] have empirically found recently that the anomalous lattice parameters of 3d alloys are related to the magnitude of the local magnetic moment rather than the spontaneous magnetization. Their empirical formula is $\Omega = \Omega_v + k \langle |m_i|^2 \rangle$ where Ω_v is the volume which is determined from Vegard's law in the nonmagnetic state, k is a concentration-independent constant and $\langle |m_i|^2 \rangle$ is the average of the squares of the local moment. However, the theoretical base for the expression has not been elucidated yet although it is confirmed from this empirical formula that the amplitude of the local magnetic moment has an important role.

We will give a theoretical base to their empirical

formula and will discuss its propriety. That is, we will show that the magnetic pressure is proportional to a linear combination of the squares of the local magnetic moments in the lowest order expansion for the magnetic moment and does not depend on the detail of the electronic structure such as the density of states (DOS) at the Fermi level. This property can be understood roughly as follows. The magnetic pressure is proportional to the change of the bonding energy due to the magnetic state as seen in eq.(1) if we neglect the sd charge transfer. On the other hand, the change of the bonding energy is equal to the minus change of the coulomb energy, which is expressed as a linear combination of the squares of the local moments, in the lowest order since the energy is stationary against a change of the magnetic state. Therefore the magnetic pressure (or the magnetic contribution to the volume) is proportional to the linear combination of the squares of the local moments. We will verify that this approximate expression describes qualitatively the magnetic pressures in 3d metal alloys.

The alloying effect in the bulk modulus for the 3d magnetic alloys has not been studied systematically in detail. However, it is known well that the elastic constants of the Fe-Ni alloy and the Fe-Pt alloy cause the softening in the invar region and their bulk moduli become about half of the value which is expected from the additive law. Usually, these phenomena are considered to be caused by the rapid decrease of

the spontaneous magnetization with the decrease of the volume.[20] But, such a consideration is based on the rigid band Stoner model and has not been established sufficiently. It has not been elucidated yet how the change of the electronic structure due to alloying contributes to the bulk modulus.

We will propose an expression about bulk modulus for any magnetic and atomic configurations from the point of view of the virial theorem. We can understand from the expression that an important factor which causes the softening is not the derivative of the spontaneous magnetization but the derivative of the magnitudes of the local magnetic moments with respect to the volume. On the basis of the expression, we will elucidate the softenings of some bulk moduli due to alloying.

The formation energy of 3d transition metal alloy has been calculated by Van der Rest et al.[21] using the off-diagonal CPA and the observed trends across the periodic table have been elucidated qualitatively. There are many points which are not considered in their calculation although their conclusion that the formation energy ΔH is determined by the band energy is very valuable. Firstly, the effect of the magnetic energy is not taken into account though ΔH is of the same order as the magnetic energy. Experiments are performed at the high temperature (500K~1000K). However many 3d transition metal alloys have the local magnetic moment above the Curie temperature.[22],[23] Therefore we can not neglect the magnetic contribution to ΔH. The second point is the effect of the repulsive energy.

In the alloy having a large volume difference between two components, the size effect due to the repulsive energy will be important. Another effect which is not considered in their calculation is the effect of the s-d hybridization. It may be important in the noble metal base 3d alloys to some extent.

We will take account of the first effect and will explain the observed trend of the formation energy in 3d metal alloys qualitatively, assuming the charge neutrality condition at each site. We will also show that there are indeed changes in the sign of ΔH due to the gain of the magnetic energy in some alloys.

We impose, in the real calculation through Part I and Part II, the charge neutrality condition, which is considered to be reasonable in the transition metal alloys. The charge neutrality condition suppresses the electron transfer from site to site. Such an effect plays an important role to obtain a good agreement of the lattice parameter with the observed value, for example, in Cu-Mn alloy.

Our model contains three factors which mainly determine the cohesive properties of transition metal alloys. They are the d-d bonding effect, the s-d charge transfer effect and the change of the magnitude of the local magnetic moment.

The gain of the bonding energy between the d electrons on alloying leads to a negative ΔH and causes a contraction of the volume. We will find these behaviors in the results of the calculation for the cohesive properties of the Pd base 4d transition metal alloys in Part I, Fe-Ti

alloy and Ni-Ti alloy in Part II. The gain of the bonding energy also causes the softening of the bulk modulus. However , the hardening of the modulus for the repulsive core part (the first term of r.h.s. of eq.(1)) with lattice contraction always cancels the softening. Therefore, the effect of the gain of the bonding energy does not appear in the bulk modulus explicitly in many cases.

The s-d charge transfer effect with alloying is an important factor for the lattice parameters and the bulk moduli. The volume contraction is caused by the electron transfer from the s orbital to the d orbital since the pressure due to the s electron is positive and the pressure due to the d electron is negative at the equilibrium volume. Furthermore it causes the softening in the bulk modulus. These behaviors will be found in the Fe-Ti and Ni-Ti alloys as shown in Part II. The importance of the s-d charge transfer effect on the lattice parameter was pointed out by Teraoka and Kanamori[24] for the first time. However, they discussed only the contribution from the band energy after all, and could not calculate the lattice parameter and bulk modulus of alloys because the repulsive force was treated as an external parameter.

The magnitude of the local magnetic moment is the most important factor to understand the cohesive properties of 3d transition metal alloys. The growth of the magnitudes of the local magnetic moment due to alloying contributes negatively to ΔH since it causes the gain of the exchange energy. The

negative ΔH in Ni-Mn and Ni-Fe is essentially due to the effect as will be shown in Part II. As has been mentioned already, the magnetic pressure can be approximated with the linear combination of the squares of the local moments. The change of the volume which is characterized by the magnitudes of the local moments is the most conspicuous in Cu-Mn alloy and the Fe base 3d alloys since their alloys change largely the amplitudes of the local moments with alloying. We can also show that the change of the volume derivative of the amplitude of the local moment with the concentration causes the softening in the bulk modulus. The softening in Fe-Co, Fe-Ni and Fe-Cu is due to the mechanism as shown in §3 of Part II. We believe that the softenings in many invar alloys, perhaps, are caused by the instability of the magnitudes of the local moments with respect to the volume.

In Part I and II, the ground state properties of transition metal alloys are discussed. In Part III, we will try to extend our approach to the finite temperature.

The magnetovolume effect in the invar problem has been discussed on the basis of the Stoner model considering the d electron band energy only.[20] However, the Stoner model gives a completely nonmagnetic state above the Curie point Tc although the existence of the local magnetic moment above Tc is verified by recent theoretical[22] and experimental studies[23] for 3d metals. Because of the uniform vanishing of the local moments, the spontaneous volume magnetostriction of Fe and Mn in the Stoner model amounts to about 10%[10] while

the observed spontaneous volume magnetostrictions are usually about 0.1~1.0%.[15] Therefore, the Stoner model largrly overestimates the spontaneous volume magnetostriction and will not describe the magnetovolume effect in the 3d transition metal alloys at the finite temperature.

On the other hand, it is well known from the point of view of the local moment model that the Weiss model[25] (or the two state model) explains the many phenomena for Fe-Ni invar alloys, particularly in the high temperature. The most fatal fault in this model is the lacking of the theoretical support.

However, recently it has been shown that the local moment model in 3d metals can be derived with use of the functional integral method.[22] In Part III, we will derive an expression of the pressure at finite temperatures by using the functional integral method in order to remove some faults in the Stoner model and to elucidate the role of the amplitude of the local moment in the cohesive properties of the 3d transition metal alloys at the finite temperature, which is essential in the magnetovolume effect in the ground state as has been mentiond.

We will use the static approximation. The effect of the spin wave in the magnetovolume effect is not taken into account, which will be important in the low temperature. Furthermore, we neglect the fluctuation terms in many cases. Nevertheless, we can obtain some important properties for the magnetovolume effect in the finite temperature.

We propose an expression for the spontaneous volume magnetostriction ω_s, the anomalous thermal expansion α_M, the forced magnetostriction $\partial\omega/\partial h$ and the bulk modulus B. From our point of view, we can show that an empirical formula that the spontaneous magnetostriction is proportional to the change of the linear combination of the squares of the local magnetic moment is also justified in the finite temperature if the thermal fluctuation around the saddle points is neglected, and show that the Weiss model which is believed to be a correct model by many experimenters can be naturally derived.

We should emphasize that there are two origins for the magnetovolume effect of invar alloys. One is the change of the amplitude of the local moment. The other is the s-d charge transfer effect. Especially, the former gives us a new recognition for the influence of the magnetism on the cohesive properties. Indeed, we will show that the changes for the magnetic state influence all physical quantities which can be derived from the pressure, that is, ω_s, α_M, $\partial\omega/\partial h$ and B through only the amplitudes of the local magnetic moments when the s-d charge transfer effect is neglected.

Although the calculation in the limit of the CPA method is directly possible, the results of the actual calculation will be scarcely mentioned. Only the result of the preliminary calculation for αFe will be shown and will be discussed in comparison with the Stoner model. The detailed results of the calculation will be published elsewhere in future.

Part I

Cohesive Properties of 4d Transition Metal Alloys

Outline of Part I

A method to calculate the pressure-volume relation in alloys is given and it is shown that the method is useful to study the cohesive properties for transition metal alloys (TMA). First of all, Liberman-Pettifor's virial theorem is represented with the L.C.A.O. assuming the ideal substitutional alloy as has been mentioned in the introduction. The theory is based on the two-band model where the s-d hybridization is neglected and the five-fold degenerate d orbitals are replaced by five times the single orbital. The two-center approximation is made for the matrix element in the pressure expression and the ratio of the matrix element combining the different sites in the pressure expression to the transfer matrix is approximated to be independent of the sites, the types of the atoms and the volume. As the result, a simple expression for the pressure in alloy is obtained. The parameters are determined from the correspondence of our expression to Pettifor's expression which is based on the first principle energy band calculation. The expression obtained for the pressure is applied to the calculation of the lattice constant and the bulk modulus of Nb-Zr alloy as a test and the propriety is discussed. The electronic structure of the alloy is calculated with use of the off-diagonal CPA. In §3, the deviations from Vegard's law of the Pd base 4d transition metal alloys are calculated with use of our approach. A semi-quantitative agreement with experiments is obtained. The results are analyzed and interpreted in terms of the 'relative' pressure. It is also verified with

use of the same parameters that the observed trends for the formation energies of their alloys across the periodic table can be explained only by the band energy. The conclusion in Part I is given in §4.

§1. Formulation

We start from the virial theorem derived by Liberman[26]. For simplicity, let us consider the ideal substitutional alloy that can be divided into the geometrically equivalent unit cells with one atom. It is assumed that the nucleus lies at the center of each cell. The virial theorem is expressed in Ry atomic unit as follows:

$$3PV = \sum_{\alpha}\left[\frac{1}{2}\sum_{i}^{occ}\int_{\alpha}\left\{\nabla\psi_i^*((\mathbf{r}-\mathbf{r}_\alpha)\cdot\nabla)\psi_i - \psi_i^*\nabla((\mathbf{r}-\mathbf{r}_\alpha)\cdot\nabla)\psi_i + c.c.\right\}d\mathbf{S} + \int_{\alpha} n^2(\mathbf{r})\frac{\partial\epsilon_{xc}}{\partial n}(\mathbf{r}-\mathbf{r}_\alpha)\cdot d\mathbf{S}\right]$$

$$+ \sum_{\alpha}\sum_{\beta}{}'(\mathbf{r}_\alpha-\mathbf{r}_\beta)\int_{\alpha}d\mathbf{r}\,(n(\mathbf{r})-\rho(\mathbf{r}))(-\nabla)\int_{\beta}\frac{n(\mathbf{r}')-\rho(\mathbf{r}')}{|\mathbf{r}-\mathbf{r}'|}d\mathbf{r}', \qquad \text{(I.1.1)}$$

where the ψ_i is the occupied one electron wave function, ϵ_{xc} is the exchange and correlation energy density and n(r) (ρ(r)) is the electron density (the nuclear density). Integrations are performed over the unit cell at the site α or its surface.

The last term of r.h.s. of eq.(I.1.1) expresses the contribution from the interatomic coulomb energy. Liberman has misunderstood this term and neglected. However, this term becomes important in alloys. The detailed discussion about this point is given in Appendix I.

In order to calculate 3PV easily, we rewrite eq. (I.1.1) in terms of the L.C.A.O., that is, we expand one electron wave function ψ_i by orthogonal atomic-orbitals $\{\Phi_\mu\}$ where μ denotes the orbital and the site. The first term of r.h.s. of eq.(I.1.1), $3P_eV$, is expressed as

$$3P_e V = \frac{(-)}{2\pi} \int \sum_{\alpha}^{EF} \mathrm{Im}\ \mathrm{tr}\,(D^{\alpha} \cdot G)\, d\epsilon \quad , \tag{I.1.2}$$

$$D^{\alpha}_{\mu\nu} \equiv \int_{\alpha} \{ [(\nabla \varphi_{\mu}^{*} ((r - r_{\alpha}) \cdot \nabla) \varphi_{\nu} - \varphi_{\mu}^{*} \nabla ((r - r_{\alpha}) \cdot \nabla) \varphi_{\nu} + c.c.] + \frac{2}{3} \varphi_{\mu}^{*} \cdot (r - r_{\alpha}) \cdot \epsilon_{xc} \varphi_{\nu} \} dS \quad , \tag{I.1.3}$$

where we assumed the Slater exchange potential ϵ_{xc}, G is the one-electron Green function in the atomic-orbital representation. Hereafter, we adopt the single orbital model, and assume that φ_{μ} only depends on the type of atom on the μ-th site and that ϵ_{xc} is independent of the type of atom on the cell boundary. Then $D^{\alpha}_{\mu\nu}$ does not depend on the type of atom at the site α.

In the next step, we adopt the two-center approximation to the $D^{\alpha}_{\mu\nu}$, that is, we neglect the $D^{\alpha}_{\mu\nu}$ whose indices α, μ and ν are all different from one another. With this approximation,

$$\begin{aligned} 3P_e V = {} & \frac{1}{2} \sum_{\alpha} \left(\sum_{\beta} D^{\beta}_{\alpha\alpha} \right) n_{\alpha} \\ & + \frac{1}{2} \sum_{\alpha} \sum_{\beta}{}' \left\{ D^{\alpha}_{\alpha\beta} \left(\frac{-1}{\pi} \cdot \int^{EF} \mathrm{Im}\, G_{\beta\alpha}\, d\epsilon \right) \right. \\ & \left. + D^{\alpha}_{\beta\alpha} \cdot \left(\frac{-1}{\pi} \cdot \int^{EF} \mathrm{Im}\, G_{\alpha\beta}\, d\epsilon \right) \right\} \quad , \end{aligned} \tag{I.1.4}$$

where n_{α} is the electron number on the site α. $\sum_{\beta}'$ means the lattice sum except for the site α. If we approximate that the ratio of $D^{\alpha}_{\alpha\beta}$ to the transfer matrix $t_{\alpha\beta}$ depends on neither

the sites α and β, nor the type of the atom at each site, the second term of r.h.s. of eq.(I.1.4) becomes

$$\frac{D}{t}\cdot\left(\frac{-1}{\pi}\right)\sum_{\alpha}\int^{EF} Im \sum_{\beta}{}' t_{\alpha\beta}\, G_{\beta\alpha}\, d\epsilon \quad , \tag{I.1.6}$$

where

$$\frac{D}{t} \equiv \frac{1}{z}\,\frac{D^{\alpha}_{\alpha\beta} + D^{\beta}_{\alpha\beta}}{t_{\alpha\beta}} \quad . \tag{I.1.7}$$

And then, using the locator expansion $G_{\alpha\alpha} = L_{\alpha} + L_{\alpha}\sum_{\beta}{}' t_{\alpha\beta}\, G_{\beta\alpha}$ where L_{α} is the locator on the site α, we can rewrite eq. (I.1.6) in the form:

$$-\frac{D}{t}\sum_{\alpha}\int^{EF}(\epsilon_{\alpha}-\epsilon)\,\rho_{\alpha}(\epsilon)\,d\epsilon \quad , \tag{I.1.8}$$

where ϵ_{α} is the atomic level and $\rho_{\alpha}(\epsilon)$ is the local density of states (DOS) at the site α.

For the pure metal, eq.(I.1.8) agrees with Pettifor's expression (see eq.(13) and (14) of ref.3). This fact suggests that the above mentioned approximation is correct for A-A pair. Furthermore, in his expression, (D/t) is nearly independent of the volume. Hereafter, we assume that (D/t) does not depend on the volume in alloys. For the alloy, the approximation $D^{\alpha}_{\alpha\beta}/t_{\alpha\beta}$=constant is reasonable when we can assume for the A-B pair that $D_{AB}(t_{AB})$ is equal to the geometrical mean of $D_{AA}(t_{AA})$ and $D_{BB}(t_{BB})$.

Applying the point charge approximation to the inter atomic coulomb term (the last term of r.h.s. of eq.(I.1.1)), and with eqs.(I.1.4) and (I.1.8), we can finally write the

virial theorem as follows:

$$3PV = \sum_{\alpha} \left(\sum_{\beta} \frac{1}{Z} D_{00}^{\beta} \right)_I n_{\alpha} - \frac{D}{t} \sum_{\alpha} \int^{EF} (\epsilon_{\alpha} - \epsilon) \rho_{\alpha}(\epsilon) \, d\epsilon + \sum_{\alpha} \sum_{\beta}{}' \frac{q_{\alpha} q_{\beta}}{|r_{\alpha\beta}|} , \qquad \text{(I.1.9)}$$

where $(\sim)_I$ expresses the matrix element for pure metal specified by the type I atom at the site α. The q_{α} is the total charge in the α-th cell. The first term of the r.h.s. is the core-repulsion term which is mainly caused by the increase of the kinetic energy. The second term is an attractive term due to the gain of the bond energy. We call this term the bond energy term. The third term is, as is known well, the Madelung term.

When we consider the completely disordered alloys and the single site approximation, the Madelung term vanishes and so,

$$3P\Omega = \sum_{I} c_I \left(\sum_{\beta} \frac{1}{Z} D_{00}^{\beta} \right)_I \tilde{n}_I - \frac{D}{t} \tilde{E}_b , \qquad \text{(I.1.10)}$$

$$E_b \equiv \sum_{I} c_I \int^{EF} (\epsilon_I - \epsilon) \, \tilde{\rho}_I(\epsilon) \, d\epsilon , \qquad \text{(I.1.11)}$$

where $\tilde{n}_I$ and $\tilde{\rho}_I$ are respectively the averaged electron number of an I-type atom and the average local density of states of the I-type atom.

We define the core-part partial pressure of the I-type

atom at the site α by

$$(3P_c\Omega)_{\alpha I} = \left(\sum_\beta \frac{D^\beta_{\alpha\alpha}}{z}\right)_I n_\alpha \quad , \tag{I.1.12}$$

the bond part of the partial pressure of the I type of atom at the site α by

$$(3P_b\Omega)_{\alpha I} = -\frac{D}{t}\int^{EF}(\epsilon_\alpha - \epsilon)\rho_\alpha(\epsilon)\,d\epsilon \quad , \tag{I.1.13}$$

and the total partial pressure of the I-type atom at the site α by

$$(3P\Omega)_{\alpha I} = (3P_c\Omega)_{\alpha I} + (3P_b\Omega)_{\alpha I} + \frac{1}{N}\sum_\beta{}' \frac{q_\alpha q_\beta}{|r_{\alpha\beta}|} \quad , \tag{I.1.14}$$

Then eq.(I.1.10) is

$$3P\Omega = \sum_I c_I (3\widetilde{P}\Omega)_I \quad , \tag{I.1.15}$$

where $(3\widetilde{P}\Omega)_I$ is the averaged partial pressure, $(3\widetilde{P}_c\Omega)_I + (3\widetilde{P}_b\Omega)_I$. The partial pressure should not be regarded as the real pressure of atom at the site. Their interrelation is elucidated in Appendix II.

Equation (I.1.9) has been derived with the orthogonal A.O.. But we can also derive the expression corresponding to eq.(I.1.9) from non-orthogonal Anderson's A.O. $\{\phi_\mu\}$[27]. In this case, $D^\alpha_{\mu\nu}$ is replaced with the matrix expressed by ϕ_μ and ϕ_ν, not by φ_μ and φ_ν. The n_α should be regarded as the electron number for ϕ_μ :

$$\frac{(-)}{\pi}\int^{EF} \mathrm{Im}\, \mathcal{G}_{\alpha\alpha}\, d\epsilon$$

where $\mathcal{G}$ is the Grimley's Greenian[28] defined by $(\epsilon S-H)\mathcal{G} = 1$. Furthermore, the partial density of state in the bond energy term must be regarded as the gross density:

$$\rho_\alpha(\epsilon) = \frac{(-)}{\pi}\,\mathrm{Im}\,(\mathcal{G}S)_{\alpha\alpha}$$

where $S_{\alpha\beta}$ is the overlap matrix element between α and β.

We can also find the cohesive energy by integrating eq.(I.1.9). The repulsive energy is obtained from the first term of the r.h.s.. The bond energy is obtained from the second term, and the Madelung energy from the third term. In the lattice gas model and the phenomenological elastic theory in alloys, it is assumed that the repulsive energy consists of pairs. But our repulsive force is a volume force and so such an assumption is not realistic.

Up to now, we have not specified the class of alloys, particularly . Hereafter, we consider the transition metal alloys (TMA), where the pseudo potential approach can not be applied.

We neglect the s-d hybridization. Therefore, the total pressure is just the sum of the d and s part pressures. It is known that this approximation is qualitatively good for the cohesive properties[3].

Parameters $(\sum_\beta D_{oo}^\beta/2)_I$ and D/t can be easily determined from Pettifor's expression[3]. For the s part,

$$\frac{D}{t} = z\left(1 + \frac{3}{z}\frac{\delta\mu_s}{\mu_s} - (B_s - \epsilon_{xc})R^2 a_s\right),$$

$$\left(\sum_\beta \frac{D_{oo}^\beta}{z}\right) = \frac{D}{t}(\epsilon_s - B_s) + \frac{3(B_s - \epsilon_{xc})}{\mu_s}, \qquad \text{(I.1.16)}$$

and for the d part,

$$\frac{D}{t} = 5\left(1 + \frac{z}{5}\frac{1}{\mu_d} - \frac{z}{5}(\epsilon_d - \epsilon_{xc})R^2 a_d\right),$$

$$\left(\sum_\beta \frac{D_{oo}^\beta}{z}\right) = \frac{z(\epsilon_d - \epsilon_{xc})}{\mu_d}, \qquad \text{(I.1.17)}$$

where μ_s and μ_d are the s band and d band effective masses, $\delta\mu_s = 1-\mu_s$, and a_d and a_s are the logarithmic parameters which are given in Pettifor's paper[3]. R is the Wigner-Seitz radius. B_s is the bottom of the conduction band. $\epsilon_s - B_s$ is derived from the Laurent form[29] about the logarithmic derivatives and taking up to the linear term of $\epsilon_s - B_s$, we obtain

$$\epsilon_s - B_s \approx \frac{3}{1+a_s}\cdot\frac{1}{\mu_s R^2}. \qquad \text{(I.1.18)}$$

Other parameters for pure metal are assumed according to Pettifor[29], as follows:

$$\mu_d R^2 \propto R^n,$$

$$\epsilon_{xc} = -\frac{3}{z}\frac{Z_{w.s}}{R},$$

$$\epsilon_d = \epsilon_d^a + Q R^{-q} ,$$

$$\beta_s = \frac{3 Z_A}{\mu_s R} \left\{ \left(\frac{r_A}{R} \right)^2 - 1 \right\} ,$$

$$W_d \propto \frac{1}{\mu_d R^2} , \qquad \text{(I.1.19)}$$

where ϵ_d^a is the atomic d level. r_A is the core atomic radius. Z_A is the effective charge which the s electron on the W.S. sphere feels and $Z_{W.S}$ is also the effective charge similar to Z_A. W_d is the d band width. See ref.(29) for the values of the parameters $Z_{W.S}$, Z_A, Q, q and r_A.

As mentioned previously, the bond energy part in the pressure mainly originates from the derivative of the bond energy with respect to the volume. Therefore, $(D/t)_s$ and $(D/t)_d$ should be close to 2 and n respectively. From this point of view, we assumed in the real calculation that $(D/t)_s$ =2 and $(D/t)_d$=n where n is the exponent for the R dependence of the d band width. For the 4d transition metals, if we calculate (D/t) using Pettifor's parameter, $(D/t)_s$=2.5~3.0, $(D/t)_d \approx$n-1, but these discrepancies will not be important qualitatively.

In the following section, we will show the results of numerical calculations on the pressure-volume relations of

completely disordered transition metal alloys. The s part DOS is approximated by the free-electron like rigid band model because it has not a complex form. That is, we assumed that $\rho_s(\epsilon)=\sum_I c_I \rho_{sIf}(\epsilon)$ where $\rho_{sIf}(\epsilon)$ is the free electron DOS of the I-type pure metal with the effective mass μ_s.

The volume dependence of μ_s is neglected for simplicity. The d-part DOS's are calculated by using the off-giagonal CPA formulated by Shiba[30]. The volume dependence of the model d band can be assumed as $\rho(\epsilon)=\hat{\rho}(\epsilon/W)/W$ because of the single band model. The quantity $(D/t)_d$ is not exactly the same values over the all transition metals. When $(D/t)_{dA} \neq (D/t)_{dB}$, we replace $(D/t)_d$ by $c_A(D/t)_{dA}+c_B(D/t)_{dB}$. Although the level ϵ_d and B_s do not necessarily agree with the values for the pure state in eq.(I.1.19) in alloys, they are initially assumed to be equal to those in eq.(I.1.19), and then if the calculated electron number violates the charge neutrality condition at each site, we shift ϵ_d and B_s of B atom (or A atom) by a same amount until the condition is satisfied. Lang and Ehrenreich[31] also have found that the volume dependence of the Curie temperature in Cu-Ni alloy is explained by the minimum polar model such that the charge neutrality is satisfied within each atom, rather than by the ionic regid band model.

In the concentration c=0.0 and 1.0, if we directly use Pettifor's parameters, the equilibrium lattice constants calculated by the above mentioned scheme often show the

deviations of about 10% from the observed values. Therefore, we have adjusted $(\mu_s, \mu_d)_A$ and $(\mu_s, \mu_d)_B$ so that the calculated lattice parameters and bulk moduli agree with the observed values[32] for both constituents. Other parameters except for μ_s and μ_d are quoted from Pettifor's paper, and the detailed difference in parameters between the crystal structures is neglected.

§2. Nb-Zr Alloy

The β-phase Nb-Zr alloy forms a continuous series of solid solutions at high temperature with the b.c.c. structure. Lattice parameter shows the negative deviation from Vegard's law. Recently the bulk modulus has been measured by Walker et al.[33]. It shows the negative deviation from the linearly interpolated value.

As the first example, we calculated the pressure-volume relation of this system. The input parameters are as follows. $\mu_{sNb}=0.5484$, $\mu_{dNb}=2.046$, $\mu_{sZr}=0.6396$, $\mu_{dZr}=2.465$. These values are determined by previously mentioned procedure. Band width is $W_{Nb}=W_{Zr}=0.7\cdot(R/3.0713)^{-4}$. Other parameters are taken from Pettifor's paper.

In Fig.I.1, the assumed model d band and the volume dependence of the d DOS at c=0.5 are shown. Since Nb and Zr are adjacent to each other on the periodic table and we apply the charge neutrality condition, the calculated d bands are similar to the common bands. However, the band width is extended due to alloying and the position of Fermi level is shifted upward and passes through a peak of the d band with the decrease of the volume. This is caused by the fact that the bottom of the conduction s band relative to the d level is pushed up due to large core radii, as the result, the electron transfer from the s band to the d band occurs.

We show the pressure-volume relation in Fig.I.2. The variation of the pressure with the concentration is approxima-

tely linear. In Fig.I.3, the calculated lattice parameters are shown. The negative deviations from Vegard's law qualitatively agree with the observed trends[34]. In order to understand the roles of the s and d electrons, it may be suitable that we plot the difference between the partial pressures when the alloy is completely separated to the pure metals and those when the alloy is completely disordered. (When completely separated, of course, the Vegard law $\Omega_V = c_A\Omega_A + c_B\Omega_B$ is satisfied.) In connection with this, the relative d-core part pressure of A atom is defined by

$$\delta(3P_c\Omega)_{dA} \equiv c_A\left[(3\tilde{P}_c\Omega)_{dA}\Big|_{\Omega=\Omega_V} - (3P_c\Omega)_{dA}\Big|_{\substack{\Omega=\Omega_A \\ c_A=1}}\right] .$$

The relative d bond part pressure of A atom $(3P_b\Omega)_{dA}$ is also defined in the same way, but the suffix c is replaced by b. The relative d-part pressure of A atom is defined by

$$\delta(3P\Omega)_{dA} \equiv \delta(3P_c\Omega)_{dA} + \delta(3P_b\Omega)_{dA} .$$

The relative s-part pressure is also defined in the same way. We show the results of those relative pressures in Fig.I.4. We find that the both s and d electrons contribute attractively to the deviation from Vegard's law.

Figure I.4(b) shows the contributions from the partial pressures of A and B atom. The s part pressure always increases the repulsive character with the decrease of the volume. Therefore the relative s pressure at Zr site is positive because the equilibrium volume of pure Zr, Ω_{Zr} is

larger than $\Omega_v = c_{Zr}\Omega_{Zr} + c_{Nb}\Omega_{Nb}$ and oppositely the relative s-part pressure at Nb site is negative because $\Omega_{Nb} < \Omega_v$. As the total, the negative partial s-pressure at the Nb site overcomes that at the Zr site. Therefore the s part pressure causes the volume contraction relative to the volume Ω_v.

The total relative pressure of the d core part is also attractive because of the behavior similar to the above mentioned s-part pressure. Since the d bond part always has the opposite sign and the different volume dependence from the core-repulsion part at the Nb site, its relative pressure is positive. On the other hand, the d bond part of the relative pressure at the Zr site is negative. The total relative pressure of the d-bond part is positive because of the large positive pressure at Nb site.

In the adjacent type of alloy on the periodic table such as Nb-Zr, the above mentioned analysis is not intuitive although such an analysis is useful in the case of the Pd base 4d transition metal alloys as shown in the following section. It is easy to consider as follows in the adjacent type of alloys. Let us assume that the deviations $R_{eq}-R_A$ and $R_{eq}-R_B$ are small where R_{eq} is the equilibrium atomic radius of the alloy and R_I is the equilibrium atomic radius of the pure metal of the type I and assume that the partial pressure $(3P\Omega)_I$ is equal to the pressure of the pure metal of the type I. Expanding $\sum_I c_I (3P\Omega)_I (R_{eq}) = 0$ for $R_{eq}-R_I$ to the first order, we can easily obtain the equilibrium radius R_{eq}:

$$\frac{R_{eq} - R_B}{R_A - R_B} = \frac{c_A}{c_A + c_B \frac{R_B^2}{R_A^2} \cdot \frac{B_B}{B_A}} ,$$

where B_I is the bulk modulus of the pure metal I. Therefore, the deviation from $R_V = \sum_I c_I R_I$ is

$$\frac{R_{eq} - R_V}{R_A - R_B} = \frac{c_A c_B \left(1 - \frac{R_B^2 B_B}{R_A^2 B_A} \right)}{c_A + c_B \frac{R_B^2 B_B}{R_A^2 B_A}} . \qquad \text{(I.2.1)}$$

With the approximation $R_B^2/R_A^2 \simeq 1$, we can obtain

$$(R_{eq} - R_V)/(R_A - R_B) = c_A c_B \left(1 - \frac{B_B}{B_A} \right) \Big/ \left(c_A + c_B \frac{B_B}{B_A} \right) . \qquad \text{(I.2.2)}$$

In the case of $c_A \ll 1$, we get $(R_{eq}-R_V)/(R_A-R_B) = c_A(B_A/B_B-1)$ which is equal to Friedel's formula[8] except for the factor $(1+(1+\nu)B_A/2(1-2\nu)B_B)^{-1}$ where ν is the Poisson's ratio. We remark that the R_{eq} in eq.(I.2.1) has not the extreme value in the region $0<c_A<1$. Therefore, eq.(I.2.1) does not explain the minimum volume in Pd-Mo alloy and the maximum volume in Cu-Mn alloy[34]. Equation (I.2.1) qualitatively describes the deviation from Vegard's law of the iso-electronic or adjacent type of alloy such as Nb-Zr. The deviation from Vegard's law calculated from eq.(I.2.1) is shown in Fig.I.3(a) by the dashed line. As known from eq.(I.2.1), the fact that the Nb-part contribution is main in Fig.I.4(b) is roughly due to $B_{Nb} > B_{Zr}$. Hereafter, we call this kind of classical behavior in the partial pressures as the normal behavior. In many transition metal alloys of the adjacent type , $B_A > B_B$ if $R_A < R_B$.

Therefore, such an alloy always tends to exhibit a negative deviation from Vegard's law.

The charge neutrality condition is important to some extent. For example, when the electron number in the site deviates by more than 0.6 per atom from the charge neutrality, the positive deviation from Vegard's law occurs at $c=0.5$.

It is observed that the bulk moduli of the $Nb_{1-c}Zr_c$ change linearly with $c<0.2$, while for $c>0.2$, they deviate downward from the linear extrapolation for concentration. (See Fig.I.3(b).). Our results for the completely disordered Nb-Zr system show an approximately linear change over all concentration. So, for $c>0.2$, the result does not agree with the observed negative deviation from the linear variation. Many causes are considered for this disagreement. The most important one seems to be the short range order effect. In fact, Nb-Zr system separates into two phases at low temperature and at high concentration (20at%~90at%Zr). B.c.c. β-phase is formed above about at 900 °C[35]. Since the crystal is annealed at about 1000°C during the whole growth processes, we can always expect the short range order. In Fig.I.3(b), the bulk modulus of the solution of the completely separated Nb-Zr is shown by dotted line, and it seems to agree with the observed trends.

§3. Pd-Base 4d Transition Metal Alloys

In this section, we discuss the change of the lattice parameters of the Pd base 4d TMA and its microscopic interpretation, then the calculated bulk moduli will be also shown. At the end of this section, the formation energy will be discussed.

It is observed that the lattice parameter of the Pd base 4d TMA shows a negative deviations from Vegard's law and the negative deviations change parabolically across the periodic table. Particularly, the deviations in Pd-Zr and Pd-Y are large, and it has been believed that the deviation relates to the charge transfer effect[36] (or the ionization effect). Later in this section, it will be shown that their large deviations are partly due to the deformation effect of the d density of states at the Pd site and partly due to the charge transfer effect from s band to d band within the impurity site, but not due to that from the impurity atom to the host atom.

Figure I.5 shows the model band and the impurity site partial density of states for c=0.1 at the equilibrium position of pure Pd. As we remarked previously, it is not necessary that ϵ_d and B_s are given by eq.(I.1.19) in alloys. If A atom has, for example, a larger core than B atom, it may be more reasonable to consider that the real level of A atom is close to the level obtained from eq.(I.1.19) into which a larger radius R_A is substituted in stead of the cell radius

R per atom because the average wave function on the A atom will tend to extend outward so as not to increase the kinetic energy. But, even if such a procedure were followed, the level of A atom relative to the level of B atom would not be so different from the relative levels determined by the procedure in the previous section when we assume the charge neutrality condition.

In Fig.I.6(a), the results of the calculation for the deviation from Vegard's law are shown. The agreement between the observed and the calculated values is good.

Friedel's phenomenological theory is not good in agreement with the observed value except for Pd-Ag and Pd-Rh alloys. These disagreements are caused by the characteristic d band effects as will be shown soon later.

In order to show the roles of the s and d electrons and those of the Pd and impurity atoms, we consider the partial pressures relative to the separated phase in Fig.I.6(b). Since the relative pressure which has been defined in the previous section is approximately proportional to the relative deviation, we can understand from the figure that the negative deviations from the Vegard law are mainly due to d part pressures and that the calculated deviation dip at Ru occurs because of the contribution from the s part pressure.

Let us examine each partial relative-pressure in detail. The s part partial pressures behave normally in the sense mentioned in the previous

section and are determined by the deviations from each equilibrium position (See Fig.I.6(c).). The relative pressure of the d core part are also normal as shown in Fig.I.6(d). The d core part pressure at the impurity site dominates the sign of the total relative pressure of the d-core part because of large core radius of the impurity. The relative partial pressures of the d bond part at the impurity site (dbA) are also normal. But the partial pressures of the d-bond part at the Pd site are abnormal. When the Pd-Zr and Pd-Nb alloys expand, we expect that the relative d-bond contribution at Pd site is positive since the magnitude of the negative d bond contribution of the pure Pd decreases with the volume expansion. But the results in Fig.I.6(d) do not behave so. These anomalies are due to the alloying effect of the d band at the Pd site.

As an example, let us see the alloying effect of the $Pd_{80}Nb_{20}$ at the equilibrium atomic radius of the pure Pd in Fig.I.7. The sharp peak near the top of the local density of states at the Pd site is shaven off due to the mixing with the Nb impurity states above that. The shaved states partially extend upward, and partially contribute to the bonding state. This change causes the gain of the bond energy at the Pd site, therefore causes the negative bond contribution of the relative partial pressure at Pd site. Recently, Pettifor characterizes this bonding effect as an effective increment of the d band width in the alloy.

Next, we show the calculated bulk moduli in Fig.I.8.

These changes $\Delta B/c$ tend to deviate in the positive direction from the linear variation. But for c=0.2, $\Delta B/c$ lies in the concentration-linear line. These variations will relate to the change of the DOS at Fermi level. In the case of the bulk moduli, the s-part contribution and the hybridization effect are comparatively important according to the pure metal calculations. Therefore, it may not be quantitatively good that the rigid-band like approximation is applied to the calculation of the electronic structure of the s electrons.

The experimental studies of the transition metal alloys for the bulk moduli have not been done systematically. Detailed experimental studies at this field are expected in future. We postpone more detalied discussion to future, waiting for the systematic experiments.

Finally , we discuss the formation energy of the Pd base 4d TMA. It may also be important to show that the alloy formations should be qualitatively explained by using the same parameters as those in this section. If we apply the point charge approximation to the interatomic coulomb energy, the configurationally averaged total energy is

$$\langle E_{tot} \rangle = \sum_I c_I \left[\tilde{n}_{dI} \epsilon_{dI} + \tilde{n}_{sI} \epsilon_{sI} \right.$$

$$+\int^{EF}(\epsilon-\epsilon_{dI})\,\tilde{\rho}_{dI}\,d\epsilon+\int^{EF}\epsilon\,\tilde{\rho}_{sI}\,d\epsilon$$

$$-\frac{1}{2}\int_{o}\tilde{n}_{I}(\mathbf{r})\,\tilde{v}_{eI}(\mathbf{r})\,d\mathbf{r}-\frac{1}{3}\int_{o}\tilde{n}_{I}(\mathbf{r})\,\tilde{\epsilon}_{xc}\,d\mathbf{r}\Big] \qquad \text{(I.3.1)}$$

where the spatial integration is performed over the Wigner-Seitz cell. The $\tilde{n}_I$ and $\tilde{v}_{eI}$ are respectively the averaged density and the intra-atomic coulomb potential when the site o is occupied by the atom I. As verified by Gelatt et al.[5] and Pettifor[3], the large cancellation between the level-shift energy and the double counting energy occurs near the equilibrium position, so that they do not qualitatively contribute to the cohesive energies. Therefore, we assume that the formation energy which is defined by the energy difference between the completely disordered state and the completely separated state is approximately described by the bond energy only.

So that, our estimation for the formation energy is essentially the same as that discussed by Friedel, Cyrot and Cyrot-Lackman[7] and Gautier et al[6].. The different points are as follows. (1) We take account of the volume effect of the bonding energy in alloys. (2) We use the relative levels shifted by the charge neutrality condition, and do not use the atomic level. (3) The s part contribution of the band energy is also added.

The calculated formation energies are shown in Fig.I.9.

The obtained signs are similar to those obtained by Cyrot and Cyrot-Lackman[7] although our values are fairly larger than their values.

§4. Conclusion

We have proposed a method to calculate the pressure-volume relation in alloys and have shown that the pressure-volume dependence and the related cohesive properties of the 4d TMA are qualitatively explained by the virial theorem and the simple two-band model. The s-d hybridization has been neglected. The sp band and the d band were approximated by the single bands, and the former was regarded as the concentration average of the free electron like DOS of each component and the latter was treated in Shiba's off-diagonal CPA.

The negative deviation from Vegard's law and the linear change of the bulk moduli of Nb-Zr can be explained qualitatively, but the negative deviation from the linear change of the bulk modulus in $c>20$ at%Zr can not be explained by our completely disordered model which assumes the charge neutrality condition. It was suggested from the estimation in the separated-phase limit that the disagreement in the bulk modulus is due to the short range order effect.

We have calculated the lattice parameters, bulk moduli and the formation energies for Pd-base 4d TMA, and have obtained the following conclusions.

(1) The negative deviations from Vegard's law are mainly due to the d part pressures. Particularly, the gain of the d-bond energy which is due to the destruction of the sharp peak at the top of the Pd-site partial density of states

when alloying, contributes mainly to the negative relative-pressure of the d part. In the Pd-Zr and Pd-Nb alloys, the reduction of the s part pressures caused by the charge transfer effect from the s band to the d band also contributes to the negative deviations. The s part pressures cause the dip at Ru for the deviation on the periodic table.

(2) The calculated bulk moduli tend to be larger than the concentration-linear values for c=0.1, but for c=0.2,are approximately equal to the concentration-linear values.

We have discussed the large d band effect at Pd site to the cohesive properties. However, in the case of Ag-base 4d TMA, such a large d band effect can not be expected. Indeed, we have verified to be so. For example, the deviation from Vegard's law of $Ag_{80}Zr_{20}$ is only one-third of that of $Pd_{80}Zr_{20}$.

In spite of the simplicity of the model, we believe that our approach is useful for elucidating the cohesive properties of the transition metal alloys. However, there are many points which seem to be excessively simplified.

Firstly, we neglected the s-d hybridization effects. For this reason, the charge transfer from the s band to the d band indicated in the Pd-Zr alloy may not be so large as to be expected from the present model, because the s-d hybridization expels the sp states from the energy region of the d states so that the sp density of states at the Fermi level is small. Also, the bonding effect due to s-d hybridization might explain the formation of the Pd-Ag alloy.

Secondly, we do not take account of the concentration dependence of the bottom of the sp band. It is not so difficult to take this effect into account. However, for integrated quantities such as the sp electron numbers and sp band energy, we believe that our approximation correctly describes the trends of them because the sp density of states is not complicated and because our approximation is correct up to the second order moment μ_2. Of course, the more detailed calculations are necessary for the cohesive properties of alloys, especially the noble metal- noble metal alloys (Cu-Ag , Cu-Au etc) and the transition metal- nontransition metal alloys (Fe-Al, Ag-Al etc) which are not considered in this paper. We leave these for the future problems.

Part II

Cohesive Properties of 3d Transition Metal Alloys

Outline of Part II

The purpose of Part II is to elucidate the formation energy, the lattice parameter and the bulk modulus of 3d transition metal alloys in the ground state on the basis of the electronic structures.

The calculation is performed with use of the method developed in Part I. The method is reviewed briefly in §1 and a useful and approximate expression for the magnetic pressure is derived. Furthermore, an expression which is used in the calculation of the formation energy is derived.

Cu-Mn alloy is discussed in §2, and then the cohesive properties of the αFe-base and the Ni-base 3d transition metal alloys are studied in §3 with the assumption of the charge neutrality condition. The concentration dependence and the systematic variation on the periodic table for the formation energy, lattice constant and bulk modulus reproduce the observed trends qualitatively well except for a few alloy systems.

In the formation energy of 3d transition metal alloys, the effect of the gain in the exchange energy is emphasized in comparison with the formation energy in the nonmagnetic state. It is shown that the origin of the deviation from Vegard's law lies in the change of the magnitude of the local magnetic moment and the s-d charge transfer effect in alloys, and it is verified theoretically that the empirical formula for the deviation from Vegard's law proposed by Shiga and

Schlosser is qualitatively correct for many 3d transition metal alloys. For the bulk moduli, the softenings due to alloying are discussed.

In the last section, the conclusion and a brief discussion for the Fe-Pt invar alloy are given.

§1. Formulation

The formulation is essentially the same as in Part I. The different point from the previous method is that the electronic structure of the s electron part is also calculated with use of the CPA and so, the alloying effect of s electron is taken into account.

By neglecting the s-d hybridization, the virial theorem is written in the tight binding representation as follows (See eq.(I.1.9) in Part I) :

$$3PV = 3P_s V + 3P_d V + \sum_{\alpha}\sum_{\beta}{}' \frac{q_\alpha q_\beta}{|r_\alpha - r_\beta|}, \qquad \text{(II.1.1)}$$

$$3P_l V = \sum_{\alpha\sigma} \left(\sum_{\beta} \frac{D^{\beta}_{\alpha\alpha}}{2}\right)_{l\sigma} n_{\alpha l\sigma} - \left(\frac{D}{t}\right) \sum_{\alpha\sigma} \int^{EF} (\epsilon_{\alpha l\sigma} - \epsilon) \rho_{\alpha l\sigma}\, d\epsilon, \qquad \text{(II.1.2)}$$

where σ means the electron spin state. $3P_l V$ is the partial pressure of the orbital l. The first term of r.h.s. of eq. (II.1.2) is the core part pressure due to the l-orbital electron. $(\sum_{\beta} D^{\beta}_{\alpha\alpha}/2)_l$ is a volume dependent factor of the atom at the site α. The second term of r.h.s. of eq.(I.1.2) is the bonding energy term. $(D/t)_l$ is the volume independent factor of the orbital l. $\rho_{\alpha l\sigma}(\epsilon)$ is the partial density of states (DOS) of the orbital l and the spin state σ at the site α. Although the spin dependence of the factor $(\sum_{\beta} D^{\beta}_{\alpha\alpha}/2)$ is not important, we assumed its spin dependence due to the change of the local magnetic moment since we formulated the pressure on the basis of the local spin density functional theory (LSD).

These parameters are determined in the same way as in the case of eq.(I.2.1)

and (I.2.2) in Part I by use of Pettifor's expression[3] of the pure metal:

$$\left(\sum_{\beta}\frac{D^{\beta}_{\alpha\alpha}}{z}\right)_{dI\sigma} = \frac{z(\epsilon_{dI\sigma}-\epsilon_{xc})}{\mu_{dI}}\,, \tag{II.1.3}$$

$$\left(\sum_{\beta}\frac{D^{\beta}_{\alpha\alpha}}{z}\right)_{sI} = \xi_I\left[\left(\frac{D}{t}\right)_{sI}(\epsilon_s-B_s)+\frac{3(B_s-\epsilon_{xc})}{\mu_s}\right], \tag{II.1.4}$$

$$\left(\frac{D}{t}\right)_{\ell} = \sum_I c_I\left(\frac{D}{t}\right)_{\ell I}\,, \tag{II.1.5}$$

$$\left(\frac{D}{t}\right)_{dI} = \left[5+\frac{z}{\mu_d}-z a_d(\epsilon_d-\epsilon_{xc})R^2\right]_I\,, \tag{II.1.6}$$

$$\left(\frac{D}{t}\right)_{sI} = 2\eta_I\left[1+\frac{3}{z}\frac{\delta\mu_s}{\mu_s}-(B_s-\epsilon_{xc})a_s R^2\right]_I, \tag{II.1.7}$$

where $\epsilon_{dI\sigma}$ is assumed to be equal to $\epsilon_{dI}-(U_I/2)m_I\cdot\sigma$. ϵ_s and ϵ_{dI} are respectively the centers of the gravity of s and d electrons of the nonmagnetic pure metal of the type I, m_I is the local moment at the site and U_I is the exchange parameter of atom of the type I. The fitting factors ξ_I and η_I are respectively introduced to the r.h.s. of eq.(II.1.4) and eq. (II.1.7) so that both the lattice parameter and bulk modulus of pure metal are reproduced correctly. In Part I, the effective mass μ_s and μ_d were the adjusting parameters for the same purpose.

In the case of the disordered alloy which we discuss, the Madelung energy vanishes. Therefore,

$$3\tilde{P}\Omega = 3\tilde{P}_s\Omega + 3\tilde{P}_d\Omega$$

$$3\tilde{P}_{\ell}\Omega = \sum_{I\sigma} c_I \left(\sum_{\beta} \frac{D_{oo}^{\beta}}{z}\right)_{\ell I\sigma} \tilde{n}_{\ell I\sigma} - \left(\frac{D}{t}\right)_{\ell} \sum_{I\sigma} c_I \int^{EF} (\epsilon_{\ell I\sigma} - \epsilon)\, \tilde{\rho}_{\ell I\sigma} d\epsilon . \tag{II.1.8}$$

In this paper, $3\tilde{P}_1\Omega$ is calculated in the off-diagonal CPA assuming the geometrical mean.

As shown easily by the analysis of the first three moments, the volume dependence of the DOS, the center of gravity and the transfer integrals are all determined only by that of the band width W.

$$\begin{aligned} &\rho(\epsilon) = \frac{1}{W}\hat{\rho}\left(\frac{\epsilon - \epsilon_b}{W}\right), \\ &\epsilon_o - \epsilon_b \propto W, \\ &\sum_j |t_{oj}|^2 \propto W^2, \end{aligned} \tag{II.1.9}$$

where $\hat{\rho}(\omega)$ is a volume independent function, ϵ_b is the bottom of the energy band and ϵ_0 is the center of gravity. The level of the I type atom in the magnetic alloys are assumed to be as follows.

$$\begin{aligned} &\epsilon_{dI\sigma} = \epsilon_{dI}(pure) - \frac{1}{2} v_I m_I \cdot \sigma + \Delta V \cdot \delta_{IA}, \\ &\epsilon_{sI} = \epsilon_{sI}(pure) + \Delta V \cdot \delta_{IA}, \\ &\epsilon_{dI}(pure) = \epsilon_{dI}^{a} + Q_I R^{-n_I}, \\ &\epsilon_{sI}(pure) = B_{sI}(pure) + \omega_s, \end{aligned} \tag{II.1.10}$$

where ϵ_{dI}(pure) and ϵ_{sI}(pure) are the centers of gravity of d and s electrons in the nonmagnetic state. U_I is the exchange parameter and assumed to be equal to $U_{0I}(1+\gamma U_{0I}/W_{dI})$ where U_{0I} and γU_{0I} are adjustable parameters and W_{dI} is the d band width of the pure metal I. The volume dependence of the d band width is described by $W_d \propto R^{-n}$. R is the cell radius corresponding to the atomic volume. ϵ^a_{dI} is the atomic d level of the atom I. B_{sI}(pure) is the bottom of the pure s energy band of the type I and is assumed to be equal to $3Z_A((r_A/R)^2-1)/\mu_s R$ which was suggested by Pettifor and used in Part I. r_A is the core atomic radius and Z_A is the effective charge which the s electron on the W.S. sphere feels. We assume that the s band DOS of the pure metal is a semi-ellipsoidal DOS and define w_s by one half of the s band width. The volume dependence of w_s is proportional to R^{-2} because of the neglect of the volume dependence of μ_s (See eq.(I.1.18) in Part I.). The magnetic polarization of the s band is neglected. ΔV is determined from the charge neutrality condition in a site. δ_{IA} is the Kronecker δ. The volume dependence of ϵ_{dI}(pure)$-\epsilon^a_{dI}$ is assumed to agree with that of W_d. In the 4d metals, this assumption is justified numerically. This point is different from the method in Part I.

Expanding eq.(II.1.2) with the atomic magnetic moments, we can get an approximate magnetic pressure. Integrating by parts, let us transform the bonding energy of the orbital l,

$-E_{bl}=\int^{EF}\sum_{\alpha\sigma}(\epsilon-\epsilon_{\alpha l\sigma})\rho_{\alpha l\sigma}(\epsilon)\,d\epsilon$, to the following form.

$$-E_{bl} = \sum_{\alpha\sigma}(EF-\epsilon_{\alpha l\sigma})n_{\alpha l\sigma} - \int^{EF}\sum_{\alpha\sigma} n_{\alpha l\sigma}(\epsilon)\,d\epsilon \quad , \quad \text{(II.1.11)}$$

where $n_{\alpha l\sigma}(\epsilon)=\int^{\epsilon}\rho_{\alpha l\sigma}(\omega)\,d\omega$, $n_{\alpha l\sigma}=n_{\alpha l\sigma}(EF)$. Local magnetic moments contribute to the bonding energy through each atomic level $\epsilon_{\alpha l\sigma}$. The change of the bonding energy ($-E_{bl}$) due to the first order change of the atomic levels is

$$\delta(-E_{bl}) = \sum_{\alpha\sigma}(EF-\epsilon_{\alpha l\sigma})\,\delta n_{\alpha l\sigma} \quad , \quad \text{(II.1.12)}$$

where we used the relation $\delta\sum_{\alpha} n_{\alpha l\sigma}(\epsilon)=-\sum_{\alpha}\rho_{\alpha l\sigma}(\epsilon)\cdot\delta\epsilon_{\alpha l\sigma}$. According to the selfconsistent condition (II.1.10), the above expression is

$$\delta(-E_{bl}) = \sum_{\alpha}(EF-\epsilon_{\alpha l})\,\delta n_{\alpha l} + \delta\left(\frac{1}{4}\sum_{\alpha} v_{\alpha} m_{\alpha}^{2}\right)\delta_{ld} .$$

Therefore, the magnetic pressure defined by the magnetic 3PV minus the nonmagnetic 3PV becomes approximately the following form.

$$(3PV)_{mag} \approx \sum_{\alpha}\left[\frac{1}{4}\left(\frac{D}{t}\right)_{d}-\frac{1}{\mu_{d\alpha}}\right] v_{\alpha} m_{\alpha}^{2} + \sum_{\alpha l}\left[\left(\sum_{\beta}\frac{D_{\alpha\alpha}^{\beta}}{z}\right)_{l}+\left(\frac{D}{t}\right)_{l}(EF-\epsilon_{\alpha l})\right]\delta n_{\alpha l} \quad . \quad \text{(II.1.13)}$$

Of course, in the ferromagnetic pure metal, the first term of r.h.s. of eq.(II.1.13) agrees with the formula derived by Andersen et al.[37] in the first order expansion. The second term is the charge transfer term due to the change of the local magnetic moment. Since $(D/t)_d \approx (D/t)_s$ (See Table 1)

and the charge neutrality within the site is satisfied, this term hardly depends on the Fermi level and is smaller than the first term as numerically verified in the later section. It is remarkable that the first term does not depend on the detail of the electronic structure since $(D/t)_d$ and μ_d are determined by the atomic d wave function. The first term of r.h.s. of eq.(II.1.13) gives a theoretical base to the empirical formula found by Shiga[17] and Schlosser[18].

The expression for the bulk modulus can be derived in the same manner. In the present case, the following expression is obtained in stead of eq.(II.1.12) as there is the volume change of the transfer integrals.

$$V\frac{d(-E_{b\ell})}{dV} = \sum_{\alpha\sigma}(EF-\epsilon_{\alpha\ell\sigma})V\frac{dn_{\alpha\ell\sigma}}{dV} - \sum_{\alpha\sigma}\gamma_{\ell\alpha}\int^{EF}(\epsilon-\epsilon_{\alpha\ell\sigma})\rho_{\alpha\ell\sigma}(\epsilon)\,d\epsilon\,, \tag{II.1.14}$$

where we assumed the geometrical mean for the AB type transfer integral and assumed $t^1_{AA}\propto\Omega^{-\gamma_{\ell A}}$, $\gamma_{dI}=n_I/3$, $\gamma_{sI}=2/3$. Finally, we obtain the formula for B:

$$3B = \sum_{\alpha\ell\sigma}\left[-\frac{d}{dV}\left(\sum_\beta\frac{D^\beta_{\alpha\alpha}}{z}\right)_{\ell\sigma}\right]n_{\alpha\ell\sigma} + \sum_{\alpha\ell\sigma}\left[\left(\sum_\beta\frac{D^\beta_{\alpha\alpha}}{z}\right)_{\ell I\sigma}+\left(\frac{D}{t}\right)_\ell(EF-\epsilon_{\alpha\ell\sigma})\right]\left(-\frac{dn_{\alpha\ell\sigma}}{dV}\right) - \sum_\ell\left(\frac{D}{t}\right)_\ell\sum_{\alpha\sigma}\frac{\gamma_{\ell\alpha}}{V}\int^{EF}(\epsilon_{\alpha\ell\sigma}-\epsilon)\rho_{\alpha\ell\sigma}(\epsilon)\,d\epsilon$$

$$+\left[-\frac{d}{dV}\left(\sum_{\alpha}\sum_{\beta}{}'\frac{\delta_\alpha \delta_\beta}{|r_{\alpha\beta}|}\right)\right]. \qquad \text{(II.1.15)}$$

In the case of the CPA,

$$\begin{aligned} 3\tilde{B} &= \sum_{lI} c_I\left[-\frac{d}{d\Omega}\left(\sum_{\beta}\frac{D_{oo}^{\beta}}{z}\right)\right]\tilde{n}_{lI} \\ &+ \sum_{lI} c_I\left[\left(\sum_{\beta}\frac{D_{oo}^{\beta}}{z}\right)_{lI} + \left(\frac{D}{t}\right)_l (EF-\epsilon_{lI})\right]\left(-\frac{d\tilde{n}_{lI}}{d\Omega}\right) \\ &+ \sum_{I} c_I\left\{\left[\frac{d}{d\Omega}\left(\frac{v_I}{\mu_{dI}}\right)\right]\tilde{m}_I^{\,2} + z\left[\frac{1}{4}\left(\frac{D}{t}\right)_d - \frac{1}{\mu_{dI}}\right] v_I \tilde{m}_I\left(-\frac{d\tilde{m}_I}{d\Omega}\right)\right\} \\ &- \sum_{l}\left(\frac{D}{t}\right)_l \sum_{I} c_I \frac{\gamma_{lI}}{\Omega}\int^{EF}(\epsilon_{lI\sigma}-\epsilon)\,\tilde{\rho}_{lI\sigma}(\epsilon)\,d\epsilon . \end{aligned} \qquad \text{(II.1.16)}$$

The first term of r.h.s. of eq.(II.1.16) is the core part. The second term is related to the change of the electron number due to the volume variation . The third term is related to the local magnetic moment. The last term is the bonding energy term.

Next, we explain the expression used in the calculation of the formation energy. We consider only the d electron in accordance with other calculations[6],[7],[19]. The energy expression to calculate the formation energy is

$$\sum_{I\sigma} c_I \int^{EF}(\epsilon-\epsilon_{I\sigma})\,\tilde{\rho}_{I\sigma}(\epsilon)\,d\epsilon - \frac{1}{4}\lambda\sum_{I} c_I v_I \tilde{m}_I^{\,2}. \qquad \text{(II.1.17)}$$

Of course, the above expression in the nonmagnetic state agrees with the d electron part of the expression used in Part I.

We consider two values of $\lambda = 3/2, 1$. $\lambda = 1$ is correspond-

ing to the Hartree-Fock (H.F) magnetic energy. If we interpret the DOS $\rho(\epsilon)$ in the sense of the quasi-particle, $\lambda = 1$ is appropriate. If we interpret the DOS $\rho(\epsilon)$ as the DOS in the sense of the LSD theory, the double counting term is not exactly double counting and $\lambda=3/2$ is appropriate in the case of the Slater type LSD potential. Indeed, according to the LSD theory, the electronic total energy is given by

$$\int^{E_F} \epsilon \rho(\epsilon)\, d\epsilon - \frac{1}{2}\int d\mathbf{r}\, d\mathbf{r}' \frac{n(\mathbf{r})\, n(\mathbf{r}')}{|\mathbf{r}-\mathbf{r}'|} + \int d\mathbf{r}\left[n(\mathbf{r})\,\epsilon_{xc}(n(\mathbf{r})) - \sum_\sigma n_\sigma(\mathbf{r})\, v_{xc}^\sigma(\mathbf{r})\right], \qquad \text{(II.1.18)}$$

where ϵ_{xc} is the exchange-correlation energy and $v_{xc}^\sigma = \partial(n\epsilon_{xc})/\partial n_\sigma$. If we assume the Slater type potential, i.e. that with $\alpha=2/3$ in Slater's $X\alpha$ method, the third term is

$$-\frac{1}{2}\varsigma \int \sum_\sigma n_\sigma(\mathbf{r})\, v_{xc}^\sigma(\mathbf{r})\, d\mathbf{r}, \qquad \text{(II.1.19)}$$

where $\varsigma = 1/2$. Here, we define the exchange splitting parameter U_j at the site j by

$$U_j m_j \equiv \epsilon_{j\downarrow} - \epsilon_{j\uparrow} \simeq \langle \varphi_{j\downarrow} | v_{xc}^{\downarrow}(\mathbf{r}) | \varphi_{j\downarrow} \rangle - \langle \varphi_{j\uparrow} | v_{xc}^{\uparrow}(\mathbf{r}) | \varphi_{j\uparrow} \rangle,$$

where $\varphi_{j\sigma}$ is a localized orbital of σ spin state at the site j, m_j is a local magnetic moment at the site j. Then, leaving only the intraatomic d electron term, the magnetic term in eq.(II.1.19) becomes

$$\frac{1}{4}\varsigma \sum_j v_j m_j^2 .$$

Therefore, eq.(II.1.17) is obtained and $\lambda=2-\varsigma=3/2$.

§2. Cu-Mn Alloy

The lattice parameter of Cu-Mn alloy exhibits a maximum at 60 at%Mn[34] where the volume of this alloy exceeds that expected from Vegard's law by about 10%. The classical and phenomenological theory by Friedel[8] predicts the opposite sign to the observed deviation. Shiga[18] and Schlosser[19] suggested from the empirical formula that the deviation from Vegard's law is closely related to the growth of the local moment. However, the information about the magnetic properties of this alloy is not enough to elucidate the deviation, thus the origin of the deviation from Vegard's law has not been elucidated yet.

The calculation of the formation energy of Cu-Mn by means of the off-diagonal CPA is performed by Van der Rest et al.[21]. Their calculated value is about ten times larger than the observed value[38], and so, is not satisfactory.

In this section, we give the result for the lattice parameter mainly and elucidate the relation of it to the electronic structure and the magnetism.

The s-d hybridization effect changes the electron numbers by about ± 0.5 in the pure metal. However, the net change due to the alloying effect may not be so large and not important for the concentration dependence of the pressure. The concentration dependence of the lattice parameter of the Cu-Mn alloy shows the behavior similar to that of the Ni-Mn alloy experimentally. This fact suggests that the

hybridization effect in Cu-Mn is not particularly important in comparison with other transition metal alloys.

We calculate the electronic structure regarding this alloy as the magnetically and configurationally disordered alloy. In fact, the antiferromagnetic order has not been found in the low Mn concentration. In Fig.II.1, we show the DOS of γMn calculated by means of this method. The result reproduces the DOS in the antiferromagnetic state calculated by Asano and Yamashita[39] qualitatively well although we regarded the antiferromagnetic γMn as a disordered alloy.

Values of parameters are w_s(Cu)=0.626 Ry, w_s(γMn)= 0.78232 Ry, Z_A(Cu)=0.91135 and Z_A(γMn)=0.88199. The quantities w_s's are selected so that the curvature at the bottom of the s band DOS agrees with that of the free electron DOS determined by the effective mass μ_s[40]. Z_A's are estimated so that the position of the bottom of the s band agrees with the result of the band calculation. Exchange parameters are U_0(Cu)=0.0 Ry and U_0(γMn)=0.29004 Ry, γU_0(Cu)=0.0 Ry and γU_0(γMn)=2.0. In the pure metal, these values reproduce the observed Mn magnetic moment 2.4 μB and the reasonable critical pressure[41] at which the local magnetic moment vanishes. Fitting parameters ξ and η are as follows: ξ(Cu)=1.01579, η(Cu)=1.68358, ξ(γMn)=0.96533, η(γMn) =1.25716. Other parameters are given in Table 1.

The calculation for the P-V relation of γMn which is based on the energy band theory and the calculation for the

volume dependence of the magnetic moment have not been performed yet. Our model calculation in which the antiferro magnetic γMn is treated as a disordered antiferro magnetic γMn is the first one. The critical pressure such that the anomaly of the P-V relation appears together with the vanishing of the spontaneous magnetostriction, is 160 kbar, where the pressure-induced antiferro-nonmagnetic transition occurs as shown in Fig.II.2. A large increment of the pressure with the decreasing volume is seen in the nonmagnetic region from Fig.II.2 and the small increment of the pressure with the decrease of the volume, in the antiferromagnetic region. This bending of the P-V relation has not been observed yet because of the lack of the high pressure experiments on Cu-Mn alloy larger than 100 kbar. In the case of the Fe-Ni alloy, this continuous bending is observed [42]. Such a bending shows the vanishing of the localized moment. In Fig.II.2, the pressure in the magnetic state minus the pressure in the nonmagnetic state is called the magnetic pressure. Figure II.3 shows the volume dependence of this magnetic pressure. The magnetic pressure of γMn is well reproduced by the first term of eq.(II.1.13).

The electronic structure of Cu-Mn alloy is given in Fig.II.4. In Fig.II.5, the result indicated by II is calculated with the following selfconsistent condition in stead of eq.(II.1.10).

$$\epsilon_{dI\sigma} = \epsilon_{dI}(para) + \frac{1}{z} v_I (\tilde{n}_{dI} - \tilde{n}_{dI}(para)) - \frac{1}{z} v_I \tilde{m}_I \cdot \sigma ,$$

$$\epsilon_{sI} = \epsilon_{sI}(para) , \qquad \text{(II.2.1)}$$

where ϵ_{dI}(para) and ϵ_{sI}(para) show the levels in the nonmagnetic state, $\tilde{n}_{dI}$(para) is the d electron number in the nonmagnetic state. In the high Mn concentration, the result II shows the good agreement with the result I, but in the low Mn concentration, these results do not agree. In the case of the selfconsistent condition (II.2.1), the magnetic moment is larger than that determined by eq.(II.1.10) because the d electron number at Mn site decreases, being accompanied by localization of Mn with the decrease of the Mn concentration. The concentration dependence of the DOS of Cu-Mn can be easily understood since the Cu-part DOS and the Mn-part DOS are separated clearly. The low energy peak of DOS grows up with the decrease of Mn concentration, the d band width of Mn site in the high energy region becomes narrow and narrow as the interaction among Mn atoms becomes weak. In the magnetic case, the up band at Mn site mixes well with Cu. At lower concentration than 60 at%Mn, the d band of the antiferromagnetic Mn has a gap because of the exchange splitting and localization. This gap, of course, becomes

small with the decrease of the volume.

Calculated lattice parameters are shown in Fig.II.6(a). The index I is the result calculated from eq.(II.1.10) and II is based on eq.(II.2.1). The result II deviates largely from the experimental value at the low Mn concentration and is overestimated. Therefore, the selfconsistent condition (II.2.1) may be inappropiate. This overestimation of the lattice parameter is due to the fact that the d electron number at Mn site decreases by 0.4, so that, the excess electrons which flow out from the d orbital are accumulated mainly in the s orbital at Cu site.

In order to elucidate the origin of the large positive deviation of the atomic volume from Vegard's law, we define the pressure at the volume determined by Vegard's law (Ω_V) relative to the pressure in the separated phase as well as §2 in Part I as follows:

$$\delta(3\tilde{P}_\ell\Omega)(\Omega_V) = 3\tilde{P}_\ell\Omega(\Omega_V) - \sum_x c_x (3P_\ell\Omega)(\Omega_x), \quad \text{(II.2.2)}$$

$$\delta(3\tilde{P}\Omega)(\Omega_V) = \delta(3\tilde{P}_s\Omega)(\Omega_V) + \delta(3\tilde{P}_d\Omega)(\Omega_V), \quad \text{(II.2.3)}$$

where $(3P_l\Omega)_I(\Omega_I)$ is the l component of the pressure of the pure metal I at the eqilibrium volume and $3\tilde{P}_l\Omega(\Omega_V)$ is the l-component pressure of alloy at the volume determined by Vegard's law. Each component of the orbital can be decomposed into the core part and the bonding part which consist of the contributions of both types of atoms. Of course, if $\delta(3\tilde{P}\Omega)(\Omega_V)>$

0, the lattice expands relatively to the volume determined by Vegard's law. In order to claify the magnetic effect. the following magnetic pressure $(3p\Omega)_{mag}$ is useful.

$$3\tilde{P}\Omega(\Omega_v) \equiv 3\tilde{P}\Omega_p(\Omega_v) + (3\tilde{P}\Omega)_{mag}(\Omega_v), \qquad \text{(II.2.4)}$$

where $3P\Omega_p(\Omega_v)$ is the pressure in the nonmagnetic state at the Vegard law Ω_v which is obtained by intepolating the volume between the nonmagnetic Cu and the magnetic γMn. An approximate expession of the magnetic pressure is given by eq.(II.1.13). Substituting eq.(II.2.4) into (II.2.3), we obtain the relative pressure which consist of two parts i.e. the term $\delta(3P\Omega)_{mag}(\Omega_v)$ due to the change of the magnetic state with alloying and the term $\delta(3P\Omega_p)(\Omega_v)$ due to the change of the nonmagnetic part:

$$\delta(3\tilde{P}\Omega)(\Omega_v) = \delta 3\tilde{P}\Omega_{mag}(\Omega_v) + \delta 3P\Omega_p(\Omega_v). \qquad \text{(II.2.5)}$$

In Fig.II.7, each relative pressure $\delta(3P\Omega)$ is shown. Figure II.7(a) expresses the s and d contributions. Both s and d electrons make positive contributions to the relative pressre. The arrows written by the solid and dotted lines show the direction of the change of the relative s and d pressures when the volume changes from Ω_v to the equilibrium volume. Since the s electron part of the pressure generally increases rapidly with the decrease of the volume and d electron part pressure decreases with the expansion, $\delta(3P_s\Omega)$ becomes negative and

then balances with the relative d pressure which is positive at the equilibrium volume. As shown in Fig.II.7(b), the origin of the large expansion at 60 at%Mn is due to the change of the magnetic pressure. Since the magnetic pressure is approximately proportional to the linear combination of the squares of the local magnetic moment, we can interpret that this large expansion is due to the increment of the Mn magnetic moment. The increment of the Mn magnetic moment is caused by the reason that the bonding of the Mn atoms is broken with the decrease of the Mn concentration and the magnetic moment is localized. The main part of the magnetic pressure originates in the bonding pressure of the d part. So, we can give also the interpretation that the loss of the bonding energy at Mn site becomes large with the increase of the Mn magnetic moment and it causes the relatively repulsive pressure. (See Fig.II.7(c).)

There are two origins of the positive deviation from Vegard's law in the low Mn concentration. One origin lies in the relative pressure of the s part. The d electrons at Cu site mix with the d electrons at Mn site which is in the higher energy region, and so the d hole is produced at Cu site. Therefore the charge transfer from d orbital to s orbital at Cu site occurs. It causes the excess repulsive s pressure. Another origin lies in the loss of the bonding energy due to the narrowing of the DOS at Mn site. This effect is, though large, not predominant compared with the former.

These two effects are conspicuous in the case of the nonmagnetic state as can be seen from Fig.II.7(d). In this case, the effect due to the loss of the bonding energy is larger than the s-d charge transfer effect. The positive deviation from Vegard's law in the nonmagnetic state results from these two mechnisms, so that, the phenomenological theory by Shiga and Sclosser is not correct because of the assumption of Vegard's law in the nonmagnetic state. However, their suggestion that the lattice parameter is related to the increment of the local magnetic moment, is qualitatively correct.

By the way, we note that the behavior of the lattice parameter of Ag-Tc is different from the nonmagnetic Cu-Mn alloy. The 4d TMA Ag-Tc causes the negative deviation from Vegard's law by $(\Omega-\Omega_V)/\Omega_{Ag}c=-0.012$ at 10 at%Tc according our calculation in terms of the same method in Part I. This seems to be based on the reason that the magnitude of the negative relative-pressure at Tc site is larger than the case of Cu-Mn alloy since the volume derivative of the core part pressure of Tc is larger than that of Mn. This different behavior may be caused by the more violent increase of the kinetic energy of 4d metal than the 3d metal because of the difference of the number of the node between the 4d metal wave function and the 3d metal wave function.

In spite of the large volume expansion, the bulk modulus changes linearly as shown in Fig.II.6(b). Although the increase of the

bond energy term in the bulk modulus is obtained as in the case of the pressure according to eq.(II.1.16), the increase of this term is compensated by the decrease of the core part (the first term of r.h.s. of eq.(II.1.16)) due to the volume expansion as seen from Fig.II.8. It is also caused by the volume expansion due to the appearance of the local moment that the bulk modulus in the nonmagnetic state is larger than that in the magnetic state. The experimental study of Cu-Mn about Young's modulus has been reported, but the bulk modulus has not been done yet.

At the end of this section, we discuss the formation energy ΔH of Cu-Mn. The calculated value in the nonmagnetic state is more than twice the value of Van der Rest et al[21]. as shown in Fig.II.6(c). This is mainly due to the fact that the bonding energy of pure γMn is enhanced by the contraction larger than 10% due to the magnetovolume effect. If we estimate the formation energy of the nonmagnetic Cu-Mn along Vegard's law in the magnetic state, the same order of the value as their result is obtained. In the magnetic state, the formation energy is reduced as compared with the nonmagnetic case because of the gain of the exchange energy due to the increase of the localized Mn magnetic moment. But the agreement with the experimental value is poor.

Equation (II.1.17) is not sufficient to explain the formation energy of Cu-Mn alloy.

There are many effects which must be considered. For

example, (1) The estimation of the repulsive energy term due to the shift of the atomic level. Especially, the large volume dependence of the formation energy in the nonmagnetic state should be reduced by this repulsive term. In the case of the magnetic state, this effect will contribute negatively to ΔH in the Mn rich region and will suppress ΔH evaluated by eq.(II.1.17). One method which takes account of the repulsive term is to integrate the pressure expression of eq.(II.1.8). From this point of view, we tried to evaluate the ΔH assuming the volume dependence of the parameters in eq.(II.1.8), but did not succeed because of the inaccuracy caused by the assumed volume dependence. Other effects which must be considered are as follows. (2) The effect of the s electron. (3) The correlation effect of d electron. (4) Temperature effect. The experiment is performed at high temperature ($\sim$1000K). It is difficult at the present stage to get the correct value of the order of 0.001 Ry confirming the importance of these effects theoretically.

§3. αFe and Ni Base 3d Transition Metal Alloys

In this section, the results of the calculation for the cohesive properties of the αFe and Ni base 3d TMA, that is, the formation energy, the change of the lattice parameter and the bulk modulus are mentioned.

The parameters which is used to calculate these quantities are listed in Table 1. The d band width is estimated from the formula $25/\mu_d R^2$. However, in the case of V, the width is selected to be smaller than $25/\mu_d R^2$ by 0.05 Ry and in Ni and Cu, to be larger than $25/\mu_d R^2$ by 0.02 and 0.06 Ry respectively. These values agree with the results of the energy band calculation[43],[44]. The exponent n which expresses the volume dependence of the d band width is assumed to be equal to the exponent of the 4d metal[29] corresponding to the same column on the periodic table. The atomic core radius r_A is calculated from the Herman-Skillmann's table[45] by means of the method suggested by Pettifor. The effective masses μ_s and μ_d are taken from Table 1 in Andersen's paper[40]. $(D/t)_s$ and $(D/t)_d$ are also estimated from Andersen's parameters. The parameter Z_A which characterizes the bottom of the s band of the pure metal is assumed to be equal to 1.0 except for V. Quantities Z_A of 4d metals are nearly equal to 1.0. In the case of V metal, the bulk modulus of V is not reproduced well with Z_A=1.0. Therefore, we assumed that Z_A=1.2. The half of semi-ellipsoidal s band width, w_s, is selected so that it does not contradict the result of the band calculation[43],[44] and

the s electron number is about 1.0. Q and $Z_{W.S}$ are evaluated by using ϵ_d and ϵ_{xc} deduced from the band calculation. These parameters reproduce the volume dependent quantities of Ti[4], Fe and Ni[11] which have been calculated selfconsistently.

The model DOS is shown in Fig.II.9. In the case of the b.c.c. structure, the model DOS which is used by Akai et al.[46] is assumed, and the f.c.c. model DOS is quoted from Connolly's[47] DOS. The tail of the length of a half of the d band width is added in order to take account of the s-d hybridization effectively. This tail is important for the volume dependence of the magnetic moment of Co and Ni.

The parameters U_0 and γU_0 are selected so that the magnetic moment and its volume dependence at the equilibrium position are reproduced for the assumed DOS. In the case of V, they are selected so that the magnetic moment of V in $\alpha Fe_{90}V_{10}$ alloy is reproduced and so that V causes the magnetic instability at the W.S. radius $R \approx 3.35$ a.u.[9]. The values in Ti and Cr are assumed to be equal to the values in V for simplicity.

The fitting factors ξ and η are determined to reproduce the observed lattice parameter and bulk modulus. In the case of Cr, they are determined assuming that the magnetic pressure is given by the first term in eq.(II.1.13) and the expression of the bulk modulus is equal to the expression of the bulk modulus in the nonmagnetic state.

In general, the fact that the values η are fairly larger

than 1.0 may be due to the overestimation of the s-d charge transfer effect. Indeed, if we assume the s DOS whose value at the Fermi level is about a half of the present DOS , we get, for example, ξ_{Fe}=1.26, η_{Fe}=1.14.

Atomic radii in the nonmagnetic state, the partial pressures of the s parts and the components of the bulk modulus calculated with use of the parameters listed in Table 1 are shown in Fig.II.10. The results of the calculation for the spontaneous magnetostrictions defined by $(\Omega-\Omega_0)/\Omega_0$ (where Ω_0 is the volume in the nonmagnetic state), are 0.003 for Cr, 0.140 for γMn, 0.067 for αFe, 0.041 for f.c.c. Co and 0.013 for Ni. The values calculated by Janak and Williams[10] are 0.071 for αFe and 0.005 for Ni, and these values agree with our results well. The s part pressures in the nonmagnetic state at equilibrium position agrees roughly with the pressures of 4d metals. However in the magnetic state, they decrease because of the volume expansion.

In Fig.II.10(c), the components of the bulk modulus are shown. The dominant part in the magnetic-moment term is related to the volume-derivative of the magnetic moment. For example, in the case of αFe, the third term of eq.(II.1.16) is -0.0031 Rya.u. and the volume-derivative term of the magnetic moment in it is -0.0024 Rya.u.. The main term in the bulk modulus is the s part as indicated by Pettifor[3]. However, when we consider the alloying effect, the s-d charge transfer term (the second term of eq.(II.1.16)) and the

magnetic moment term (the third term of eq.(II.1.16)) are also important.

According to the expression of the approximate magnetic pressure, (II.1.13), the change of the magnitude of the local magnetic moment is important in alloys. The calculated magnetic moments at the impurity site do not change very much from the magnetic moments in the impurity limit as shown in Fig.II.11. The $Fe_{10}Mn_{90}$ alloy just lies in the boundary between the ferromagnetic phase and the antiferromagnetic phase, and so, it should be treated as a quaternary alloy. But, the electronic structure is calculated with respect to three phases of binary alloy, that is, the antiparallel Mn moment in ferromagnetic phase, the parallel Mn moment in the ferromagnetic phase and the disordered antiferromagnetic phase for simplicity. The calculation in the parallel Mn moment configuration is performed with the parameter $w_s(Mn) = 0.78232$ which is used in the previous section because $w_s(Mn) = 0.650$ does not cause the solution of the parallel Mn moment in the ferromagnetic medium. In the αFe base alloys, the changes of the magnetic moment of Fe are mainly effective to ΔH and $\Omega - \Omega_v$, and in the Ni base alloys, the changes of the impurity magnetic moment are important.

§3.1. Formation energy

The calculated result of ΔH in the 3d metal alloys is shown in Fig.II.13 . The values of ΔH are evaluated at the equilibrium volume calculated from eq.(II.1.8) in the magnetic state or nonmagnetic state.

In α Fe-base alloys, the double counting term is important and the $\lambda = 3/2$ scheme explains ΔH qualitatively well. The result in the nonmagnetic state and the result by Van der Rest et al.[21] also explain the trend. The differences from their scheme of calculation are following three points: (1) We assume the charge neutrality within a site. (2) In our energy comparison, the magnetic energy is included. (3) The volume change of the bonding energy between the magnetic and nonmagnetic state is considered. Although experiments[38] are performed at high temperature, about 1000K , according to the recent experimental and theoretical studies[22],[23] of the 3d ferromagnetic metal, the local magnetic moment remains even at the high temperature more than 1000K. Therefore, it may be reasonable to estimate ΔH as the magnetic alloys.

An interesting result in connection with this circumstance is that the ΔH of Ni-Mn can not be explained as the nonmagnetic alloy. The origin of the negative ΔH in this alloy lies in the gain of the exchange energy with the increase of the Mn magnetic moment according to our calculation. Van der Rest et al. also present the negative ΔH of Ni-Mn in their nonmagnetic calculation.

According to their calculation , the origin is due

to the gain of the bonding energy. However, this mechanism is dubious if we consider a large magneto-volume effect of Mn. Indeed, the reason for the nearly zero ΔH in the nonmagnetic Ni-Mn alloy as shown in Fig.II.13 is that the gain of the bonding energy of pure γMn increases since the volume in the nonmagnetic state contracts more than 10 at% due to a large magneto-volume effect, and so the alloy tends to separate two metals. If we evaluate ΔH in the nonmagnetic state at the volume determined from Vegard's law in the magnetic state, we obtain ΔH=-0.0046 Ry/atom which is a comparable order with their result. Of course, it is not sufficient to discuss with eq.(II.1.17) for the alloy having a large spontaneous magnetostriction as mentioned in the previous section. Nevertheless, this alloy is interesting as an example that the magnetovolume effect influences the formation energy. The disagreements with the results of Van der Rest et al.[21] are also found in αFe-Cr and Ni-Fe. Our results give a correct trend in agreement with the observed value.

§3.2. Deviation from Vegard's Law

The deviation of the volume from Vegard's law is shown in Fig.II.13(a),(b). The agreement with the experimental values is not so good as in the case of 4d metal alloys. However, the trend through the periodic table is reproduced well. In αFe-Mn alloy, the antiparallel Mn moment configuration in the ferromagnetic phase is suitable since it explains the sign of ΔH and $(\Omega - \Omega_V)/\Omega_B c$. In the following analysis, this configuration is assumed. The deviation from Vegard's law in αFe-V is not explained by the common b.c.c. model DOS. This alloy will be discussed later. The experimental tendency can not be explained by the result of the nonmagnetic calculation, especially, in Ni-Cr, Ni-Mn, Ni-Co , αFe-Co, αFe-Ni and αFe-Cu alloys.

The relative pressures at the volume determined from Vegard's law are shown in Fig.II.15 in the same way as the previous section in order to elucidate the mechanisms of the deviation and the magnetic contribution . The relative pressure is defined by eq.(II.2.3). From these figures, we can conclude as follows.

Firstly for the αFe base 3d alloys, (1) The main origin of the deviation from Vegard's law is the magnetovolume effect except for αFe-Ti and αFe-V. The positive deviation in αFe-Co , αFe-Ni and αFe-Cu is mainly due to the increase of the magnetic moment at the host Fe site since the magnetic pressure is approximately proportional to the linear combination of the squares of each local magnetic moment. In αFe-Mn alloy,

the increase of the magnetic moment at Mn site is also important. (2) In the case of the above mentioned alloys, the nonmagnetic part of the relative pressure nearly vanishes, and the magnetic pressure is qualitatively reproduced by the first term of eq.(II.1.13). These facts show that the empirical formula proposed by Shiga and Schlosser,

$$\Omega \sim \Omega_V + \delta \left(\sum_I c_I k_I m_I^2 \right) \qquad \text{(II.2.6)}$$

is qualitatively correct where $k_I = \left[(D/t)_d / 4 - 1/\mu_{dI} \right] U_I / 3B$, Ω_V is the volume determined from Vegard's law. δ indicates the difference relative to the separated phase. (3) The negative deviation in αFe-Ti is due to the nonmagnetic effect of the negative relative pressure which is caused by the d-d bonding effect and s-d charge transfer effect as in the case of Pd-Zr alloy in Part I.

The disagreement in αFe-V with the observed value is not improved even if the parameter Z_A is changed by ± 0.1, and the result is also not sensitive to the parameter U_0 and γU_0 of V as shown in Fig.II.13 .

On the other hand, the atomic volume of Ni-V alloy is reproduced comparatively good for the same parameter, Therefore it is inferred that this disagreement is due to the detail of the b.c.c. model DOS. So, we calculated the lattice parameter with the new model DOS of V which is taken from the DOS calculated by Boyer et al.[48]. The new DOS is characterized by a more deep valley due to the bonding-antibonding effect, a sharp peak in the center of the band due to the $d\varepsilon$ state and an additional peak just below the large peak due to the $d\gamma$ state.

The decrease of the magnetic moment at the host Fe site and the increase of the bonding energy gain relative to the result of the previous DOS, are caused. For example, the magnetic moments at Fe and V sites are respectively 2.069 μB and -1.099 μB, while these are 2.223 μB and -0.957 μB in the old DOS. The new DOS also leads to the large negative deviation from Vegard's law at the nonmagnetic V-rich region contrary to the case of the previous DOS. The origin of this negative deviation can be considered to be due to the bonding effect caused by the breaking of the large peak of the d state at the center where the Fermi level lies and by the accumulation of the states on the valey of the b.c.c. DOS. It is due to these nonmagnetic contributions that Schlosser[18] could not elucidate the change of the lattice parameter of αFe-V.

Next , for the Ni base 3d alloys, the following three conclusions are obtained from Fig.16(b). (1) The nonmagnetic parts of the relative pressure are small except for Ni-Ti, Ni-Mn and Ni-Cu and so, eq.(II.2.6) is qualitatively correct. (2) The positive deviations from Vegard's law of Ni-Mn and Ni-Fe are mainly due to a magnetovolume effect. These are caused by the increase of the Mn and Fe magnetic moment. The negative deviations of Ni-Cr, Ni-V and Ni-Ti are also due to the magnetic effect caused by the decrease of the host Ni magnetic moment. This phenomenon is well known with respect to the deviation from the Slater-Pauling curve.

(3) The negative deviation in Ni-Ti is mainly due to the d-d bonding effect and the s-d charge transfer effect as in the case of αFe-Ti.

Until now, we have elucidated the origin of the deviation remarking the change of the magnetic pressure. However, we can also interpret it as the change of s and d parts of the relative pressure. Figure II.16(c) and (d) are analyses from this point of view. For example, the positive deviation of Ni-Fe alloys can be explained as follows. The repulsive relative pressure of the s part is caused by the repulsive relative pressure at Fe site due to the relative contraction. On the other hand, in the case of the nonmagnetic state, the relative d part pressure is negative as well as Pd-Tc in Part I. However, in the case of the magnetic state, this relative pressure of the d part nearly vanishes because of the loss of the bonding energy with the increase of the moment at the Fe site. Then, only the contribution of the relative pressure of the s part remains. This is another interpretation why the lattice parameter of Ni-Fe deviates positively from Vegard's law.

Finally, we point out that the change of the lattice parameter of the nonmagnetic Ni-base 3d alloys across the periodic table is different from the Pd base 4d alloys. As shown in Fig.II.16, the behavior of the relative pressure of the s part is always positive and is different from the case of the Pd base alloys although the relative d part pressures behave in the same way. This difference is caused by the

difference of the relative weight between the relative s pressure at the impurity site and the host one since the relative magnitude of lattice parameters of Cr, Mn, Fe and Co with respect to that of Ni has the opposite tendency to those of Mo, Tc, Ru and Rh compared with Pd.

§3.3. Bulk Modulus

The result of the calculation for the bulk modulus is shown in Fig.II.14. In the case of Ni-Co, Ni-Fe and Ni-Mn, it changes linearly with concentration. The others deviate negatively from the linear dependence. The origin of the softening in Ni-Ti, Ni-V, Ni-Cr, αFe-Ti and αFe-Cr is mainly due to the s-d charge transfer induced by the volume change. (See Fig.II.17.) The change of the bulk modulus of αFe-V calculated by the modified model band is $\Delta B/c=2.06$ which is of opposite sign to the modulus calculated by the old model band. In order to get the reliable result, it is necessary to calculate more accurately. The origin of the softening in αFe-Co, αFe-Ni and αFe-Cu is , in addition to the s-d charge transfer effect, partially due to the increase of the derivative of the local magnetic moment with respect to the volume and partially due to the decrease of the rigid part with the volume expansion. The rigid part in the bulk modulus is defined by the first and third terms of r.h.s. of eq.(II.1.15).

The observed values of αFe-Cr, αFe-Ni and αFe-Co agree with the trend of the result of the calculation. The systematic experiment is desirable so as to check whether the softenings in αFe-Ti and Ni-Ti type alloys are observed or not.

§4. Conclusion and Discussion

We have calculated the cohesive properties of Cu-Mn and the αFe and Ni base 3d TMA on the basis of the tight binding model and the virial theorem, and then discussed the mechnism. Our result and conclusion are summarized as follows.

Firstly, for the formation energy ΔH, we have taken account of the volume dependence of the bonding energy and evaluated ΔH by the d electron magnetic energy (II.1.17). The trend for ΔH was reproduced also in the case of the magnetic state. In the αFe base 3d alloys, the formation energies calculated with the $\lambda=3/2$ scheme in eq.(II.1.17) agree with the experimental values qualitatively. We pointed out that the nonmagnetic evaluation of ΔH can not explain the negative ΔH of Ni-Mn and Ni-Fe if we take account of the magnetovolume effect since ΔH is fairly sensitive to the volume change. The small positive ΔH of Cu-Mn could not be explained by eq.(II.1.17). In the case of such a system which shows the large magneto-volume effect, (for example, Cu-Mn), the evaluation of the repulsive energy term will be important.

Secondly, we have calculated the volume dependence of the magnetic moment and the pressure of the disordered antiferromagnetic γMn which has a large pressure dependence of the Neel point. We did not find the first order change of the magnetic moment induced by the pressure as in γFe[11], [14]. With the stretching of the d band width, the magnitude of the local moment decrease continuously and, at the volume at which the local moment vanishes, a bending of the P-V

relation appears.

The deviations of the lattice parameters from Vegard's law were also qualitatively elucidated. There are several origins for the deviation from Vegard's law.

One is the magnetovolume effect due to the change of the local magnetic moment. When the magnetic pressure is expanded in powers of the local magnetic moments for any magnetic and atomic configurations, it consists of the terms of the squares of the local magnetic moment and the s-d charge transfer term due to the change of the magnetic moment in the lowest order expansion. We have verified that the latter term is not important for many 3d metal alloys and the magnetic pressure is qualitatively described well by the former term only. This approximate expression does not depend on the details such as the Fermi level and the DOS. So, we have given a theoretical basis to the empirical formula proposed by Shiga and Schlosser. The alloys in which the deviation from Vegard's law is mainly caused by the magnetic pressure are αFe-Mn, αFe-Co, αFe-Cu, Ni-V, Ni-Cr, Ni-Fe and Cu-Mn.

The other origins are the d-d bonding effect and the s-d charge transfer effect. These effects were the origin of the deviation from Vegard's law in the Pd base 4d alloys. In 3d alloys, the deviations from Vegard's law of αFe-Ti, Ni-Ti, V rich αFe-V and Cu rich Cu-Mn alloys are also caused by these mechanisms.

The linear change of the bulk modulus with concentration of Cu-Mn which is contrary to the behavior of the lattice parameter is due to the fact that the relatively negative modulus of the core part caused by the volume expansion cancels the relatively positive modulus of the bonding part as has been shown in §2.

The magnitude of the bulk modulus is determined mainly by the core term (the first term of r.h.s. of eq.(II.1.16)) and the bonding term (the fourth term of r.h.s. of eq.(II.1.16)). However, for the changes of the bulk moduli in alloys, the s-d charge transfer term and the magnetic moment term for the volume derivative (the second and third terms of r.h.s. in eq.(II.1.16)) are also important. Especially, the softenings of αFe-Ni, αFe-Co and αFe-Cu are due to the two origins, that is , the increase of the sd charge transfer for the volume derivative and of the magnetic moment term for the volume derivative. These effects will be important in the so-called invar region. The softenings of Ni-Ti, Ni-V, αFe-Ti and αFe-Cr are also due to the former origin. The experimental bulk modulus of αFe-Cr supports this trend.

These are our conclusions at the present stage. We have calculated the electronic structure as a binary system for all alloys. The electronic structures of αFe-Mn and Ni-Mn which are sensitive to the magnetic configuration and its pressure dependence, are not sufficient in our calculation, and the calculation as a ternary or quaternary alloy will be necessary in order to reproduce the electronic structure more reasonably. The

cohesive properties of αFe-V are not also elucidated sufficiently. The s electron number of V is 1.38 according to our parameter listed in Table 1. This value is clearly overestimated. On the other hand, if we assume Z_A to be equal to 1.0, the s electron number is about 1.0, but the lattice parameter and bulk modulus are not reproduced reasonably. These inconsistencies seem to be caused by the fact that the semi-ellipsoidal s DOS overestimates the s-d charge transfer effect. In other words, it may indicate that the s-d hybridization effect is important. It was needed to modify the model d DOS in order to get the correct lattice parameter of $Fe_{90}V_{10}$ alloy. This suggests that the cohesive properties of αFe-V depend on the detail of the assumed model DOS. Therefore, for this alloy, we must carry out a more exact calculation.

Finally, we discuss an extention to the finite temperature and the invar problem. To the ground state properties of the magnetovolume effects and the bulk moduli of the invar alloys such as Fe-Ni and Fe-Pt, our method is applicable straight forwardly and the calculations are in progress. However, it is well known that the electronic structure in the critical concentration at which the ferromagnetic state vanishes, is not sufficiently described by the simple CPA. So, the theoretical elucidation in this concentration of Fe-Ni alloy at 0K is not easy in the existing circumstances. On the other hand, we have shown that the first term of eq.(II.1.13)

describes the magnetovolume effect qualitatively. According to this expression, for example, the behavior of the lattice parameter of Fe-Ni can be understood by considering only by the magnitude of the local magnetic moments even in the critical concentration. From this point of view, Shiga et al.[18] have discussed the invar alloy.

In connection with this, it is claimed from the experimental viewpoint that the theoretically calculated magnetovolume term $\left[(D/t)_d /4-1/\mu_{dI}\right]U_I/3B$ is overestimated by the factor 5~10 times[50]. We point out that the claim is based on the inappropriate analysis.

In the usual phenomenologicall theory, the spontaneous magnetostriction is assumed to be proportional to the square of the magnetization. However, according to the approximate expression (II.1.19), it is proportional to the linear combination of the squares of the local moment. On the other hand, the local magnetic moment remains above the Curie temperature according to the recent studies of the magnetism of Fe[22],[23]. Therefore, the spontaneous magnetovolume striction is approximately

$$\omega_s \equiv \frac{\delta\Omega}{\Omega} \sim \sum_I c_I \left[\frac{1}{4}\left(\frac{D}{t}\right)_d - \frac{1}{\mu_{dI}}\right] v_I \left(m_I^z - m_{Io}^z\right)/3B\Omega , \qquad \text{(II.4.1)}$$

where B is the bulk modulus, m_I is the local moment at 0K and m_{I0} is the local moment above the Curie temperature.

Let us consider Fe_3Pt alloys as an example. We neglect the local moment at Pt site and assume $m_{Fe0}/m_{Fe}=0.9$. Using the observed value $\omega_s=0.018$, $m_{Fe}=2.7\,\mu B$, we can evaluate $\{[(D/t)_d/4-1/\mu_d]U\}_{Fe}/3B \approx 0.017$ from eq.(II.4.1). On the other hand, we obtain $\{[(D/t)_d/4-1/\mu_d]U\}_{Fe}/3B = 0.022$ with use of the observed values $B(Fe_3Pt)=0.00682$ Rya.u., $\Omega=93.4$ a.u. since $\{[(D/t)_d/4-1/\mu_d]U\}_{Fe}$ is 0.0421 Ry if we use the parameters in Table 1. This value is roughly equal to the experimentally deduced value 0.017.

In the case of finite temperatures, if we use the two-field functional integral method[51] and apply the static approximation, eq.(II.1.2) is replaced by

$$3P_\ell V = \sum_{\alpha\sigma}\left(\sum_\beta \frac{D^\beta_{\alpha\alpha}}{z}\right)_{\ell\sigma} \left\langle \int d\omega\, f(\omega)\, \rho_{\alpha\ell\sigma}(\omega)\right\rangle_{\xi\eta} + \left(\frac{D}{t}\right)_\ell \int d\omega\, f(\omega) \left\langle \sum_{\alpha\sigma}(\omega-\epsilon_{\alpha\ell\sigma}+\mu)\,\rho_{\alpha\ell\sigma}(\omega)\right\rangle_{\xi\eta},$$

where $f(\omega)$ is the Fermi distribution function, μ is the chemical potential and $\langle\sim\rangle_{\xi\eta}$ expesses the classical thermal average about ξ and η. As known from this expression, the change of the bonding energy caused by the thermal excitation which changes the amplitude of the local magnetic moment, is important for invar alloy. Essential properties of magneto-volume effects in the finite temperature will be elucidated in the following Part III.

Part III

A Theory of the Magnetovolume Effect at Finite Temperatures

Outline of Part III

The method of the calculation for the pressure in alloys proposed in Part I is extended to finite temperatures in order to elucidate the magnetovolume effect in the 3d metals and alloys such as invar alloys. Liberman-Pettifor's expression at finite temperatures is derived from the virial theorem from the most general point of view. In §2, the expressions for the spontaneous volume magnetostriction, the forced volume magnetostriction, the magnetic contribution to the thermal expansion and the bulk modulus are obtained with use of the static approximation in the functional integral method. It is shown that the empirical formula with respect to the magneto-volume effect can be obtained also in the finite temperature case if the fluctuation term around saddle points are neglected. It is concluded that the anomalous magnetovolume effect in the 3d alloys is mainly caused by the change of the magnitude of the local magnetic moment and the s-d charge transfer effect. Furthermore, it is shown that the Weiss model in the invar problem can be derived from our point of view. At the end of §2, the result of the preliminary calculation for αFe is given and discussed in comparison with the result based on the Stoner model.

§1. The Virial Theorem at Finite Temperatures

In this section, we derive Liberman-Pettifor's expression at finite temperatures from a general point of view.

The virial theorem for a total system is given by

$$\begin{aligned} 3PV = & \; 2\langle T_n \rangle + \langle \Sigma \phi_{nn} \rangle \\ & + 2\langle T_e \rangle + \langle \Sigma \phi_{ee} \rangle \\ & + \langle \Sigma \phi_{ne} \rangle + \sum_{\mu} \langle \mathbf{r}_\mu \cdot \mathbf{F}_\mu^{ex} \rangle , \end{aligned} \tag{III.1.1}$$

where $\langle \sim \rangle$ expresses the thermal average for the total system. T_n (T_e) is the kinetic energy of the nuclear system (the electron system). ϕ_{nn} is the coulomb interaction between the nuclei. ϕ_{ee} is the coulomb interaction in the electron system. ϕ_{ne} is the coulomb interaction between the nuclear system and the electron system. $\mathbf{F}_\mu^{ex}$ is an external force which acts on the μ-th particle (a nucleus or an electron) and is defined by $\mathbf{F}_\mu^{ex} = -\partial H_1 / \partial \mathbf{r}_\mu$ where H_1 is an external perturbation. We neglect the electron-phonon interaction so that the system can be separated into a phonon system and an electron system. Let $X_\alpha(k)$ denote the α-th component of the nuclear coordinate at the site k. If we expand the coordinates $\{X_\alpha(k)\}$ in terms of $\{u_\alpha(k)\}$, the displacements from the average values $\{\langle X_\alpha(k) \rangle\}$, we find that the thermodynamical potential $3PV$

can be divided into two parts, a phonon part $3P_{ph}V$ and an electron part $3P_eV$:

$$3PV = 3P_{ph}V + 3P_eV , \tag{III.1.2}$$

$$3P_{ph}V = 2\langle T_n\rangle_{ph} + \frac{1}{2}\sum_{\alpha k}\sum_{\alpha' k'} \frac{\partial^2\langle 2T_e + U\rangle_e}{\partial u_\alpha(k)\,\partial u_{\alpha'}(k')} \cdot \langle u_\alpha(k)\,u_{\alpha'}(k')\rangle_{ph} , \tag{III.1.3}$$

$$3P_eV = 2\langle T_e\rangle_e + \langle U^0\rangle_e , \tag{III.1.4}$$

where U is the coulomb energy of the total system defined by $\Sigma\phi_{ee}+\Sigma\phi_{en}+\Sigma\phi_{nn}$. $\langle U^0\rangle_e$ is the coulomb energy of the total system such that the coordinates of nuclei are replaced by their average values. The last term of r.h.s. of eq.(III.1.1) is neglected considering only the spacially uniform external magnetic field. After this, we do not enter into the details of the phonon part pressure.

We consider the electronic system whose Hamiltonian is

$$H = \int \psi^\dagger(\mathbf{r})(-\nabla^2)\psi(\mathbf{r})\,d\mathbf{r} - \int \frac{\psi^\dagger(\mathbf{r})\psi(\mathbf{r})\rho(\mathbf{r}')}{|\mathbf{r}-\mathbf{r}'|}\,d\mathbf{r}\,d\mathbf{r}'$$
$$+ \frac{1}{2}\int \frac{\psi^\dagger(\mathbf{r})\psi^\dagger(\mathbf{r}')\psi(\mathbf{r}')\psi(\mathbf{r})}{|\mathbf{r}-\mathbf{r}'|}\,d\mathbf{r}\,d\mathbf{r}'$$
$$- \int \psi^\dagger(\mathbf{r})\,\boldsymbol{\sigma}\psi(\mathbf{r})\cdot\mathbf{h}\,d\mathbf{r} , \tag{III.1.5}$$

where $\psi^\dagger(\mathbf{r})$ and $\psi(\mathbf{r})$ are respectively the creation and the annihilation field operators. $\rho(\mathbf{r})$ is the nuclear charge density. $\mathbf{h}$ is the uniform magnetic field. $\boldsymbol{\sigma}$ is the Pauli

spin matrix. Now, we show that an expression similar to eq.(I.2.1) holds generally. However, in the expression, one electron wave function should be replaced by the field operator $\psi(\mathbf{r})$ and the conjugate complex (c.c.) should be replaced by the hermite conjugate (h.c.).

First of all, we rewrite the following expression with use of Green's theorem.

$$\left\langle \frac{1}{2} \int d\mathcal{S} \left[(\nabla \psi^{\dagger}(\mathbf{r}))(\mathbf{r}\cdot\nabla)\psi(\mathbf{r}) - \psi^{\dagger}(\mathbf{r})\nabla(\mathbf{r}\cdot\nabla\psi(\mathbf{r})) + h.c. \right] \right\rangle_e . \tag{III.1.6}$$

Then, the above expression becomes equal to

$$2\langle T_e \rangle_e + \left\langle \frac{1}{2} \int d\mathbf{r} \left[(\nabla^2\psi^{\dagger}(\mathbf{r}))(\mathbf{r}\cdot\nabla)\psi(\mathbf{r}) - \psi^{\dagger}(\mathbf{r})(\mathbf{r}\cdot\nabla)\nabla^2\psi(\mathbf{r}) + h.c. \right] \right\rangle_e , \tag{III.1.7}$$

where we used the fact that the kinetic energy is hermite ($\langle \int d\mathbf{r}\, \psi^{\dagger}(\mathbf{r})\nabla^2\psi(\mathbf{r}) \rangle = \langle \int d\mathbf{r}\, (\nabla^2\psi^{\dagger}(\mathbf{r}))\psi(\mathbf{r}) \rangle$.) .

If we note a commutation relation,

$$\nabla^2\psi_\alpha(\mathbf{r}) = -[\psi_\alpha(\mathbf{r}), H] + \mathcal{W}_\alpha(\mathbf{r})$$

$$\mathcal{W}_\alpha(\mathbf{r}) \equiv -\int \frac{\rho(\mathbf{r}')\,d\mathbf{r}'}{|\mathbf{r}-\mathbf{r}'|}\psi_\alpha(\mathbf{r}) + \int \frac{\psi^{\dagger}(\mathbf{r}')\psi(\mathbf{r}')}{|\mathbf{r}-\mathbf{r}'|} d\mathbf{r}'\psi_\alpha(\mathbf{r}) - (\varpi)_{\alpha\alpha'}\psi_{\alpha'}(\mathbf{r})\,\hbar ,$$

and $\mathrm{tr}(e^{-\beta(H-\mu N)}[H, \psi_\alpha]) = 0$, the integrand of the second term of eq.(III.1.7) can be written as follows.

$$\frac{1}{2}\left\langle \left\{ W^{\dagger}(\mathbf{r})\,(\mathbf{r}\cdot\nabla\psi(\mathbf{r})) - \psi^{\dagger}(\mathbf{r})\,(\mathbf{r}\cdot\nabla)\,W(\mathbf{r}) \right\} \right\rangle_e$$

$$= \frac{-1}{2}\cdot\left\langle \psi^{\dagger}(\mathbf{r}) \left\{ (\mathbf{r}\cdot\nabla)\left(-\int \frac{\rho(\mathbf{r}')\,d\mathbf{r}'}{|\mathbf{r}-\mathbf{r}'|} + \int \frac{\psi^{\dagger}(\mathbf{r}')\psi(\mathbf{r}')}{|\mathbf{r}-\mathbf{r}'|} d\mathbf{r}' \right) \right\} \psi(\mathbf{r}) \right\rangle_e .$$

Therefore, with use of eq.(III.1.7), eq.(III.1.6) becomes

$$\left\langle \frac{1}{2}\int d\mathcal{S} \left[(\nabla\psi^{\dagger}(\mathbf{r}))\,(\mathbf{r}\cdot\nabla\psi(\mathbf{r})) - \psi^{\dagger}(\mathbf{r})\,\nabla\,(\mathbf{r}\cdot\nabla\psi(\mathbf{r})) + h.c. \right] \right\rangle_e$$

$$= 2\langle T_e \rangle_e + \left\langle \frac{1}{2}\int d\mathbf{r}\,d\mathbf{r}' \frac{\psi^{\dagger}(\mathbf{r})\,\psi^{\dagger}(\mathbf{r}')\,\psi(\mathbf{r}')\,\psi(\mathbf{r})}{|\mathbf{r}-\mathbf{r}'|} \right\rangle_e$$

$$- \left\langle \int d\mathbf{r}\, \psi^{\dagger}(\mathbf{r})\psi(\mathbf{r})\,(\mathbf{r}\cdot\nabla) \int \frac{(-\rho(\mathbf{r}'))\,d\mathbf{r}'}{|\mathbf{r}-\mathbf{r}'|} \right\rangle_e$$

$$+ \left\langle \int d\mathbf{r}\, \psi^{\dagger}(\mathbf{r})\, \varpi\,((\mathbf{r}\cdot\nabla)\,\mathbb{h})\,\psi(\mathbf{r}) \right\rangle_e .$$

(III.1.8)

Eliminating $2\langle T_e \rangle$ from eqs.(III.1.8) and (III.1.4), the following expression is obtained.

$$3 P_e V$$

$$= \left\langle \frac{1}{2}\int d\mathcal{S} \left[(\nabla\psi^{\dagger}(\mathbf{r}))\,(\mathbf{r}\cdot\nabla\psi(\mathbf{r})) - \psi^{\dagger}(\mathbf{r})\,\nabla(\mathbf{r}\cdot\nabla\psi(\mathbf{r})) + h.c. \right] \right\rangle_e$$

$$- \int d\mathbf{r}\,\rho(\mathbf{r})\,(\mathbf{r}\cdot\nabla) \left[\sum_i{}' \int_j \frac{\rho(\mathbf{r}')\,d\mathbf{r}'}{|\mathbf{r}-\mathbf{r}'|} - \int \frac{\langle \psi^{\dagger}(\mathbf{r}')\,\psi(\mathbf{r}') \rangle}{|\mathbf{r}-\mathbf{r}'|} d\mathbf{r}' \right] .$$

(III.1.9)

The procedure after this is similar to the derivation of eq.(A.I.4) from eq.(A.I.1) in Appendix I. That is, in order to transform the surface integral term of eq.(III.1.9) to the surface integral form at each cell, we must add the following relation to eq.(III.1.9) and subtract that.

$$\left\langle \frac{1}{2}\int_j \left[(\nabla\psi^t(\mathbf{r}))(\mathbf{r}_j\cdot\nabla)\psi(\mathbf{r}) - \psi^t(\mathbf{r})\nabla(\mathbf{r}_j\cdot\nabla\psi(\mathbf{r})) + \text{h.c.}\right] d\mathcal{S}\right\rangle_e$$

$$= -\left\langle \int_j d\mathbf{r}\int_j d\mathbf{r}'\left[\psi^t(\mathbf{r})\psi^t(\mathbf{r}')\psi(\mathbf{r}')\psi(\mathbf{r}) - \psi^t(\mathbf{r})\psi(\mathbf{r})\rho(\mathbf{r}')\right](\mathbf{r}_j\cdot\nabla\frac{1}{|\mathbf{r}-\mathbf{r}'|})\right\rangle_e$$

$$-\sum_i{}' \int_j d\mathbf{r}\int_i d\mathbf{r}'\left\langle \psi^t(\mathbf{r})\psi(\mathbf{r})\left(\psi^t(\mathbf{r}')\psi(\mathbf{r}') - \rho(\mathbf{r}')\right)(\mathbf{r}_j\cdot\nabla\frac{1}{|\mathbf{r}-\mathbf{r}'|})\right\rangle_e ,$$

where $\int_j d\mathbf{r}$ expresses the integration over the cell at the j-th site and we have used the relation $\nabla^2\psi_\alpha = -[\psi_\alpha, H] + W_\alpha(\mathbf{r})$. As the result, we obtain Liberman-Pettifor's expression in the most general form.

$$3P_e V$$

$$= \sum_j \frac{1}{2}\left\langle \int_j d\mathcal{S}\left[(\nabla\psi^t(\mathbf{r}))((\mathbf{r}-\mathbf{r}_j)\cdot\nabla\psi(\mathbf{r})) - \psi^t(\mathbf{r})\nabla((\mathbf{r}-\mathbf{r}_j)\cdot\nabla\psi(\mathbf{r})) + \text{h.c}\right]\right\rangle$$

$$+\frac{1}{2}\sum_i\sum_j{}'(\mathbf{r}_i-\mathbf{r}_j)\int_i d\mathbf{r}\left(\langle\psi^t(\mathbf{r})\psi(\mathbf{r})\rangle - \rho(\mathbf{r})\right)$$

$$\times(-\nabla)\int_j d\mathbf{r}'\frac{\left(\langle\psi^t(\mathbf{r}')\psi(\mathbf{r}')\rangle - \rho(\mathbf{r}')\right)}{|\mathbf{r}-\mathbf{r}'|}$$

$$+\frac{1}{2}\sum_i\sum_j{}'(\mathbf{r}_i-\mathbf{r}_j)\int_i d\mathbf{r}\int_j d\mathbf{r}\left\langle\delta(\psi^t(\mathbf{r})\psi(\mathbf{r}))\cdot\delta(\psi^t(\mathbf{r}')\psi(\mathbf{r}'))\right\rangle$$

$$\times(-\nabla)\frac{1}{|\mathbf{r}-\mathbf{r}'|} \qquad \text{(III.1.10)}$$

where the index e in the average is omitted and $\delta(\psi^{\dagger}(\mathbf{r})\psi(\mathbf{r})) = \psi^{\dagger}(\mathbf{r})\psi(\mathbf{r}) - \langle\psi^{\dagger}(\mathbf{r})\psi(\mathbf{r})\rangle$. The first term is the surface integral term at each cell. The second term is the interatomic electrostatic energy term. The third term is the inter-atomic coulomb energy term due to the charge fluctuation.

The second and third terms in eq.(III.1.10) will not be important for alloys that satisfy the charge neutrality condition. So, we consider only the first term of the r.h.s. of eq.(III.1.10) and define $(3P_eV)_{cell}$ by this term. The field operator can be expanded by the orthogonalized atomic orbitals $\{\varphi_{\mu\sigma}\}$ as follows:

$$\psi_\sigma(\mathbf{r}) = \sum_\mu \varphi_{\mu\sigma}(\mathbf{r})\, a_{\mu\sigma} ,$$

where μ specifies both site and orbital. Substituting this expression into $(3P_eV)_{cell}$ and defining $\bar{D}^{ij}_{\mu\nu}$ by $(D^{ij}_{\mu\nu}+D^{ji}_{\nu\mu})/2$, we obtain

$$(3PeV)_{cell} = \sum_{j\sigma}\sum_{\mu\nu} \bar{D}^{j}_{\mu\nu} \langle a^{\dagger}_{\mu\sigma} a_{\nu\sigma}\rangle /2 . \qquad \text{(III.1.11)}$$

With use of the same procedure as in Part I, we obtain the following expression.

$$(3PeV)_{cell} = 3P_sV + 3P_dV,$$

$$3PeV = \sum_i \Big(\sum_j \frac{D^{i}_{ii}}{z}\Big)_{\ell} \langle n_{\ell i}\rangle + \Big(\frac{D}{t}\Big)_{\ell} \sum'_{ij\sigma} \langle t^{\ell}_{ij}\, a^{\dagger}_{i\sigma} a_{j\sigma}\rangle .$$

(III.1.13)

This expression corresponds to eq.(I.1.9) in Part I or eq.(II.2.2) in Part II. In eq.(II.2.2), we have assumed the

spin dependence of $(\Sigma D/2)_{1i}$. But it is not important and therefore we neglected it in eq. (III.1.13). After all , the quantities which must be calculated are the electron number and the bond energy.

§2. Magnetovolume effect in the Static Approximation

We estimate an expression of the pressure (III.1.13) with use of the functional integral method which enable us to have a definite physical picture intuitively.

The model Hamiltonian is as follows:

$$
\begin{aligned}
H &= H_d + H_s + \sum_i U_i^{sd} n_{di} n_{si} \\
H_l &= \sum_{i\alpha} \epsilon^0_{li\alpha} n_{li\alpha} + \sum_{\substack{i\neq j \\ \alpha}} t_{ij}^{l} a^{\dagger}_{li\alpha} a_{lj\alpha} \\
&\quad + \sum_i \left(\frac{1}{4} J_i^l n_{li}^z - U_i^l S_{liz} \right) ,
\end{aligned}
\tag{III.2.1}
$$

where $\epsilon^0_{li\alpha}$ is the center of gravity of the l orbital and α spin state. t^l_{ij} is the transfer integral of the orbital l between the i-th site and the j-th site. U_i^{sd} means the intraatomic coulomb energy between s and d electrons at the site i. J_i^l (U_i^l) is the intra-atomic coulomb energy (exchange energy) of the orbital l at the site i. S_{liz} is the z component of the spin operator and defined by $S_{liz}=(n_{li\uparrow}-n_{li\downarrow})/2$. We apply the two-field method[53] for each of s and d, which is consistent with the Hartree-Fock (H.F.) approximation in the ground state.

The partition function in the static approximation is

$$
Z_{stat} = \int \left[\prod_i d\xi_{di}\, d\eta_{di}\, d\xi_{si}\, d\eta_{si} \right] e^{-\beta E[\xi\eta]} ,
$$

$$E[\xi\eta] = F^{\circ}[\xi\eta] + \sum_i \left[\sum_l \frac{1}{4} \left(J_i^l \eta_{li}^z + v_i^l \xi_{li}^z \right) + v_i^{sd} \eta_{si} \eta_{di} \right],$$

$$F^{\circ}[\xi\eta] = F_s^{\circ} + F_d^{\circ}, \qquad \text{(III.2.3)}$$

where ξ_{1i} and η_{1i} are fields of the 1 orbital at the site i. We averaged Z_{stat} over all directions of the quantized axis at each site by the method proposed by Hubbard[53]. $F_1^0[\xi,\eta]$ is one electron state free energy which is described by the following Hamiltonian of the orbital 1 in random fields $\{\xi_{li}\eta_{li}\}$.

$$H_{l\lambda} = \sum_{i\alpha} \left[\epsilon_{li}^{\circ} - \mu - \left(\frac{1}{z} J_i^l i \eta_{li} + v_i^{sd} i \eta_{l'i} \right) \right] n_{li\alpha}$$

$$+ \lambda_l \sum_{\substack{i \neq j \\ \alpha}} t_{ij}^l a_{li\alpha}^{\dagger} a_{lj\alpha}$$

$$- \sum_i \left(v_i^l \xi_{li} + z h \right) \cdot s_{li}, \qquad \text{(III.2.4)}$$

where μ is the chemical potential. We introduced a parameter λ_1 for convenience. $F_{1\lambda}^0$ is also expressed by the integrated number of states $N_{1\lambda}(\omega)$ as follows.

$$F_{l\lambda}^{\circ} = -\int d\omega \, f(\omega) N_{l\lambda}(\omega), \qquad \text{(III.2.5)}$$

where $f(\omega)$ is the Fermi distribution function. $N_{1\lambda}(\omega)$ can be calculated from

$$N_{l\lambda}(\omega) = \frac{(-)}{\pi} Im \, tr \, ln \left(L^{-1} - \lambda_l t \right), \qquad \text{(III.2.6)}$$

where L^{-1} is the locator, t is the transfer matrix, which

are defined by

$$(\mathcal{L}^{-1})_{i\alpha\, j\beta} = \left[\omega - \{\epsilon_{\ell i} - \mu - (\tfrac{1}{2} v_i^{\ell} \xi_{\ell i} + h)\cdot\sigma\}\right]_{\alpha\beta} \delta_{ij} ,$$

$$(t)_{i\alpha\, j\beta} = t_{ij}^{\ell}\, \delta_{\alpha\beta} ,$$

$$\epsilon_{\ell i} = \epsilon_{\ell i}^{o} - (\tfrac{1}{2} J_i^{\ell}\, i\eta_{\ell i} + v_i^{sd}\, i\eta_{\ell' i}) , \qquad \text{(III.2.7)}$$

where i and j are the site indices, α and β are the spin indices. σ is Pauli's spin matrix. The total free energy is

$$F_\lambda = -\beta^{-1} \ln Z_{stat} . \qquad \text{(III.2.8)}$$

The bond energy in the static approximation can be obtained as follows.

$$\Big\langle \sum_{\substack{i\neq j \\ \alpha}} t_{ij}^{\ell}\, a_{\ell i\alpha}^{\dagger}\, a_{\ell j\alpha} \Big\rangle$$

$$= -\left[\partial F_\lambda / \partial \lambda_\ell\right]_{\lambda=1}$$

$$= \int \left[\prod_i d\xi_i\, d\eta_i\right] e^{-\beta E} \left(\frac{\partial E_\lambda}{\partial \lambda_\ell}\right)_{\lambda=1} \Big/ \int \left[\prod_i d\xi_i\, d\eta_i\right] e^{-\beta E}$$

and

$$\left(\frac{\partial E_\lambda}{\partial \lambda_\ell}\right)_{\lambda=1} = -\int d\omega\, f(\omega) \left(\frac{\partial N_{\ell\lambda}(\omega)}{\partial \lambda_\ell}\right)_{\lambda=1}$$

$$= \sum_{i\alpha} \int d\omega\, f(\omega) \frac{(-)}{\pi} \mathrm{Im}\left[\{\omega - (\epsilon_{\ell i} - \mu - (\tfrac{1}{2} v_i^{\ell} \xi_{\ell i} + h)\cdot\sigma)\}\, G_i^{\ell}\right]_{\alpha\alpha} ,$$

where $G^{l}(\omega)$ is one electron Green function of the orbital l which corresponds to the Hamiltonian (III.2.4). Therefore,

$$\left\langle \sum_{\substack{i\neq j \\ \alpha}} t_{ij}^{l}\, a_{li\alpha}^{\dagger} a_{lj\alpha} \right\rangle$$

$$= \sum_{i\alpha} \Big[\int d\omega f(\omega) \left\langle (\omega - \epsilon_{li} + \mu) \rho_{li}(\omega) \right\rangle_{\xi\eta} + \left\langle \left(\frac{1}{z} v_i^{l} \xi_{li} + h\right) \cdot m_{li}^{0} \right\rangle_{\xi\eta} \Big] ,$$

(III.2.9)

where $\langle \sim \rangle_{\xi\eta}$ means the classical average for fields $\{\xi_{li}, \eta_{li}\}$, $\int d\xi d\eta\, e^{-\beta E(\sim)} / \int d\xi d\eta\, e^{-\beta E}$. m_{li}^{0} is the local magnetic moment of the orbital l at the site i which is described by the Hamiltonian (III.2.4). $\rho_{li}(\omega)$ is the local DOS of the orbital l at the site i.

After all, eq.(III.1.13) is expressed in the static approximation as follows.

$$3P_l V = \langle 3P_l^{0} V \rangle_{\xi\eta}$$

$$3P_l^{0} V = \sum_i \left(\Sigma \frac{D}{z}\right)_{li} n_{li}^{0} + \left(\frac{D}{t}\right)_l \sum_i \Big[\int d\omega f(\omega) (\omega - \epsilon_{li} + \mu) \rho_{li}(\omega) + \left(\frac{1}{z} v_i^{l} \cdot \xi_{li} + h\right) \cdot m_{li}^{0} \Big] ,$$

(III.2.10)

where $3P_l^{0}V$ is the pressure of one electron state described by the Hamiltonian (III.2.4). n_{li}^{0} and m_{li}^{0} are respectively the electron number and local magnetic moment of the orbital l at the site i.

The equilibrium volume per atom Ω is determined by the condition of $3P\Omega[\Omega,T]=0$. Spontaneous volume magnetostriction is defined by the volume expansion due to the appearance of the magnetization. Then,we define the volume Ω_p in the paramagnetic state at any temperature as follows.

$$[3P\Omega(\Omega_p,T)]_{para} \equiv 0 \quad .$$

The 'paramagnetic state' means that the classical thermal average $\langle\sim\rangle_{\xi\eta}$ in the physical quantities is replaced by $\langle\sim\rangle_{\xi\eta\,para} \equiv \int d\xi\, d\eta\, e^{-\beta^* E}(\sim) \,/\, \int d\xi\, d\eta\, e^{-\beta^* E}$.
$T^* = \beta^{*-1} (\gg Tc)$ is the temperature where there are no short range order. Then, the following equation is obtained.

$$3P\Omega(\Omega,T) - [3P\Omega(\Omega,T)]_{para} = -([3P\Omega(\Omega,T)]_{para} - [3P\Omega(\Omega_p,T)]_{para}).$$

Since the magneto-volume striction is less than a few percent of the volume, it can be obtained by expanding the r.h.s. of the above equation to the first order of $\Omega-\Omega_p$. As the result,

$$\omega_s(T) = (\Omega(T) - \Omega_p(T))/\Omega_p(T) = \frac{3P\Omega(\Omega,T) - [3P\Omega(\Omega,T)]_{para}}{3B_p(\Omega_p,T)\Omega_p}, \qquad \text{(III.2.12)}$$

where B_p is the bulk modulus in the paramagnetic state defined by

$$3B_p(\Omega_p,T) \equiv -\frac{\partial}{\partial\Omega}\left[3P\Omega(\Omega_p,T)\right]_{para}, \qquad \text{(III.2.13)}$$

B_p is not anomalous for the temperature variation at all. Since B_p changes only a few percent at about 1000K, it can be replaced by $B_p(\Omega_p(0),T=0K)$ at 0K. The spontaneous volume magnetostriction can be calculated from eq.(III.2.10) and eq.(III.2.12) since only the electronic part pressure will contribute to $3P\Omega-[3P\Omega]_{para}$.

The bulk modulus of the electronic part is obtained by differentiating eq.(III.2.10) with respect to the volume:

$$3B_e = \sum_\ell \left\langle \left[-\frac{d}{d\Omega}(3P_\ell^\circ\Omega)\right]\right\rangle_{\xi\eta} - \beta\left\langle \Delta P^1 \cdot \Delta\sum_\ell 3P_\ell^\circ\Omega\right\rangle_{\xi\eta}, \qquad \text{(III.2.14)}$$

where the second term of the r.h.s. is a classical fluctuation term. $P^1=-\partial E[\xi\eta]/\partial\Omega$, $\Delta 3P_1^0\Omega=3P_1^0\Omega-\langle 3P_1^0\Omega\rangle_{\xi\eta}$ and $\Delta P^1=P^1-\langle P^1\rangle_{\xi\eta}$. In order to rewrite $[-d(3P_1^0\Omega)/d\Omega]$ to obtain an easily understandable expression , it is convenient to transform the bond energy after integrating by parts, into

$$\int d\omega\, f(\omega)\frac{(-)}{\pi}\,\mathrm{Im}\sum_{i\alpha}\left[\left\{\omega-\left(\epsilon_{\ell i}-\mu-\left(\frac{1}{2}v_i^\ell\xi_{\ell i}+h\right)\cdot\varpi\right)\right\}G_i^\ell\right]_{\alpha\alpha}$$

$$= F_\ell^\circ[\xi\eta]$$

$$+ \int d\omega \left(-\frac{\partial f(\omega)}{\partial \omega}\right) \sum_{i\alpha} \frac{(-)}{\pi} \mathrm{Im}\left[\left\{\omega - (\epsilon_{\ell i} - \mu - (\frac{1}{z} v_i^\ell \xi_{\ell i} + h)\cdot \varpi)\right\} \times \int_d^\omega d\omega' G_i^\ell(\omega')\right]_{\alpha\alpha} . \qquad \text{(III.2.15)}$$

The derivative of this term with respect to the volume becomes as follows in the same way as the derivation of eq. (II.2.15) in Part II.

$$\sum_i \left[(\mu - \epsilon_{\ell i}) \frac{\partial n_{\ell i}^\circ}{\partial \Omega} + (\frac{1}{z} v_i^\ell \xi_{\ell i} + h) \cdot \frac{\partial m_{\ell i}^\circ}{\partial \Omega}\right]$$

$$+ \int d\omega \left(-\frac{\partial f(\omega)}{\partial \omega}\right) \omega \frac{\partial N_\ell(\omega)}{\partial \Omega}$$

$$+ \int d\omega f(\omega) \sum_{i\alpha} \frac{\gamma_{\ell i}}{\Omega} \frac{(-)}{\pi} \mathrm{Im}\left[\left\{\omega - (\epsilon_{\ell i} - \mu - (\frac{1}{z} v_i^\ell \xi_{\ell i} + h)\cdot \varpi)\right\} G_i^\ell\right]_{\alpha\alpha} . \qquad \text{(III.2.16)}$$

Therefore, the bulk modulus of the electronic part in the static approximation is

$$3B_e = \sum_{\ell i} \left[-\frac{d}{dV}\left(\Sigma \frac{D}{z}\right)_{\ell i}\right] \langle n_{\ell i}^\circ \rangle_{\xi\eta}$$

$$+ \sum_{\ell i} \left\langle \left[\left(\Sigma \frac{D}{z}\right)_{\ell i} + \left(\frac{D}{t}\right)_\ell (\mu - \epsilon_{\ell i})\right] \left(-\frac{d n_{\ell i}^\circ}{dV}\right) \right\rangle_{\xi\eta}$$

$$+ \sum_\ell \left(\frac{D}{t}\right)_\ell \sum_i \left\langle \left(\frac{1}{z} v_i^\ell \xi_{\ell i} + h\right) \cdot \left(-\frac{d m_{\ell i}^\circ}{dV}\right) \right\rangle_{\xi\eta}$$

$$+\frac{1}{3}\left(\frac{\pi}{\beta}\right)^2\sum_{\ell}\left(\frac{D}{t}\right)_{\ell}\left\langle\left(-\frac{d\rho_{\ell}(0)}{dV}\right)\right\rangle_{\xi\eta}$$

$$+\sum_{\ell i}\left(\frac{D}{t}\right)_{\ell}\frac{\gamma_{\ell i}}{V}\left\langle\int d\omega\, f(\omega)\left(\omega-\epsilon_{\ell i}+\mu\right)\rho_{\ell i}(\omega)\right.$$

$$\left.+\left(\frac{1}{2}v_i^{\ell}\xi_{\ell i}+lh\right)\cdot m_{\ell i}^{\circ}\right\rangle_{\xi\eta}$$

$$-3\beta\Omega\sum_{\ell}\left\langle\Delta P_{\ell}^{\circ}\cdot\Delta P'\right\rangle_{\xi\eta}, \qquad \text{(III.2.17)}$$

where $\int d\omega\left(-\frac{\partial f}{\partial\omega}\right)\omega N_{\ell}(\omega)$ term is approximated by $\frac{1}{3}\left(\frac{\pi}{\beta}\right)^2\rho_{\ell}(0)$. $\rho_1(0)$ is the DOS of the orbital 1 at the Fermi level.

In the saddle point approximation, the following conditions are added.

$$\xi_{\ell i}=m_{\ell i}^{\circ}\quad,\quad \eta_{\ell i}=i\,n_{\ell i}^{\circ}. \qquad \text{(III.2.18)}$$

Substituting this condition into eq.(III.2.17) and neglecting the fluctuation term, we obtain

$$3B_e=\sum_{\ell i}\left[-\frac{d}{dV}\left(\Sigma\frac{D}{z}\right)_{\ell i}\right]\left\langle n_{\ell i}^{\circ}\right\rangle$$

$$+\sum_{\ell i}\left\langle\left[\left(\Sigma\frac{D}{z}\right)_{\ell i}+\left(\frac{D}{t}\right)_{\ell}(\mu-\epsilon_{\ell i})\right]\left(-\frac{dn_{\ell i}^{\circ}}{dV}\right)\right\rangle$$

$$+\sum_{\ell}\frac{1}{4}\left(\frac{D}{t}\right)_{\ell}\sum_{i}\left\langle v_i^{\ell}\left(-\frac{dm_{\ell i}^{\circ 2}}{dV}\right)+4lh\cdot\left(-\frac{dm_{\ell i}^{\circ}}{dV}\right)\right\rangle$$

$$+\frac{1}{3}\left(\frac{\pi}{\beta}\right)^2\sum_{\ell}\left(\frac{D}{t}\right)_{\ell}\left\langle\left(-\frac{d\rho_{\ell}(0)}{dV}\right)\right\rangle$$

$$+\sum_{\ell i}\left(\frac{D}{t}\right)_{\ell}\frac{\gamma_{\ell i}}{V}\Big\langle\int d\omega\, f(\omega)\,(\omega-\epsilon_{\ell i}+\mu)\,\rho_{\ell i}(\omega)$$
$$+\left(\frac{1}{z}\,v_i^{\ell}\,m_{\ell i}^{o\,z}+h\cdot m_{\ell i}^{o}\right)\Big\rangle,$$

(III.2.19)

where $\langle\sim\rangle$ means a classical average for all sets of local minimum points, $\sum_s e^{-\beta E_s}(\sim)/\sum_{s'} e^{-\beta E_{s'}}$. This is an extention of eq.(II.2.15) in Part II to the finite temperature.

We write the expression (III.2.10) in the saddle point approximation in addition.

$$3P_{\ell}V$$
$$=\langle 3P_{\ell}^{o}V\rangle$$
$$=\sum_i\left(\Sigma\frac{D}{z}\right)_{\ell i}\langle n_{\ell i}^{o}\rangle$$
$$+\left(\frac{D}{t}\right)_{\ell}\sum_{i\alpha}\Big\langle\int d\omega\, f(\omega)\,(\omega-\epsilon_{\ell i}+\mu)\,\rho_{\ell i}(\omega)$$
$$+\left(\frac{1}{z}\,v_i^{\ell}\,m_{\ell i}^{o}+h\right)\cdot m_{\ell i}^{o}\Big\rangle$$

(III.2.20)

where we neglected the fluctuation term around the saddle points.

Next, let us derive an approximate expression for the volume change $\delta\Omega_{\mathrm{mag}}$ due to the magnetic pressure. For that purpose, we need to define the nonmagnetic state at an arbitrary

temperature. In the Hartree-Fock approximation, the state is determined by a set of the locally minimum points $\{\xi_{\ell is}, \eta_{\ell is}\}$. We define the 'nonmagnetic state' by the state in which the classical average in the physical quantities $\langle\sim\rangle_{\xi\eta}$ is replaced with $\int d\xi\, d\eta\, \delta(\xi)\, e^{-\beta E}(\sim) \,/\, \int d\xi\, d\eta\, \delta(\xi) e^{-\beta E}$. Then, a classical thermal average $\langle A(\xi\,\eta)\rangle_{\text{nonmag}}$ of any physical quantity $A(\xi\eta)$ in the nonmagnetic state becomes $A(0\ \eta^0)$ where η^0 is the minimum point in the sense of the saddle point approximation. We take the difference between the nonmagnetic state $\{0\ \eta^0_{\ell i}\}$ and the magnetic state $\{\xi_{\ell is}, \eta_{\ell is}\}$. With use of $\delta E_s = -N_s \delta\mu$ and after neglect of the fluctuation of the total number N, we obtain

$$\delta\, 3P_e V = \sum_\ell \langle \delta\, 3P_\ell^\circ V \rangle .$$

$3P_1^0 V$ can be easily obtained with use of eq.(III.2.15). The result is

$$\begin{aligned}\delta\, 3P_\ell^\circ V = {} & \sum_i \left[\left(\Sigma \frac{D}{2}\right)_{\ell i} + \left(\frac{D}{t}\right)_\ell (\mu - \epsilon_{\ell i}) \right] \delta n^\circ_{\ell i} \\ & + \left(\frac{D}{t}\right)_\ell \sum_i \left[\frac{1}{4} v_i^\ell\, \delta(m^{\circ 2}_{\ell i}) + \text{h.} \cdot \delta m^\circ_{\ell i} \right] \\ & + \frac{1}{3} \left(\frac{D}{t}\right)_\ell \left(\frac{\pi}{\beta}\right)^2 \delta\, \rho_\ell(0) \quad . \end{aligned} \tag{III.2.21}$$

Therefore, we obtain an approximate expression for the magnetic pressure $3PV_{\text{mag}}$:

$$[3PV]_{mag} \equiv 3P_eV - [3P_eV]_{nonmag}$$

$$\approx \sum_{\ell i}\left[\left(\Sigma\frac{D}{z}\right)_{\ell i} + \left(\frac{D}{t}\right)_{\ell}(\mu - \epsilon_{\ell i})\right]\delta\langle n^{o}_{\ell i}\rangle$$

$$+\sum_{\ell}\left(\frac{D}{t}\right)_{\ell}\left[\sum_{i}\frac{1}{4}v_i^{\ell}\langle m^{o}_{\ell i}{}^{2}\rangle + \sum_{i} h\cdot\langle m^{o}_{\ell i}\rangle\right]$$

$$+\frac{1}{3}\left(\frac{\pi}{\beta}\right)^{2}\sum_{\ell}\left(\frac{D}{t}\right)_{\ell}\delta\langle P_{\ell}(0)\rangle\ . \qquad \text{(III.2.22)}$$

The volume change due to the magnetic pressure $\delta\Omega_{mag}$ is obtained from the following expression.

$$\frac{\delta\Omega_{mag}}{\Omega} \simeq \frac{[3P\Omega]_{mag}}{3B_0\Omega_0}\ , \qquad \text{(III.2.23)}$$

where B_0 is the bulk modulus in the nonmagnetic state defined by

$$3B_0(\Omega_0,T) \equiv -\frac{\partial}{\partial\Omega}[3P\Omega(\Omega_0,T)]_{nonmag}. \qquad \text{(III.2.24)}$$

Ω_0 is the volume in the nonmagnetic state.

Equation (III.2.22) is also correct in the 'paramagnetic state'. Therefore, we can obtain an approximate spontaneous magnetostriction as follows.

$$\omega_s(T) \sim (3B_0V)^{-1}$$
$$\times\Big[\sum_{\ell i}\Big\{\Big(\Sigma\frac{D}{z}\Big)_{\ell i}+\Big(\frac{D}{t}\Big)_\ell(\mu-\epsilon_{\ell i})\Big\}\delta\langle n^0_{\ell i}\rangle$$
$$+\frac{1}{3}\Big(\frac{\pi}{\beta}\Big)^2\sum_\ell\Big(\frac{D}{t}\Big)_\ell\,\delta\langle\rho_\ell(0)\rangle$$
$$+\frac{1}{4}\sum_{\ell i}\Big(\frac{D}{t}\Big)_\ell v_i^\ell\,\delta\langle m^{0z}_{\ell i}\rangle+\sum_{\ell i}\Big(\frac{D}{t}\Big)_\ell h\cdot\delta\langle m^0_{\ell i}\rangle\Big] \qquad \text{(III.2.25)}$$

where δ means the difference between the real state and the paramagnetic state.

Equation (III.2.22) is an extention of eq.(II .2.13) in Part II to the finite temperature. If we substitute eq. (III.2.22) to eq.(III.2.23) and we neglect the s-d charge transfer effect and the change of the Fermi distribution function, we can obtain the empirical expression[19] at h=0:

$$\frac{\delta\Omega_{mag}}{\Omega_0}\sim\frac{(D/t)_d}{12B_0\Omega_0N}\sum_i v_i\langle m_i^{0z}\rangle. \qquad \text{(III.2.26)}$$

This expression shows that the change of the amplitude of the local magnetic moment is important for the magnetovolume effects.

The forced volume magnetostriction is obtained from the derivative of $3P\Omega(\Omega(T\ h),T,h)=0$ with respect to the magnetic field h.

$$\frac{\partial\omega}{\partial h}\equiv\Omega^{-1}\frac{\partial\Omega}{\partial h}=-\frac{\dfrac{\partial(3P\Omega)}{\partial h}}{3B_H(\Omega\ T\ h)\Omega}. \qquad \text{(III.2.27)}$$

We assume that the field h is applied in the direction of z axis. $B_H(\Omega T)$ is the bulk modulus when the magnetic field h is fixed and it is defined by

$$3B_H(\Omega,T) = -\frac{\partial(3P\Omega(\Omega T h))}{\partial\Omega} \qquad \text{(III.2.28)}$$

$\partial(3P\Omega)/\partial h$ can be obtained easily in the same way as the case of the bulk modulus:

$$\begin{aligned}
&\partial[3P_\ell V(\Omega,T,h)]/\partial h \\
&= \sum_i \left\langle \left\{ \left(\Sigma\frac{D}{z}\right)_{\ell i} + \left(\frac{D}{t}\right)_\ell (\mu - \epsilon_{\ell i}) \right\} \frac{\partial n^\circ_{\ell i}}{\partial h} \right\rangle_{\xi\eta} \\
&+ \left(\frac{D}{t}\right)_\ell \sum_i \left\langle \left(\frac{1}{z} v_i^\ell \cdot \xi_{\ell i} + h\right) \frac{\partial m^\circ_{\ell i}}{\partial h} \right\rangle_{\xi\eta} \\
&+ \beta \left\langle \left(M^\circ_{\ell z} + N^\circ_\ell \frac{\partial\mu}{\partial h} - \left\langle M^\circ_{\ell z} + N^\circ_\ell \frac{\partial\mu}{\partial h} \right\rangle \right) \right. \\
&\qquad \left. \times \left(3P^\circ_\ell V - \langle 3P^\circ_\ell V \rangle \right) \right\rangle_{\xi\eta},
\end{aligned} \qquad \text{(III.2.29)}$$

where M^0_{1z} is the magnetization of one electron state for eq. (III.2.4) in the direction of the z axis.

With use of the saddle point approximation and the neglect of the fluctuation term, we obtain

$$\frac{\partial \omega}{\partial h}$$

$$= (3 B_H V)^{-1} \sum_{\ell} \Big[\sum_i \Big\langle \Big\{ \Big(\Sigma \frac{D}{z} \Big)_{\ell i} + \Big(\frac{D}{t}\Big)_{\ell} (\mu - \epsilon_{\ell i}) \Big\} \frac{\partial n^{o}_{\ell i}}{\partial h} \Big\rangle$$

$$+ \Big(\frac{D}{t}\Big)_{\ell} \frac{1}{3} \Big(\frac{\pi}{\beta}\Big)^2 \Big\langle \frac{\partial \rho_{\ell}(o)}{\partial h} \Big\rangle$$

$$+ \Big(\frac{D}{t}\Big)_{\ell} \sum_i \Big\langle \frac{1}{4} v_i^{\ell} \frac{\partial (m^{o\,2}_{\ell i})}{\partial h} + h \cdot \frac{\partial m^{o}_{\ell i z}}{\partial h} \Big\rangle \Big] .$$

(III.2.30)

The difference between $3B_p\Omega_p$ and $3B_H\Omega$ is about several percent although $B_H(\Omega,T,h)$ contains the anomalous magnetic term. If we neglect these difference and neglect the dependence of the magnetic field in $[3P\Omega]_{para}$, we obtain $\partial\omega/\partial h \approx \partial\omega_s/\partial h$.

In the case that the s-d charge transfer and the change of the Fermi distribution function can be neglected, the forced magnetostriction at h=0 is

$$\frac{\partial \omega}{\partial h} = \frac{(D/t)_d}{3 B_H V} \frac{1}{4} \sum_i v_i \Big\langle \frac{\partial (m^{o\,z}_i)}{\partial h} \Big\rangle . \qquad \text{(III.2.31)}$$

This formula represents an important property of the forced magnetostriction. That is, the forced magnetostriction at 0K is not determined by the spontaneous magnetization and the susceptibility for the spontaneous magnetization, but by the linear combination of the products of the amplitude of the local moment and susceptibility for that amplitude.

Therefore, we can deduce that the anomalously large forced magneto-volume striction, for example, in the Fe-Ni invar[15] alloy at low temperature is caused by the anomalous increase of the amplitude of the local magnetic moment due to magnetic field if s-d charge transfer effect is not important.

The importance of the amplitude of the local magnetic moment also appears in the thermal expansion coefficient α. The electronic contribution of the thermal expansion is given as follows in the H.F. approximation in which the thermal fluctuation term $\beta^2 \langle \Delta(E-T\partial E/\partial T)\cdot \Delta \sum_l 3P_1^0 \Omega \rangle_{\xi\eta}$ is neglected:

$$\alpha_e = \frac{\left[\frac{\partial (3P_e \Omega)}{\partial T}\right]}{3 B_H (\Omega T) \Omega}$$

$$= (3 B_H V)^{-1} \left[\sum_{li} \left\langle \left[(\Sigma \frac{D}{z})_{li} + (\frac{D}{t})_l (\mu - \epsilon_{li}) \right] \frac{\partial n^0_{li}}{\partial T} \right\rangle \right.$$

$$+ \sum_{li} (\frac{D}{t})_l \left\langle \frac{1}{4} v_i^l \frac{\partial}{\partial T} (m^{0\,2}_{li}) + h \frac{\partial m^0_{liz}}{\partial T} \right\rangle$$

$$\left. + \frac{1}{3} (\frac{\pi}{\beta})^2 \sum_l (\frac{D}{t})_l \left\langle \frac{\partial \rho_l(0)}{\partial T} + \frac{N_l}{T} \right\rangle \right.$$

(III.2.32)

If we neglect the s-d charge transfer effect and the change of the Fermi distribution function due to the temperature, we can obtain the empirical expression[18),(19)] at h=0 again:

$$\alpha_e = \frac{(D/t)_d}{3B_H V} \frac{1}{4} \sum_i v_i \left\langle \frac{\partial (m_i^{\circ 2})}{\partial T} \right\rangle . \qquad \text{(III.2.33)}$$

In the actual calculation , we are forced to treat the system as a cluster like system. For example, when we calculate the partial pressure at the i-th site, $\langle 3P_{li}^{0} \Omega \rangle$, we consider a finite cluster whose center is in the site i and substitute the outside with a kind of medium. Then, $\langle 3P_{li}^{0} \Omega \rangle$ is approximated by the thermal average for all saddle points of the cluster. That is,

$$3P_\ell V = \sum_i \frac{\sum_s e^{-\beta E_s^c} [3P_{\ell i}^{\circ} \Omega]}{\sum_{s'} e^{-\beta E_{s'}^c}} , \qquad \text{(III.2.34)}$$

where E_s^c is the energy of the cluster system at a saddle point for one electron Hamiltonian, the type of eq.(III.2.4). Equation (III.2.34) can be also derived directly from the free energy in the single site CPA[22] as shown in Appendix III.

When the s-d charge transfer effect is not important, we can deduce a qualitative behavior for a temperature variation of the spontaneous volume magnetostriction from eq.(III.2.25) and eq.(III.2.34). Equation (III.2.25) shows that the spontaneous volume magnetostriction is qualitatively proportional to the linear combination of squares of the local magnetic moment. According to eq.(III.2.34), the exponential

variation with temperature is expected at high temperature. Therefore, we can expect two types of variations for the temperature above Tc even in the single site CPA. One is the case that there is one state of local magnetic moment above Tc. In this case, we can deduce the temperature variation of the spontaneous volume magnetostriction and γ type thermal expansion coefficient with the change of the magnitude of local magnetic moment as shown in Fig.III.1.9 schematically. Such a behavior is found in αFe[54],[55]. The other is the case that there are many states of the local magnetic moment whose magnitudes are different each other. In this case, it is expected that squares of the local magnetic moment above Tc or the spontaneous magnetostriction decreases exponentially above Tc. This corresponds to the so-called Weiss model[25] in the invar problem. The Weiss model was proposed to explain the invar effects of Fe-Ni alloy for the first time.

Let us examine by means of a simple model whether the spontaneous volume magnetostriction at 0K in $Fe_{66}Ni_{34}$ which amount to 2% can be obtained by the Weiss model or not. We assume that the intraatomic coulomb integral U_i and the coefficient of the s-d charge transfer term do not depend on the type of the atom. then, we obtain the following expression from eq.(III.2.25).

$$\omega_s = \omega_s^M(0) + \omega_s^{sd}(0),$$

$$\omega_s^M(0) \sim 0.017 \left[c_{Fe} W_L \left(m^z_{FeH} - m^z_{FeL} \right) + c_{Ni} \left(m^z_{Ni}|_{0K} - m^z_{Ni}|_{T \gg Tc} \right) \right],$$

$$\omega_s^{sd}(0) \sim 0.74\, \delta N_s ,$$

(III.2.35)

where we neglected the temperature change of the magnitude of the local moment in high spin state. W_L is the rate of the low spin state of Fe to the high spin state at the sufficiently high temperature above Tc, c_{FeL}/c_{FeH}. The coefficient in the above expression is estimated from the parameters listed in Table 1.

In Fig.III.2, we show the $\omega_s^M(0)$ as a function of W_L and $|m_{FeL}|$ assuming $|m_{FeH}|=2.5\,\mu B$, $|m_{Ni}|=0.8\,\mu B$[56],[57] and $|m_{Ni}|_{T \gg Tc}=0.8\,\mu B$ (or $0.0\,\mu B$), and $\omega_s^{sd}(0)$ as a function of δN_s. From this figure, it is seen that $\omega_s(0)$ is roughly equal to the observed value at $|m_{FeL}| \sim 0.5$, $W_L \sim 0.5$ and so Weiss model is a reasonable model.

Of cource, the tail of $\omega_s(T)$ above Tc can be also explained by the SRO effect. However, even in that case, the excitation which changes amplitudes of the local magnetic moment will be important, which is consistent with the rapid decrease of magnetization. It is not difficult that

we examine whether two states exist above Tc or not within the CPA. These studies are in progress together with the calculation of a temperature dependence of $\omega_s(T)$ in αFe.

In the above mentioned discussion, we applied the so-called local saddle point approximation. Such an approximation can be considered to describe the magnetovolume effects in some transition metal alloys containing Fe and Mn at high temperature. If we do not apply the saddle point approximation to the pressure, the physical picture that the magnetovolume effect is characterized by the amplitude of the local moment is not correct any longer.

The effect of the fluctuation may be important for the invar alloys. Indeed, if we perform the static approximation and the CPA calculation fully, we can expect the volume change due to the electronic contribution in the paramagnetic state because of the temperature change of the amplitude of the local moment even if there are not two minimum points for the amplitude of the field ξ.

The preliminary results of the model calculation for αFe are shown in Fig.III.4 and Fig.III.5. The shape of the s DOS is modified to the M-shape DOS since the semi-ellipsoidal DOS tends to overestimate the s-d charge transfer effect as suggested in Part II. w_s is assumed to be equal to 0.70 Ry. The ratio of intraatomic coulomb parameter J to the exchange parameter U is assumed that J/U=2.0. The calculated spontaneous magnetostriction at 0K is 0.0073 and is the same order as the experimentally deduced value. The change of

the Fermi distribution function is not considered at the present stage although it is easy to take account of it. This effect will reduce Tc about by 100K.

The changes of the calculeted $\omega_s(T)$ and $\alpha_M(T)=\partial\omega_s/\partial T$ are surely similar to the behavior shown in Fig.II.2(a). The maximum of $\omega_s(T)$ at 600K is caused by the breakdown of the charge neutrality at low temperature and by the charge transfer from d orbital to s orbital with temperature since the selfconsistent condition as well as the eq.(II.2.1) in Part II is applied in the present calculation and assumed that $U^s=U^{sd}=0$. This maximum can be removed by the large value of J/U and by considering the finite U^s and U^{sd}. $\alpha_M(T\sim Tc)$ is the same order as the observed value[54),(55)].

The temperature variation of $\alpha_M(T)$ is similar to the result calculated by Shimizu on the basis of the phenomenological Stoner theory.[20] However, the mechanism is quite different from that due to the Stoner theory. In the Stoner theory, the spontaneous magnetostriction is caused by the change of the spontaneous magnetization and the Fermi distribution function. In our calculation, it is caused by the s-d charge transfer due to the reversal of the local magnetic moments and by the decrease of the amplitude of the local magnetic moment. Indeed. the approximate expression (III.2.25) reproduces $\omega_s(T)$ qualitatively as shown in Fig.III.5 and it shows that such a picture is appropriate.

The most fatal point that the Stoner theory is inappro-

priate will be that the spontaneous volume magnetostriction of αFe at 0K based on the first principle Stoner-LSD calculation performed by Janak and Williams[10] is more than about ten times the value deduced from the observation. On the other hand, such a contradiction is not present in our scheme.

The results of the more detailed calculation for αFe and of the consideration for the possibility of the existense of the two states in Fe-Ni alloy will be published in future.

Acknowlegement

The author would like to thank Professor H. Miwa for critical reading of the manuscript and for valuable discussions. He is very grateful to Dr. M. Kaburagi for helpful discussions about the virial theorem. The author is also grateful to Dr. N. Hamada for his kind introduction to the method of the calculation for the CPA.

Appendix

Appendix I(†)

In this appendix, we discuss two points. One is the derivation of the Liberman's expression (I.2.1) for any substitutional alloys. Another is the relation between the pressure based on the direct Feynman's theorem and the pressure based on the virial theorem.

Liberman's expression[26] in the original form is as follows.

$$3PV = \sum_i^{occ} \frac{1}{2} \int \left[(\nabla \psi_i^*)(\boldsymbol{r}\cdot\nabla)\psi_i - \psi_i^* \nabla(\boldsymbol{r}\cdot\nabla)\psi_i + c.c. \right] d\boldsymbol{S}$$
$$+ \int n^2(r) \frac{\partial \epsilon_{xc}}{\partial n} \boldsymbol{r}\cdot d\boldsymbol{S}$$
$$+ \sum_\alpha \boldsymbol{r}_\alpha \cdot Z_\alpha \, \mathbb{E}(\boldsymbol{r}_\alpha) \,, \qquad \text{(A.I.1)}$$

where the third term of the r.h.s., which we call the nuclear-part pressure, is the pressure term acting on the nuclei. Z_α and $\mathbb{E}(\boldsymbol{r}_\alpha)$ are respectively the atomic number of the α-th atom and the classical electric field at $\boldsymbol{r}_\alpha$.

Liberman has neglected this nuclear-part pressure with the misunderstanding that the term vanishes because of the inversion symmetry around the nuclear position for the simple

(†) This appendix I is based on the cooperative study with Dr. M. Kaburagi.

crystals. But the crystal is finite, that is, there is the boundary, where the inversion symmetry is not satisfied. Therefore, in this region, the electric field $\mathbb{E}(\mathbb{r}_\alpha)$ has a finite value and the nuclear part pressure caused by this surface effect has a finite contribution to the bulk pressure.

On the other hand, it should be remarked that the first and the second term of the r.h.s. in eq.(A.I.1), which we call as the electronic part, are not invariant under the translational coordinate-transformation. This fact can be understood if we return to the original expression before the transformation to the form of the surface integral. It is given by

$$2\langle T\rangle + \int n(\mathbb{r})\,\epsilon_{xc}\,d\mathbb{r} - \int n(\mathbb{r})\,(\mathbb{r}\cdot\nabla)\,v_c(\mathbb{r})\,d\mathbb{r}, \tag{A.I.2}$$

where $v_c(\mathbb{r})$ is the coulomb potential at $\mathbb{r}$, $\langle T\rangle$ is the total kinetic energy. Noninvarient term is the last one.

In order to derive eq.(I.1.3), we must divide the crystal to many cells and shift the coordinates so that the center of each cell is the origin of the coordinate. As the result, the excessive term occurs in eq.(A.I.2):

$$-\sum_\alpha \mathbb{r}_\alpha \cdot \int_\alpha n(\mathbb{r})\,\mathbb{E}(\mathbb{r})\,d\mathbb{r} \tag{A.I.3}$$

After that, we transform the electronic part of the pressure at each cell to the surface integral, which gives the first term of the r.h.s. in eq.(I.1.1). Equation (A.I.3) is a pressure caused by the electrostatic field acting on the electrons. Adding the third term of the r.h.s. in eq.(A.I.1) to eq.(A.I.3), and using

the principle of actio-reactio, we get the second term of the r.h.s. of eq.(I.1.1). After all,

$$3PV = \sum_{\alpha}\Big[\frac{1}{2}\sum_{i}^{occ}\int_{\alpha}\Big\{\nabla\psi_i^*((\mathbf{r}-\mathbf{r}_\alpha)\cdot\nabla)\psi_i - \psi_i^*\nabla((\mathbf{r}-\mathbf{r}_\alpha)\cdot\nabla)\psi_i + c.c\Big\}d\mathbf{S} + \int_{\alpha} n^2\frac{\partial\epsilon_{xc}}{\partial n}(\mathbf{r}-\mathbf{r}_\alpha)\,d\mathbf{S}\Big] + \sum_{\alpha}\sum_{\beta}{}'(\mathbf{r}_\alpha-\mathbf{r}_\beta)\cdot\int_{\alpha}d\mathbf{r}\,(n(\mathbf{r})-\rho(\mathbf{r}))(-\nabla)\int_{\beta}\frac{n(\mathbf{r}')-\rho(\mathbf{r}')}{|\mathbf{r}-\mathbf{r}'|}d\mathbf{r}'. \tag{A.I.4}$$

Next, we elucidate the interrelation between the pressure based on the direct Feynman's theorem and the pressure based on the virial theorem.

If we regard a solid as a giant molecule and if we express the pressure using the direct Feynman's theorem, it is determined only by the electric field applied to nuclei. On the other hand, according to Liberman's expression, the pressure is expressed by the wave function on the cell surface and its gradient. Therefore, it is very interesting how these quite different expressions relate mutually.

For simplicity, we consider the finite system of a cubic pure crystal whose length is L. We divide it to two parts, a surface system and a bulk system (See Fig.A.1). Then, we apply the virial theorem to the total system, the surface system and the bulk system, respectively.

Let us consider the case of the application of the virial theorem to the total system. Then, the electronic

part pressure P_e defined by the surface integral, the first and second terms of r.h.s. in eq.(A.I.1), vanishes because the electron wave function is zero at infinity. Therefore, the nuclear part of the pressure, P_n defined by the third term of r.h.s. of eq.(A.I.1), becomes the total pressure P;

$$3PV = 3P_nV = Z\sum_\alpha \mathbf{r}_\alpha \cdot \left[\mathbb{E}_{e\alpha}(\mathbf{r}_\alpha) + \sum_\beta{}'(\mathbb{E}_{e\beta}(\mathbf{r}_\alpha) + \mathbb{E}_{n\beta}(\mathbf{r}_\alpha))\right] \quad \text{(A.I.5)}$$

where $\mathbf{r}_\alpha$ is the position of the nucleus at the site α, $\mathbb{E}_{e\beta}(\mathbf{r}_\alpha)$ is the electric field which electrons in the W.S. cell at the site β apply into the nucleus at the site α.

Here, we divide the pressure P_n into two parts, P_n^f and P_n^d.

$$3P_n^f V = Z\sum_\alpha \mathbf{r}_\alpha \left[\mathbb{E}^b_{e\alpha}(\mathbf{r}_\alpha) + \sum_\beta{}'(\mathbb{E}^b_{e\beta}(\mathbf{r}_\alpha) + \mathbb{E}^b_{n\beta}(\mathbf{r}_\alpha))\right], \quad \text{(A.I.6)}$$

$$3P_n^d V = Z\sum_\alpha \mathbf{r}_\alpha \left[\delta\mathbb{E}_{e\alpha}(\mathbf{r}_\alpha) + \sum_\beta{}'(\delta\mathbb{E}_{e\beta}(\mathbf{r}_\alpha) + \delta\mathbb{E}_{n\beta}(\mathbf{r}_\alpha))\right], \quad \text{(A.I.7)}$$

where P_n^f is the pressure when we replace the charge density accompanying all atoms with the bulk one. $\mathbb{E}^b_{e\beta}(\mathbf{r}_\alpha)$ is the electric field which the electron charge density in the cell at the site β replaced with the bulk charge density causes to the point $\mathbf{r}_\alpha$. The index b means that the electric field is caused by the bulk charge density. $\mathbb{E}^b_{n\beta}(\mathbf{r}_\alpha)$ is the electric field at $\mathbf{r}_\alpha$ which the nucleus at the β-th site causes in the same way. $\delta\mathbb{E}_{e\beta}(\mathbf{r}_\alpha)$ is the difference $\mathbb{E}_{e\beta}(\mathbf{r}_\alpha)$-

$\mathbb{E}^{b}_{e\beta}(r_\alpha)$. P^{d}_{n} is the pressure caused by the difference between the real charge density and the bulk charge density. The force due to the surface dipole moment on the surface is contained in the pressure P^{d}_{n}. Field $\mathbb{E}^{b}_{e\alpha}(r_\alpha)$ vanishes because of the inversion symmetry of the charge density. $\mathbb{E}^{b}_{e\beta}(r_\alpha)+\mathbb{E}^{b}_{n\beta}(r_\alpha)$ $(\alpha \neq \beta)$ is not a long range force. For example, in the case of the cubic symmetry, it decreases with the order of $|r_\alpha - r_\beta|^{-6}$. Therefore, the β sum in eq.(A.I.6) can be limited in the region of the $|r_\alpha - r_\beta| < \Lambda$ where Λ is an range of the electric field $\mathbb{E}^{b}_{e\beta}(r_\alpha)+\mathbb{E}^{b}_{n\beta}(r_\alpha)$. Then, in eq.(A.I.6), the contribution from the α sum in the bulk region of the inside of the surface vanishes because of the inversion symmetry at the point r_α. Therefore,

$$3 P^{f}_{n} V = Z \sum_{\alpha}^{s} r_\alpha \cdot \sum_{\beta}{}' \left(\mathbb{E}^{b}_{e\beta}(r_\alpha) + \mathbb{E}^{b}_{n\beta}(r_\alpha) \right), \quad \text{(A.I.8)}$$

where $\sum_{\alpha}^{s}$ means the sum about sites in the surface system of a thickness of Λ. This pressure P^{f}_{n} can be also written as follows.

$$P^{f}_{n} = \rho_s Z \sum_{j} \sum_{\beta}{}' \left(\mathbb{E}^{b}_{e\beta}(r_j) + \mathbb{E}^{b}_{n\beta}(r_j) \right)_z, \quad \text{(A.I.9)}$$

where ρ_s is the number of atoms per unit surface area, the small index z expresses the component of the normal direction to the surface of the cube and r_j is the position of an atom in the j-th surface layer.

In eq.(A.I.7), the α sum over the bulk region can be removed because the electric field caused by the deviation

from the bulk charge density can be expressed by the gradient of the electrostatic potential $\Phi^{d}(\mathbf{r})$ and in the bulk region, it is a constant surface dipole potential $4\pi D$. The other α-sum can be expressed by the sum for the surface layers as well as eq.(A.I.9):

$$P_n^d = \rho_s Z \sum_j \left(\delta E_e(\mathbf{r}_j) + \sum_\beta{}' \delta\left(E_{n\beta}(\mathbf{r}_j)\right)_z \right), \qquad \text{(A.I.10)}$$

where $\delta E_e(\mathbf{r}j)$ is $\sum_\beta \delta E_{e_\beta}(\mathbf{r}_j)$.

Adding eq.(A.I.9) to eq.(A.I.10), we obtain the following expression,

$$P_n = \rho_s Z \sum_j \left(E_e(\mathbf{r}_j) + \sum_\beta{}' E_{n\beta}(\mathbf{r}_j) \right), \qquad \text{(A.I.11)}$$

Above expression merely means that the pressure is given by the force per unit surface area acting on the atoms near the surface.

If we apply the virial theorem to the bulk region, the following expression for the pressure of the bulk region is obtained.

$$P^b = P_e^b + P_n^b, \qquad \text{(A.I.12)}$$

where the electronic part pressure of the bulk system, P_e^b is the first and second term of r.h.s. of eq.(A.I.1) expressed by the surface integral at the boundary with the surface region. P_n^b is the nuclear part pressure expressed by the third term of r.h.s. of eq.(A.I.1).

It can be shown that P_n^b is equal to the P_n^f given by

eq.(A.I.6). Indeed,

$$3P_n^b V_b = \sum_{\alpha}^{B} \mathbf{r}_\alpha \cdot \sum_{\beta}^{B'} \left(\mathbf{E}_{e\beta}^b(\mathbf{r}_\alpha) + \mathbf{E}_{n\beta}^b(\mathbf{r}_\alpha) \right), \quad \text{(A.I.13)}$$

where $\sum_{\alpha}^{B}$ expresses the summation over the bulk region. Here, if we divide the summation $\sum_{\alpha}^{B}$ to the bulk region BB inside the surface by 2Λ and the remaining bulk region BS as shown in Fig.A.1, we can obtain the following expression in the same way that we derived eq.(A.I.8) from eq.(A.I.6).

$$3P_n^b V_b = \sum_{\alpha}^{BS} \mathbf{r}_\alpha \cdot \sum_{\beta}^{B'} \left(\mathbf{E}_{e\beta}^b(\mathbf{r}_\alpha) + \mathbf{E}_{n\beta}^b(\mathbf{r}_\alpha) \right). \quad \text{(A.I.14)}$$

Although the volume of the system considered in eq.(A.I.14) is $(L-2\Lambda)^3$, the pressure P_n^b in eq.(A.I.14) is equal to P_n^f in eq.(A.I.6) in substance because $L \gg \Lambda$.

Last, let us apply the virial theorem to the surface system with a thickness of Λ. Then, the following expression is obtained:

$$3P^s V_s = -3P_e^b V + 3P_n^s V, \quad \text{(A.I.15)}$$

where P^s is the pressure applied to the surface system.

The first term of the r.h.s. is the contribution due to the electronic pressure. In the case of the surface system, there are two different boundaries, a boundary with the bulk system and a boundary at infinity. The electronic contribution at the latter boundary vanishes as in eq.(A.I.5). The contribution at the former boundary is $-3P_e^b V$.

The pressure $3P_n^s V$ is the nuclear part contribution from the surface region and can be shown to be equal to $3P_n^d V$ in the following way. Remark that the α sum over the bulk region in eq.(A.I.7) can be removed. Then, the difference $3P_n^s V - 3P_n^d V$ is

$$-\sum_{\alpha}^{S} \mathbf{r}_\alpha \cdot \sum_{\beta}^{B\prime} \left(\delta E_{e\beta}(\mathbf{r}_\alpha) + \delta E_{n\beta}(\mathbf{r}_\alpha) \right)$$
$$+\sum_{\alpha}^{S} \mathbf{r}_\alpha \cdot \sum_{\beta}^{S} \left(E^b_{e\beta}(\mathbf{r}_\alpha) + E^b_{n\beta}(\mathbf{r}_\alpha) \right) ,$$

The first term vanishes clearly. The second term is, neglecting the effect of the edge in the surface,

$$3V\rho_s \sum_j \sum_{\beta}^{S} \left(E^b_{e\beta}(\mathbf{r}_j) + E^b_{n\beta}(\mathbf{r}_j) \right)_z ,$$

which vanishes.

After all, equation (A.I.15) becomes

$$P_s \frac{V_s}{V} = -P_e^b + P_n^d$$

The l.h.s. is zero because $V_s \ll V$. Therefore,

$$P_n^f = P_n^b \quad \text{and} \quad P_n^d = P_e^b . \tag{A.I.16}$$

According to eqs.(A.I.5), (A.I.12) and (A.I.16),

$$P_n = P^b . \tag{A.I.17}$$

If we neglect the interatomic coulomb term in eq.(A.I.4) and remark eq.(A.I.11), equation (A.I.17) can be written explicitly as the following form.

$$3P\Omega = \frac{1}{2}\int_{WS}\sum_{i}^{occ}\left[\nabla\psi_i^*(\mathbf{r}\cdot\nabla)\psi_i - \psi_i^*\nabla(\mathbf{r}\cdot\nabla)\psi_i + c.c\right]d\mathbf{S}$$

$$+\int_{WS} n^2\frac{\partial\epsilon_{xc}}{\partial n}\,\mathbf{r}\cdot d\mathbf{S}$$

$$= \rho_s Z\sum_{j}\left[E_e(\mathbf{r}_j) + \sum_{\beta}{}'E_{\alpha\beta}(\mathbf{r}_j)\right]. \qquad \text{(A.I.18)}$$

That is, the pressure based on the direct Feynman's theorem surely agrees with the pressure based on the virial theorem as shown in eq.(A.I.17) and it relates with the electric field in the surface layers. The r.h.s. of eq.(A.I.18) was used by Finnis and Heine[58] in order to discuss the surface contraction of Al.

Appendix II

The real pressure of the I type atom at the site α will be defined by

$$(3P^*\Omega)_\alpha = \int_\alpha \sum_i \{\nabla\psi_i^* ((\mathbf{r}-\mathbf{r}_\alpha)\cdot\nabla\psi_i) - \psi_i^* \nabla((\mathbf{r}-\mathbf{r}_\alpha)\cdot\nabla\psi_i) + \text{c.c.} + \tfrac{2}{3}\epsilon_{xc}\cdot(\mathbf{r}-\mathbf{r}_\alpha)\} dS + \sum_\beta{}' (\mathbf{r}_\alpha-\mathbf{r}_\beta)\int_\alpha d\mathbf{r}(n(\mathbf{r})-\rho(\mathbf{r}))(-\nabla)\int_\beta \frac{n(\mathbf{r}')-\rho(\mathbf{r}')}{|\mathbf{r}-\mathbf{r}'|}d\mathbf{r}'$$

$$= \frac{(-)}{2\pi}\int^{EF} \mathrm{Im}\,\mathrm{tr}\,(D^\alpha\cdot G)\,d\epsilon + \sum_\beta{}' \frac{\delta_\alpha\delta_\beta}{|\mathbf{r}_{\alpha\beta}|}. \qquad \text{(A.II.1)}$$

The partial pressure $(3P\Omega)_\alpha$ is defined by eq.(I.1.14). The relation between $(3P^*\Omega)_\alpha$ and $(3P\Omega)_\alpha$ can be derived in the same way as eq.(I.1.9):

$$(3P^*\Omega)_\alpha = (3P\Omega)_\alpha + \sum_\beta{}' \frac{D^\alpha_{\beta\beta}}{z} n_\beta - \left(\sum_\beta{}' \frac{D^\beta_{\alpha\alpha}}{z}\right) n_\alpha. \qquad \text{(A.II.2)}$$

Therefore $(3P\overset{*}{\Omega})_\alpha$ does not agree with $(3P\Omega)_\alpha$ except for the pure metal. Summing up over the site α in eq.(A.II.2), we can obtain the total pressure again:

$$3P\Omega = \frac{1}{N}\sum_\alpha (3P^*\Omega)_\alpha = \frac{1}{N}\sum_\alpha (3P\Omega)_\alpha. \qquad \text{(A.II.3)}$$

Of course, when the system is the completely disordered alloy, eq.(A.II.2) agrees with eq.(I.1.15). Equation (A.II.3) means that the total pressure $3P\Omega$ of an alloy can be interpreted as the average of the partial pressure of each atom which is regarded as embedded in a unit cell of the alloy. For this reason, we can derive the classical formula for the lattice parameter of alloy, (I.2.5), similar to Friedel's one when we replace the partial pressure of the I type of atom

by the pressure of the pure metal of the same type as shown in §2 of Part I.

Appendix III

In this appendix, we verify that eq.(III.2.34) in Part III can be derived directly from the free energy in the CPA.

The free energy per atom, $\tilde{F}_{\lambda\,stat}/N$, can be written in the CPA[22] as follows:

$$\tilde{F}_{\lambda\,stat}/N = \sum_{\ell} \int d\omega f(\omega) \frac{1}{\pi} \mathrm{Im}\Big[\frac{1}{N} \mathrm{tr} \ln (\mathcal{L}_{\lambda\ell}^{-1} - \lambda_\ell t^\ell) + \sum_{\sigma} (\ln F_{\lambda\ell})_{\sigma\sigma} \Big] - \beta^{-1} \sum_{I} c_I \ln \sum_{s} e^{-\beta \tilde{E}_{Is}} , \tag{A.III.1}$$

where $\tilde{E}_{Is}$ is an impurity energy of the I type of atom in the state s:

$$\tilde{E}_{Is}[\xi, \eta, \alpha, \lambda] = \sum_{\ell\sigma} \int d\omega f(\omega) \frac{1}{\pi} \mathrm{Im}\Big[\ln (\mathcal{L}_{\ell Is}^{-1} - \mathcal{L}_{\lambda\ell}^{-1} + F_{\lambda\ell}^{-1}) \Big]_{\sigma\sigma} + \sum_{\ell} \frac{1}{4} (J_I^\ell \eta_{\ell Is}^2 + U_I^\ell \xi_{\ell I}^2) + U_I^{sd} \eta_{Is}^s \eta_{Is}^d \tag{A.III.2}$$

and

$$(F_{\lambda\ell})_{\sigma\sigma'} \equiv \int d\omega' \lambda_\ell^{-1} \rho_{\ell\sigma}(\lambda_\ell^{-1}\omega') (\mathcal{L}_{\lambda\ell}^{-1} - \omega')^{-1}_{\sigma\sigma'} .$$

$\rho_{l0}(\omega')$ is defined by

$$\rho_{\ell\sigma}(\omega) \equiv \frac{(-)}{\pi} \mathrm{Im}\ \mathrm{tr}\, ((\omega - t^\ell)^{-1}) .$$

$\mathcal{L}_l^{-1}$ is the coherent locator of the l-orbital electron. The parameter λ_l is inserted in order to obtain the bond energy soon later. The probability that the I type of atom lies in the state s is given by

$$c_{Is} = c_I \, e^{-\beta E_{Is}} / \left(\sum_{s'} e^{-\beta E_{Is'}} \right). \qquad \text{(A.III.4)}$$

The bond energy of the orbital l per atom is

$$\frac{1}{N} \left\langle \sum_{ij\sigma}{}' t_{ij}^{l} \, a_{li\sigma}^{\dagger} a_{lj\sigma} \right\rangle = \frac{\partial}{\partial \lambda_l} \left(\tilde{F}_{\lambda\, stat} / N \right)_{\lambda = 1}, \qquad \text{(A.III.5)}$$

where $\tilde{F}_{\lambda stat}/N$ is depend on λ_1 in the form of $\tilde{F}_{\lambda stat}[\mathcal{L}_{\lambda}^{-1}, E_{Is}(\xi_{\lambda}, \eta_{\lambda}, \mathcal{L}_{\lambda}^{-1}, \lambda), \lambda]$. The derivative of $\tilde{F}_{\lambda stat}$ through $\mathcal{L}_{\lambda}^{-1}$ with respect to λ_1 vanishes because of the stationary property of $\tilde{F}_{\lambda stat}$ for $\mathcal{L}^{-1}$:

$$\delta \tilde{F}_{stat} / \delta \mathcal{L}^{-1} = 0 . \qquad \text{(A.III.6)}$$

The derivative of $\tilde{F}_{\lambda stat}$ through $\{\xi_{\lambda}, \eta_{\lambda}\}$ with respect to λ_1 also vanishes because of the condition of saddle points:

$$\partial \tilde{E}_{Is} / \partial \xi_{lIs} = 0 , \quad \partial \tilde{E}_{Is} / \partial \eta_{lIs} = 0 . \qquad \text{(A.III.7)}$$

After all, the remained derivative is only the direct one with respect to λ_1 which explicitely appears in $\tilde{F}_{\lambda stat}/N$. Therefore,

$$\begin{aligned} &\frac{1}{N} \left\langle \sum_{ij\sigma}{}' t_{ij}^{l} \, a_{li\sigma}^{\dagger} a_{lj\sigma} \right\rangle \\ &= \int d\omega \, f(\omega) \frac{(-)}{\pi} \, Im \Big[\frac{1}{N} \, tr \left((\mathcal{L}_{l}^{-1} - t^{l})^{-1} t^{l} \right) \\ &\qquad + \sum_{\alpha} \left(F_{l}^{-1} \frac{\partial F_{\lambda l}}{\partial \lambda} \right)_{\alpha\alpha} \\ &\qquad + \sum_{Is\alpha} c_{Is} \left\{ \left(\mathcal{L}_{lIs}^{-1} - \mathcal{L}_{l}^{-1} + F_{l}^{-1} \right) \frac{\partial F_{\lambda l}^{-1}}{\partial \lambda_l} \zeta \right\}_{\alpha\alpha} \Big] . \end{aligned} \qquad \text{(A.III.8)}$$

The second term of r.h.s. of eq.(A.III.8) cancels with the third term of r.h.s. of eq.(A.III.8) because of $F^{-1}_{\lambda 1}/\partial\lambda_1 = -F^{-1}_{\lambda\ell}\frac{\partial F_\ell}{\partial\lambda_\ell}$ $\cdot F^{-1}_{\lambda\ell}$ and the selfconsistent condition of the CPA:

$$\sum_{Is} c_{Is}\left[\mathcal{L}_{\ell Is}^{-1} - \mathcal{L}_\ell^{-1} + F_\ell^{-1}\right]^{-1} = F_\ell . \qquad \text{(A.III.9)}$$

As the result,

$$\begin{aligned}
&\left\langle \frac{1}{N}\sum_{ij}{}' t^\ell_{ij}\, a^\dagger_{\ell i\sigma}\, a_{\ell j\sigma}\right\rangle \\
&= \int d\omega\, f(\omega)\frac{(-)}{\pi}\,\mathrm{Im}\,\frac{1}{N}\,\mathrm{tr}\left(\left(\mathcal{L}_\ell^{-1} - t^\ell\right)^{-1} t^\ell\right) \\
&= \int d\omega\, f(\omega)\frac{(-)}{\pi}\,\mathrm{Im}\,\frac{1}{N}\,\mathrm{tr}\left(\mathcal{L}_\ell^{-1}\left(\mathcal{L}_\ell^{-1} - t^\ell\right)^{-1} - 1\right) \\
&= \int d\omega\, f(\omega)\frac{(-)}{\pi}\,\mathrm{Im}\sum_\sigma\left(\mathcal{L}_\ell^{-1} F_\ell\right)_{\sigma\sigma} .
\end{aligned}$$

$\mathrm{Im}\,\mathcal{L}_1^{-1}F_1$ is rewritten as follows.

$$\begin{aligned}
\mathrm{Im}\,\mathcal{L}_\ell^{-1} F_\ell &= \mathrm{Im}\left[\mathcal{S}_\ell F_\ell\right] \\
&= \sum_{Is} c_{Is}\,\mathrm{Im}\,\mathcal{S}_\ell\left(\mathcal{L}_{\ell Is}^{-1} - \mathcal{S}_\ell\right)^{-1} \\
&= \sum_{Is} c_{Is}\,\mathrm{Im}\left[\mathcal{L}_{\ell Is}^{-1}\left(\mathcal{L}_{\ell Is}^{-1} - \mathcal{S}_\ell\right)^{-1} - 1\right] \\
&= \sum_{Is} c_{Is}\,\mathrm{Im}\left[\left\{\omega - \epsilon_{\ell Is} + \mu - \left(\frac{1}{z}v_I^\ell \mathfrak{F}_{\ell Is} + h\right)\cdot\sigma\right\}\tilde{G}_{\ell Is}\right] ,
\end{aligned}$$

where $\mathcal{S}_1 = (\mathcal{L}_1^{-1} - F_1^{-1})$ and the condition of the CPA, (A.III.9), has been employed. Therefore, the bond energy of the orbital 1 becomes

$$\left\langle \frac{1}{N} \sum_{ij}{}' t_{ij}^{\ell} a_{\ell i\sigma}^{+} a_{\ell j\sigma} \right\rangle$$

$$= \sum_{Is} c_{Is} \left[\int d\omega f(\omega) (\omega - \epsilon_{\ell Is} + \mu) \rho_{\ell Is}(\omega) \right.$$

$$\left. - \frac{1}{2} (v_I^{\ell} m_{\ell Is}^{\circ z} + h.m_{\ell Is}^{\circ}) \right].$$

(A.III.10)

After all, we can obtain eq.(III.2.34):

$$3\tilde{P}_{\ell} \Omega = \sum_{Is} c_{Is} ({}^3P_{\ell}^{\circ} \Omega)_{Is}$$

$$({}^3P_{\ell}^{\circ} \Omega)_{Is} = \left(\Sigma \frac{D}{z} \right)_{\ell I} n_{\ell Is}^{\circ}$$

$$+ \left(\frac{D}{t}\right)_{\ell} \left[\int d\omega f(\omega) (\omega - \epsilon_{\ell Is} + \mu) \rho_{\ell Is}(\omega) \right.$$

$$\left. - \left(\frac{1}{2} v_I^{\ell} m_{\ell Is}^{\circ z} + h.m_{\ell Is}^{\circ}\right) \right].$$

Refferences

1) V.L. Moruzzi, A.R. Williams and J.F. Janak: Phys. Rev. B15 (1977) 2854.

2) D.G. Pettifor: Commun. Phys. 1 (1976) 141.

3) D.G. Pettifor: J. Phys. F8 (1978) 219.

4) C.D. Gelatt, H. Ehrenreich and R.E. Watson: Phys. Rev. B15 (1977) 1613.

5) L. Johannes, R. Haydock and V. Heine: Phys. Rev. Letters 36 (1976) 372.

6) F. Gautier, J. van der Rest and F. Brouers: J. Phys. F5 (1975) 1884.

7) M. Cyrot and F. Cyrot-Lackmann: J. Phys. F6 (1976) 2257.

8) J. Friedel: Phil. Mag. Ser(7)46 (1955) 514.

9) T.M. Hattox, J.B. Conklin, J.C. Slater and S.B. Trickey: J. Phys. Chem. Solids 34 (1973) 1627.

10) J.F. Janak and A.R. Williams: Phys. Rev. B14 (1976) 4199.

11) O.K. Andersen, J. Madsen, U.K. Poulsen, O. Jepsen and J. Kollar: Physica 86-88B (1977) 249.

12) D.G. Glötzel: J. Phys. F8 (1978) L163.

13) J.F. Janak: Solid State Commun. 25 (1978) 53.

14) D.M. Roy and D.G.Pettifor: J. Phys. F7 (1977) L183.

15) For example, see J. Magn and Magn Materials 10 (1979).

16) C.W.F.T. Pistorius: Prog. Solid State Chem. 11 (1976) 112.

17) T. Jo: to be published.

18) M. Shiga: Solid State Commun. 10 (1972) 1233.

19) W.F. Schlosser: J. Magn and Magn Materials 1 (1976) 106, 293.

20) M. Shimizu: J. Phys. Soc. Japan 45 (1978) 1520.

21) J. van der Rest, F. Gautier and F. Brours: J. Phys. F5 (1975) 2283.

22) H. Hasegawa: J. Phys. Soc. Japan 46 (1979) 1504.

23) D.E. Eastman, F.J. Himpsel and J.A. Knapp: Phys. Rev. Letters 40 (1978) 1514.

24) Y. Teraoka and J. Kanamori: J. Magn and Magn Materials 10 (1979) 217.

25) R.J. Weiss: Proc. Phys. Soc. 82 (1963) 281.

26) D.A. Liberman: Phys. Rev. B3 (1971) 2081.

27) J.D. Weeks and P.W. Anderson and A.G.H. Devidson: J. Chem. Phys. 58 (1973) 1388.

28) T.B. Grimley: J. Phys. C3 (1970) 1934.

29) D.G. Pettifor: J. Phys F7 (1977) 613.

30) H. Shiba: Prog. theor. Phys. 46 (1971) 77.

31) N.D. Lang and H. Ehrenreich: Phys. Rev. 168 (1968) 605.

32) K.A. Gschneidner: Solid State Phys. 16 (1964) 276.

33) E. Walker and M. Peter: J. appl. Phys. 48 (1977) 2820.

34) W.B. Peason: A Handbook of Lattice Spacings and Structures of Metals and Alloys. vol 1,2 (Pergamon, New York, 1967).

35) F.A. Shunk: Constitution of Binary Alloys 2nd Suppl. (Mc-Graw Hill Comp., New York, 1969).

36) A.R. Miedema: J. Less-Common Metals 32 (1973) 117.

37) U.K. Poulsen, J. Kollar and O.K. Andersen: J. Phys. F6 (1976) L241.

38) R. Hultgren, P.D. Desai, D.T. Hawkins, M. Gleiser and K.K. Kelley: Selected Values of the Thermodynamic Properties of Binary Alloys. (Am. Soc. Metals, 1973).

39) S. Asano and J. Yamashita: J. Phys. Soc. Japan 31 (1971) 1000.

40) O.K. Andersen and O. Jepsen: Physica 91B (1977) 317.

41) A. Sawaoka, T. Soma, S. Saito and Y. Endoh: Phys. Stat. Sol (b)47 (1971) K99.

42) G. Oomi and N. Mori: J. Magn and Magn Materials 10 (1979) 170.

43) E.C. Snow and J.T. Weber: Acta Metallurgica 17 (1969) 623.

44) R.M. Niemienen and C.H. Hodge: J. Phys. F6 (1976) 573.

45) F. Herman and S. Skillman: Atomic Structure Calculations (New Jersey Prentice Hall).

46) H. Akai, J. Kanamori, N. Hamada and H. Miwa: Physica 91B (1977) 153.

47) J.W.D. Connolly: Phys. Rev. 159 (1967) 415.

48) L.L. Boyer, D.A. Papaconstantopoulos and B.M. Klein: Phys. Rev. B15 (1977) 3685.

49) D. Papantonis and W.A. Bassett: J. appl. Phys. 48 (1977) 3374.

50) Y. Nakamura, K. Sumiyama and M. Shiga: J. Magn and Magn Materials 12 (1979) 217.

51) W.E. Evanson, J. R. Schrieffer and S.Q. Wang: J. appl. Phys. 41 (1970) 1199.

52) J.C. Slater, J.B. Mann, T.M. Wilson and J.H. Wood: Phys. Rev. 184 (1969) 672.

53) J. Hubbard: Phys. Rev. B19 (1979) 2626.

54) F. Richter and U. Lotter: Phys. Status solidi 34 (1969) K149.

55) R. Kohlhaas, P.H. Dunner and N. Schmitz-Prangle: Z. angew. Phys. 23 (1967) 245.

56) G.G.E. Low and M.F. Collins: J. appl. Phys. 34 (1963) 1195.

57) Y. Ito, J. Akimitsu, M. Matsui and S. Chikazumi: J. Magn and Magn Materials 10 (1979) 194.

58) M.W. Finnis and V. Heine: J. Phys. F4 (1974) L37.

59) K.H. Hallwedge: Landolt-Börnstein vol 11, group III (Springer-Verlag, Berlin-Heidelberg, 1979).

Table and Figure

Table caption

The parameters used in this calculation. The symbol A shows the element. S, structure assumed in the pure metal. f is the f.c.c. and b is the b.c.c.. R, equilibrium cell radius in a.u.. W_d, d band width in Ry. w_s, a half of the s band width in the ellipsoidal model DOS in Ry. $Z_{W.S}$, the effective charge for the potential. r_A, atomic core radius in a.u.. ϵ_d^a, atomic level[52] in Ry. Q, a factor with respect to the volume dependence of the center of gravity of the d band. ξ and η, fitting factors. U_0 and γU_0, exchange parameters in Ry. See ref.29 for the meaning of each parameter.

Fig.I.1.

The model density of states (DOS) and the volume dependence of the DOS for $Nb_{50}Zr_{50}$. The energy zero is the d level of the pure Nb at equilibrium volume (R= 3.071 a.u.). R is the average atomic radius. EF is the Fermi energy.

Fig.I.2.

The calculated pressure-volume relations of Nb-Zr alloy for various concentrations C . R is the cell radius.

Fig.I.3.

(a) The concentration dependence of the equilibrium cell radius (R) in Nb-Zr. The solid curves are observed values[33]. The dot-dash curve is the calculated value. The dashed curve is calculated from eq.(I.2.2).

(b) The bulk modulus of Nb-Zr. The solid curves are observed values [33], the chained curve is the calculated value, and the dashed curve is the bulk modulus of the solution of two phases.

Fig.I.4.

The partial pressures relative to the separated phase at the volume Ω_v of Vegard's law.

(a) The d (chained curve) and s (dashed curve) relative partial pressures. The solid curve is the total relative pressure.

(b) Various contributions to the relative partial pressures. dbNb (dbZr) is the relative partial pressure

due to the d bond energy at the Nb (Zr) site. db tot is equal to dbNb+dbZr. d core Zr (Nb) is the relative partial pressure of the core part at the Zr(Nb) site. sZr(Nb) is the s part of the relative pressure at the Zr (Nb) site.

Fig.I.5.

The model DOS (dashed curve) at the equilibrium cell radius of pure Pd (R=2.8726 a.u.) and the impurity-site partial DOS (solid curves) of Pd-base 4d transition metal alloys at the same volume. Concentration is c=0.1. The atomic d levels relative to the Pd are as follows: 0.1923 Ry for Zr, 0.1265 Ry for Nb, 0.0905 Ry for Mo, 0.0676 Ry for Tc, 0.0438 Ry for Ru, 0.0232 Ry for Rh and -0.1181 Ry for Ag.

Fig I.6.

(a) The deviation from Vegard's law of Pd-base 4d alloy. The solid curve shows the calculated values. Open circles are observed values[34]. Different values are reported in Rh-Pd and Ru-Pd alloys. The dashed curve is the result of Friedel's theory[8].

(b) The relative s and d partial pressures at the volume $\Omega_V=0.1\cdot\Omega_A+0.9\cdot\Omega_{Pd}$.

(c) The various contributions of s-part relative partial pressures. The dashed curves is the pressure at the impurity site, the chained curve is the partial pressure at Pd site. The solid curve is the total

relative pressure of the s part.

(d) The various contributions of the relative partial pressures of the d part. dbTot=dbondA+dbondPd, dcoreTot =dcoreA+dcorePd and dTot=dbondTot+dcoreTot. The total relative pressure $\delta(3P\Omega)$ is given by dTot+sTot.

Fig.I.7.

The partial DOS(dashed curve) of Pd in $Pd_{80}Nb_{20}$ alloy. The solid curve is that of pure Pd. The energy zero is the d level of the Pd site. The Fermi energy is EF= 0.158 Ry at c=0.0, EF=0.166 Ry at c=0.2.

Fig.I.8.

The calculated bulk moduli (solid curve for c=0.1, chained curve for c=0.2). $\Delta B/c=(B(alloy)-B(Pd))/c$. The dashed curve is B(A)-B(Pd).

Fig.I.9.

The calculated formation energies (ΔH) of Pd-base alloys. The dashed curve is the s part, the chained curve is the d part and the solid curve is the total bond energy contribution.

Fig.II.1.

The model DOS and the calculated DOS of γMn with use of the CPA. The chained curve shows the model DOS. The solid curve, the DOS of γMn. The broken curve, up and down local DOS.

Fig.II.2.

The P-V relation and the volume dependence of the local magnetic moment of γMn. O : the calculated values. The broken curve shows the result in the nonmagnetic state.

Fig.II.3.

The magnetic pressure (the solid curve) of γMn and the approximate value due to the first term of r.h.s. in eq. (II.1.13) (the dotted curve)

Fig.II.4.

The DOS of Cu-Mn at the cell radius R=2.73377 a.u.. C shows the Mn concentration. The solid curve is the DOS in the magnetic state, the broken curve is the DOS in the nonmagnetic state. The vertical lines show the Fermi levels.

Fig.II.5.

The concentration dependence of Mn magnetic moment (the solid curves) and Mn d-electron number (the broken curve) of Cu-Mn alloy. Symbol I means the magnetic moment calculated with use of eq.(II.1.10). II, the magnetic moment calculated with use of eq.(II.2.1).

Fig.II.6.

(a) The concentration dependence of the cell radius of Cu-Mn. OXD show the observed values[34]. The solid curve I is the result with use of eq.(II.1.10). The chained curve II is the result calculated from eq.(II.2.1). The solid curve P is the result for the nonmagnetic state.

(b) The concentration dependence of the bulk modulus of Cu-Mn alloy. The solid curve is the bulk modulus in the magnetic state. The chained curve, in the nonmagnetic state.

(c) The formation energy ΔH of Cu-Mn. The solid curve is the ΔH calculated in the magnetic state. The chained curve is the ΔH calculated in the nonmagnetic state. The dotted curve is the ΔH in the nonmagnetic state, which is evaluated at the volume of Vegard's law in the magnetic state. O : the experimental values[38].

Fig.II.7.

(a) The relative pressures of Cu-Mn. - - - -, s part. —·—, d part. ———, the total relative pressure. The arrows show the behavior of the relative s and d pressure when the volume moves from the volume of Vegard's law to the equilibrium position.

(b) The relative pressures of Cu-Mn. —·—, the magnetic contribution. —··—, nonmagnetic contribution. ———, the total contribution. — — —, the total

relative pressure evaluated from eq.(II.1.13). ·····, the total relative pressure from the first term of r.h.s. of eq.(II.1.13).

(c) Various contributions of relative pressures of the d part. ·····, the d-core part at the Cu site. - - - -, the nonmagnetic component of the d-core part of Mn. —·—, the magnetic component of the d-core part of Mn (i.e. $\left[-U_I m_I^2/\mu_{dI}\right]_{Mn}$). —··—, the bonding parts of Cu (dbCu) and Mn (dbMn). ———, the total d-part.

(d) The relative pressures of Cu-Mn in the nonmagnetic state. - - - - , s part. —·—, d part. ———, the total relative pressure.

Fig.II.8.

The relative bulk modulus of Cu-Mn, $\tilde{B}-\sum_I c_I B_I$ where B_I is the bulk modulus of the pure metal I. ·····, the core part (the first term of r.h.s. in eq.(II.1.15)). - - - - -, the bonding term (the fourth term of r.h.s. in eq.(II.1.15)). —·—, the s-d part (the second term of r.h.s. in eq.(II.1.15)). —··—, the magnetic moment term (the third term of r.h.s. in eq.(II.1.15)). ———, the total relative bulk modulus.

Fig.II.9.

The model DOS used in the calculation of the electronic structures of αFe-base and Ni-base 3d alloys (the solid curve). The chained curve is the modified model DOS[48] used in αFe-V alloys. W_d is the d band width.

Fig.II.10.

(a) The assumed atomic radii R (the solid curve) and the calculated atomic radii in the nonmagnetic state

(the dotted curve) of the pure 3d metals.

(b) The s part pressures $3P_s\Omega$ of pure 3d metals at each equilibrium volume. The dotted curve shows the case of the nonmagnetic state.

(c) Each component of the bulk modulus in 3d metals. -----, the core part due to the s electron. ·····, the core part due to the d electron. —···—, the bonding part due to the s electron. —··—, the bonding part due to the d electron. —·—, s-d charge transfer term due to the volume derivative. — — —, the magnetic moment term. ———, real bulk modulus[31].

Fig.II.11.

(a) The magnetic moments of the αFe base 3d alloys. The concentration is c=0.1. ———, the impurity-site magnetic moment. —·—, the host magnetic moment. ----, the averaged moment. In αFe-Mn, the antiparallel Mn moment configuration in the ferromagnetic phase is assumed. The parallel Mn moment in the ferromagnetic phase is also shown.

(b) The magnetic moments of the Ni base 3d alloys at c=0.1.

Fig.II.12.

(a) The formation energy per atom of the αFe base 3d transition metal alloys at c=0.1. The solid curve shows the result which is calculated for the magnetic state with use of λ=1.5. The chained curve is the result of the

magnetic case of λ=1.0. The dotted curve is the non-magnetic case. O : the experimental values[38].

(b) The formation energy of the Ni base 3d alloys at c=0.1.

Fig.II.13.

(a) The deviation of the volume Ω in αFe-base 3d alloys from Vegard's law Ω_V at c=0.1. Ω_B is the volume of the host pure metal. In αFe-V, ● shows the result of $U_0(V)$ =0.02 Ry, $\gamma U_0(V)$=0.1. ◎ shows the result calculated with use of the modified model band. In αFe-Mn, A.P shows the antiparallel Mn moment configuration in the ferromagnetic phase. F.P, the parallel Mn moment configuration in the ferromagnetic phase. A.F, the case of the disordered antiferromagnetic state. × : observed values.[34]

(b) The deviation of the volume in the Ni base 3d alloys from Vegard's law at c=0.1.

Fig.II.14.

(a) The change of the bulk modulus in the αFe base 3d alloys at c=0.1. $B=(\tilde{B}-B_B)/c$ where $\tilde{B}$ is the bulk modulus of alloy and B_B is the host one. ——— , the magnetic case. —·—, the nonmagnetic case. ·····, the additive law B_A-B_B. O : the experimental value[49], [59]. The vertical line is the error bar.

(b) The change of the bulk modulus in the Ni base 3d alloys at c=0.1.

Fig.II.15.

(a) The relative d (the chained curve) and s (the broken curve) part pressures of αFe-base 3d alloys. The solid curve shows the total relative pressure.
(b) The relative pressure of the magnetic part (the broken curve) and the relative pressure of the nonmagnetic part (the chained curve) in αFe-base 3d alloys. In αFe-V, the result which is calculated with the modified model DOS is also given. These contributions are all lower values. In αFe-Mn, the result of the antiparallel Mn magnetic moment configuration in the ferromagnetic alloy is shown. The solid curve is the total relative pressure. The dotted curve is the relative magnetic pressure evaluated from the first term of r.h.s. in eq.(II.1.13).
(c) The relative s and d part pressures of Ni-base 3d alloys.
(d) The magnetic and nonmagnetic part of the relative pressures in the Ni base 3d alloys.

Fig.II.16.

The s part (the broken curve) and the d part (the chained curve) of the relative pressures in the nonmagnetic Ni-base 3d alloys. The solid curve is the total relative pressure.

Fig.II.17.

The relative bulk modulus $\tilde{B}-\sum_{I} c_I B_I$ in 3d alloys where B_I is the bulk modulus of the pure metal I, and $c_{Fe}=0.9$.

Symbol rg shows the contribution from the rigid part which is the first term plus the fourth term of r.h.s. of eq.(II.1.16). sd shows the contribution from the s-d charge transfer term due to the volume variation (the second term of r.h.s. of eq.(II.1.16). m shows the contribution from the local magnetic moment term (the third term of r.h.s. of eq.(II.1.16).).

Fig.III.1.

(a) The schematic temperature variation of the spontaneous volume magnetostriction $\omega_s(T)$ when there is only one state for the amplitude of the local magnetic moment ($\langle m^2 \rangle$) at $T > T_c$.

(b) The schematic variation of the magnetic thermal expansion coefficient $\alpha_M(T)$ in the case of the one state.

Fig.III.2.

(a) The schematic variation of $\omega_s(T)$ when there are two states for the amplitude of the local magnetic moment.

(b) The schematic variation of $\alpha_M(T)$ in the two states model.

Fig.III.3.

The spontaneous volume magnetostriction $\omega_s(0K)$ of $Fe_{66}Ni_{34}$ calculated from an approximate expression (III.2.35) as the function of the low spin state (M_{FeL}) and the s-d charge transfer (δN_s). W_L denotes the ratio c_{FeL}/c_{Fe} where c_{FeL} is the concentration of the low spin state of Fe and c_{Fe} is the concentration of Fe. It is assumed that the magnitude of the local magnetic moment of Ni above Tc ($m_{Ni}|_{T \gg Tc}$) is zero. The dashed line shows the observed value.[15] The dot-dash-line shows the value when we assume $m_{Ni}|_{T \gg Tc} = 0.8 \mu B$ and $W_L = 1.0$.

Fig.III.4.

The temperature variation of the magnetization M of αFe and the magnitude of the local magnetic moment $\sqrt{\langle m^2 \rangle}$ in the CPA calculation. The inset shows the s and d model DOS used in this calculation. The Curie temperature is 1530K.

Fig.III.5.

The temperature variation of the spontaneous volume magnetostriction $\omega_s(T)$ and the magnetic part of the thermal expansion coefficient $\alpha_M(T)$ in αFe. The change of the Fermi distribution function is not taken into account. The ω_s^d denoted by a dot-dash-line is the d electron contribution to ω_s. The dotted curve shows an approximate spontaneous volume magnetostriction calculated from eq.(III.2.25).

Fig.A.1.

The surface system (S) and the bulk system (B) in a finite system whose size is L. Λ is the range of the electric field in the bulk system . The bulk system is further divided into the inner region(BB) and other region (BS) by considering the rage Λ. The boundary is shown by the dashed line.

Table 1

A	Ti	V	Cr	Mn	Fe	Co	Ni	Cu
S	f	b	b	f	b	f	f	f
R	3.0765	2.8286	2.6833	2.7338	2.6671	2.6129	2.6024	2.6696
W_d	0.450	0.450	0.486	0.415	0.357	0.322	0.300	0.260
w_s	0.550	0.550	0.600	0.650	0.650	0.650	0.650	0.625
$Z_{W.S}$	0.8750	0.9581	0.9662	0.9626	0.9406	0.9086	0.9020	0.8897
r_A	2.3105	2.1841	2.1019	1.9741	1.8850	1.8045	1.7313	1.6828
$-\epsilon_d^a$	0.2013	0.2504	0.2938	0.3372	0.3769	0.4149	0.4516	0.4871
Q	29.253	20.512	24.212	28.387	28.307	29.409	29.770	41.407
$(D/t)_d$	3.2017	3.2133	3.2657	3.3743	3.5535	3.7606	3.9821	4.1962
$(D/t)_s$	3.1435	3.3782	3.3534	3.3466	3.2708	3.2484	3.2096	3.1150
ξ	1.6077	1.1299	1.5751	1.0594	1.2367	1.2226	1.2361	0.8586
η	1.7214	0.6188	2.4603	1.2113	1.5580	1.5008	1.3891	1.2063
U_0	0.03694	0.03694	0.03694	0.3277	0.1945	0.1606	0.3035	0.0
γU_0	0.1029	0.1029	0.1029	2.0000	0.9403	0.5391	1.0489	0.0

Table 1

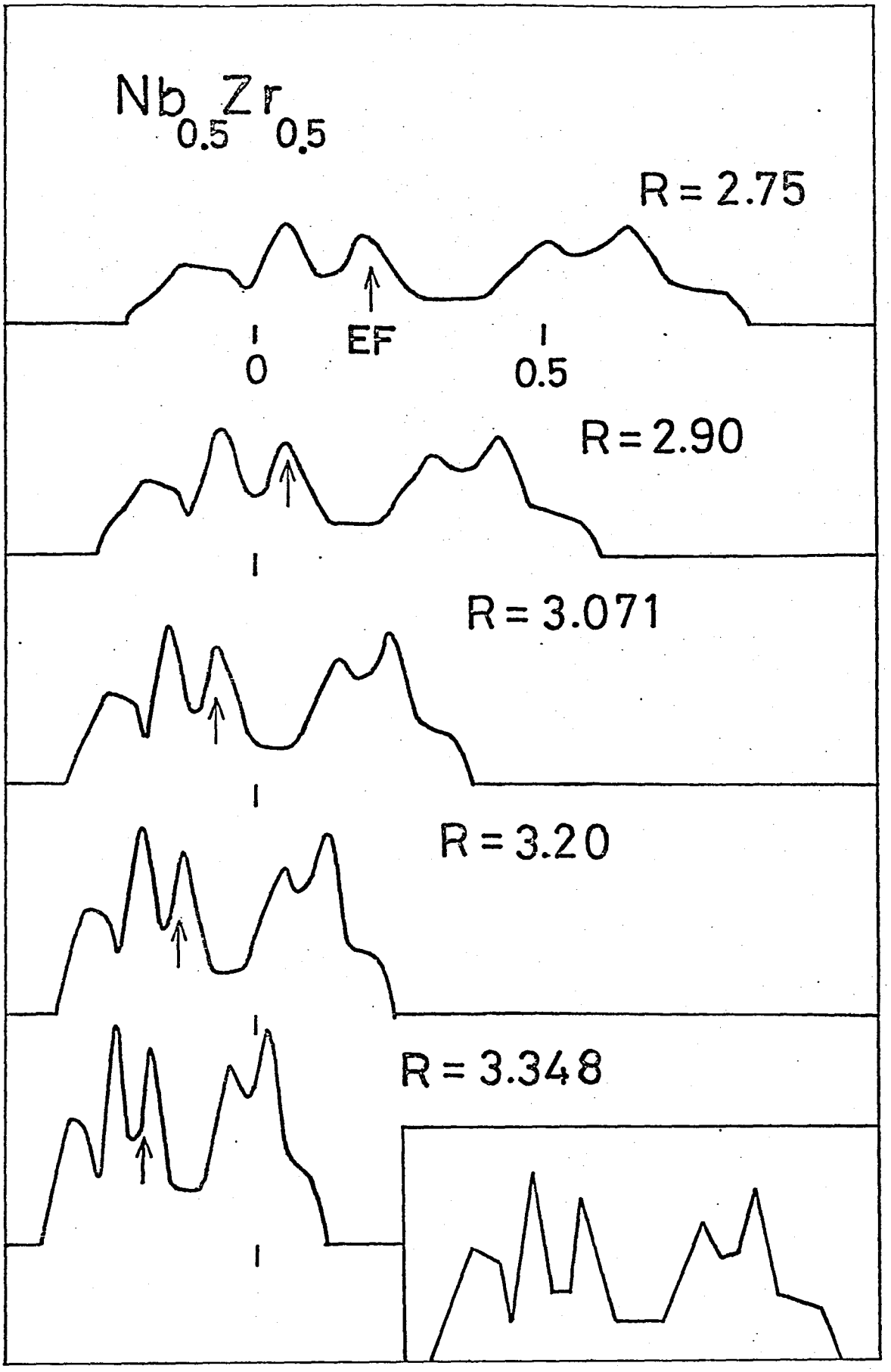

Fig.I.1

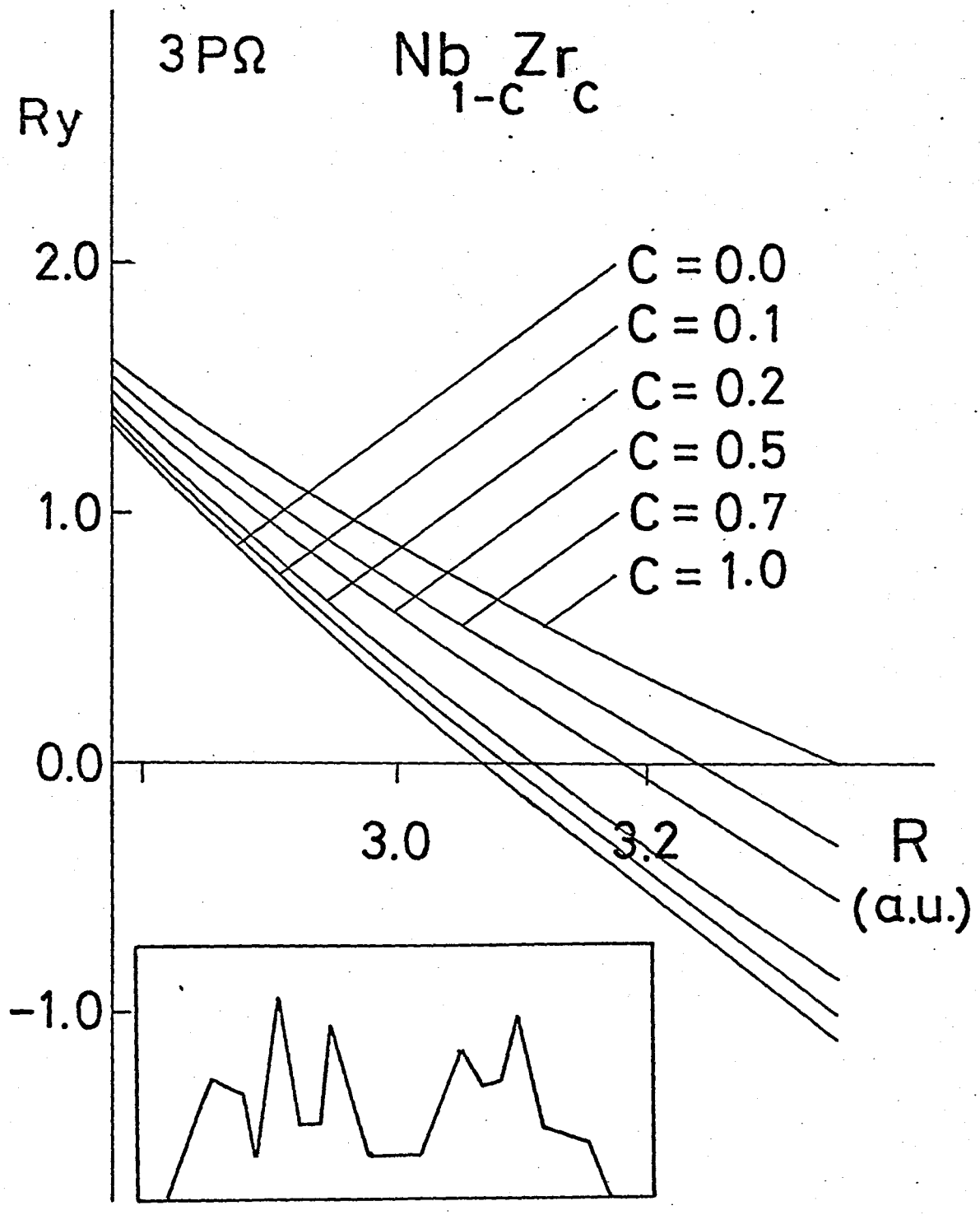

Fig.I.2

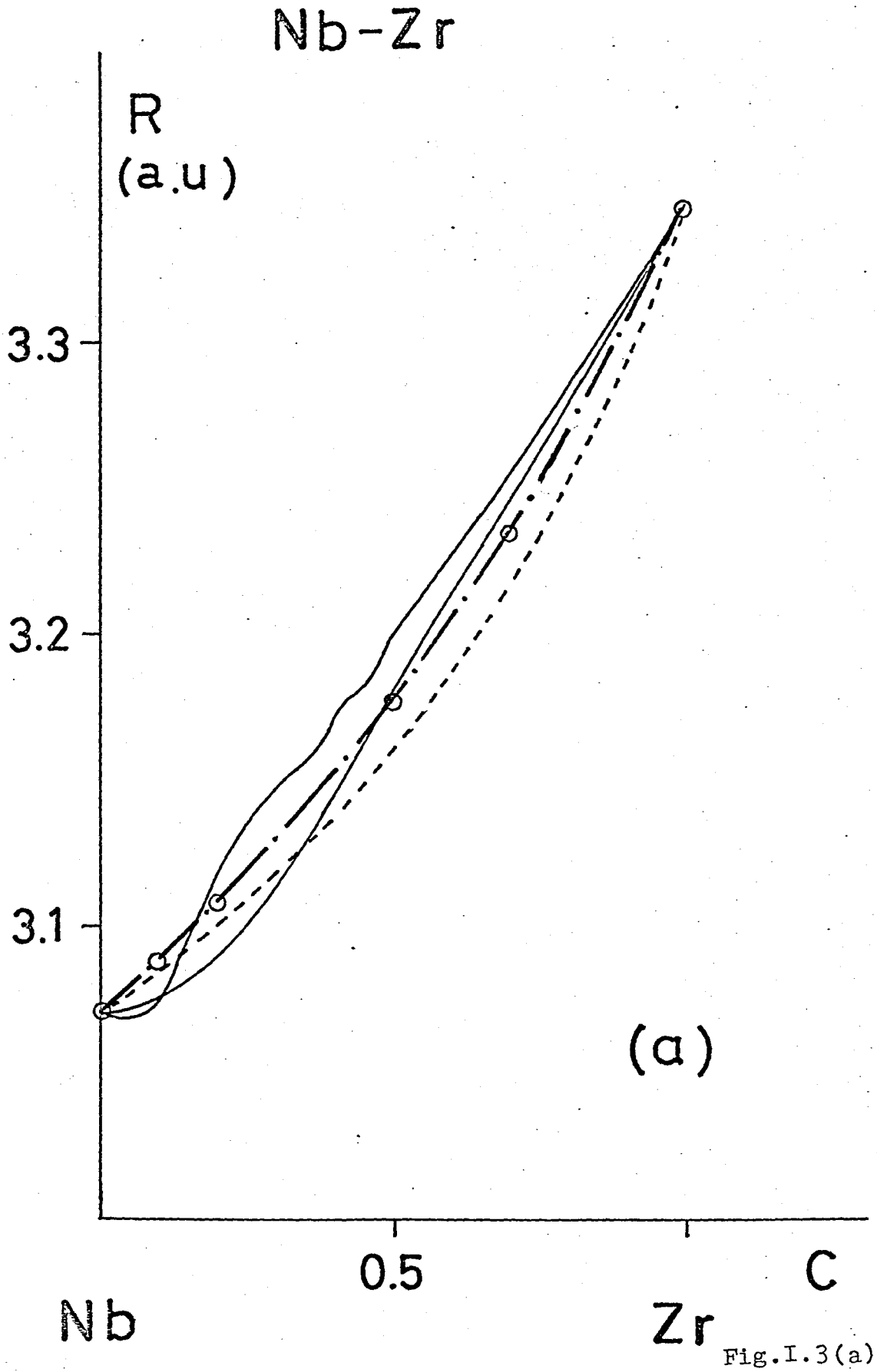

Fig.I.3(a)

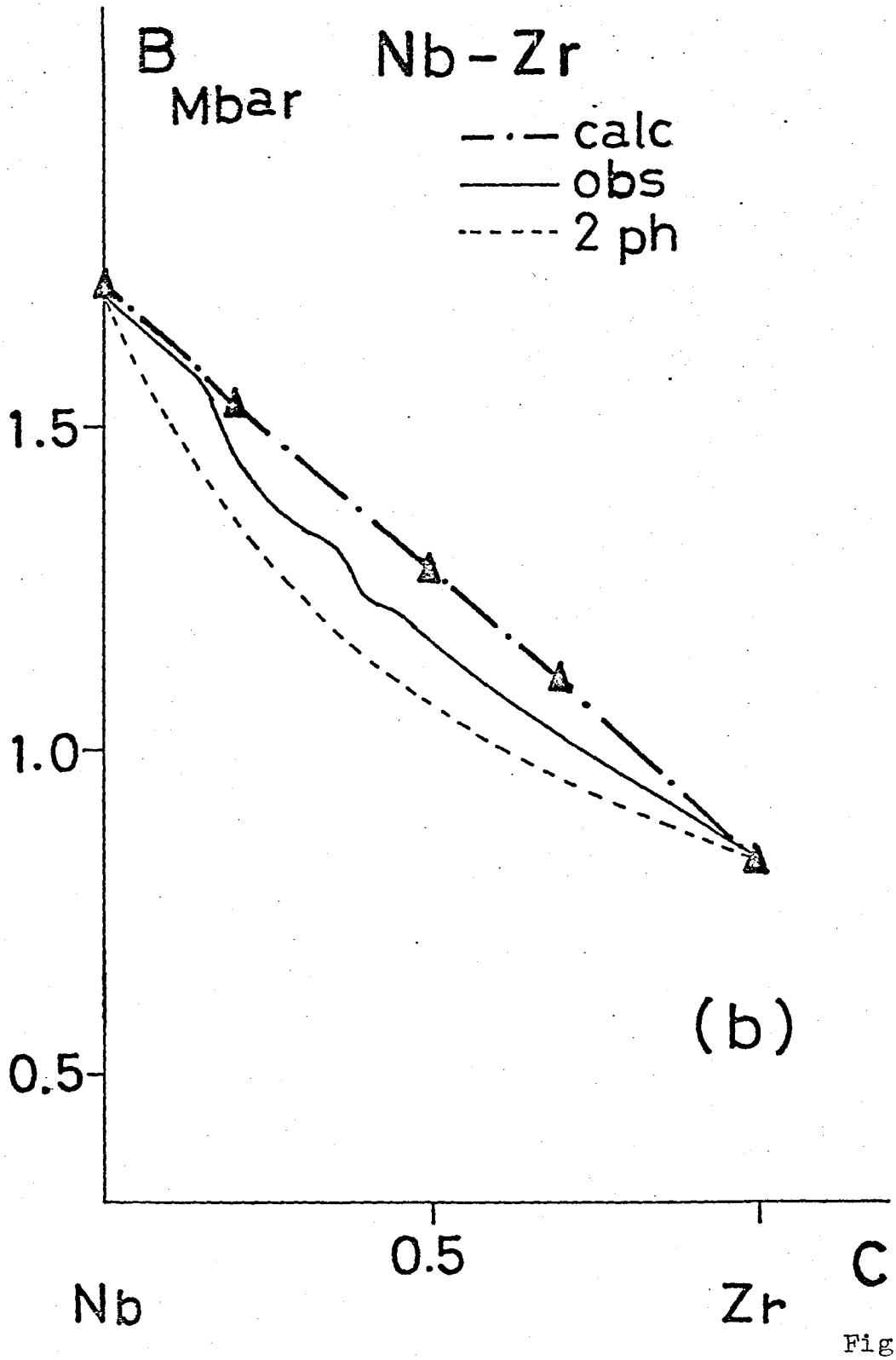

Fig. I.3 (b)

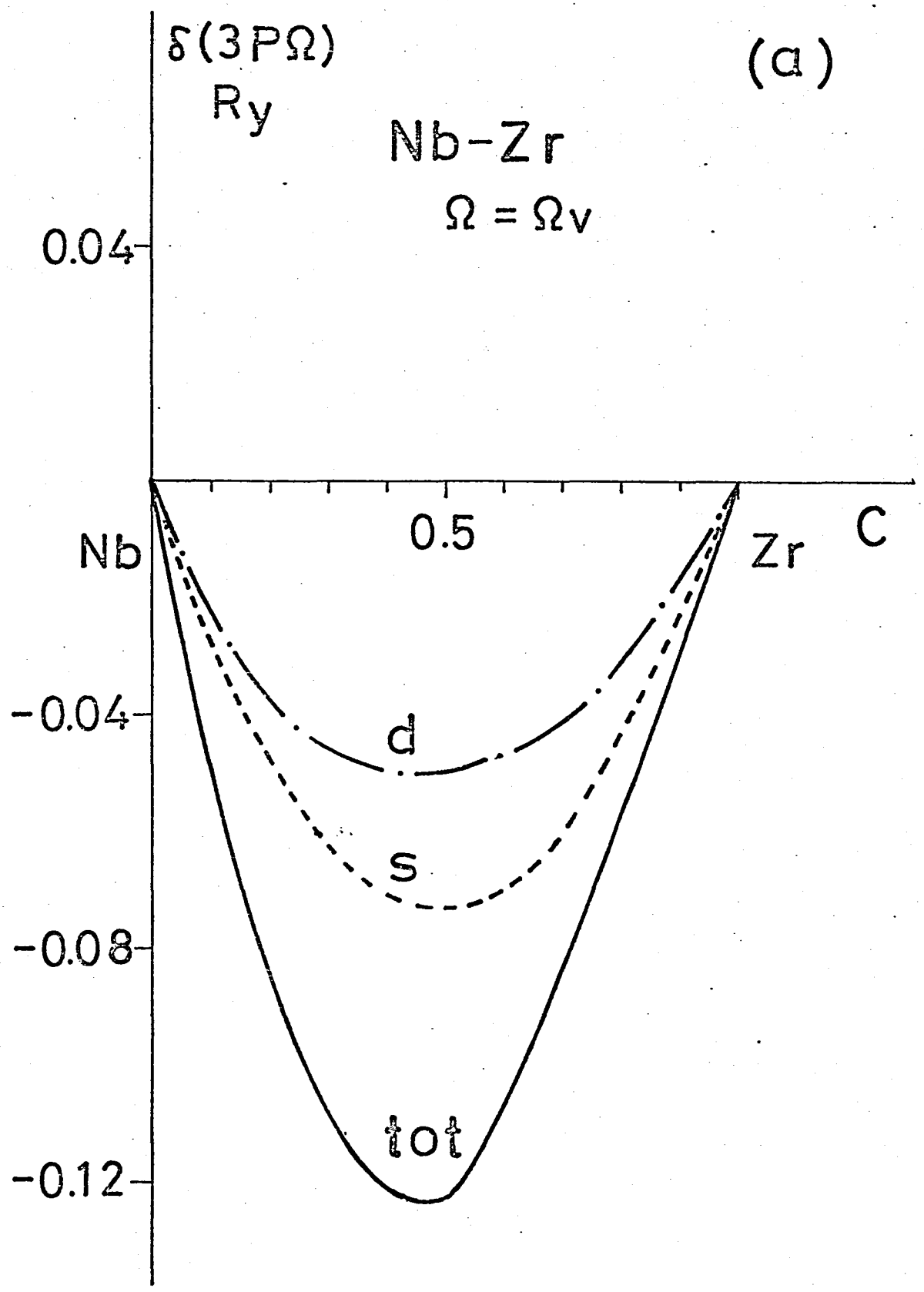

Fig.I.4(a)

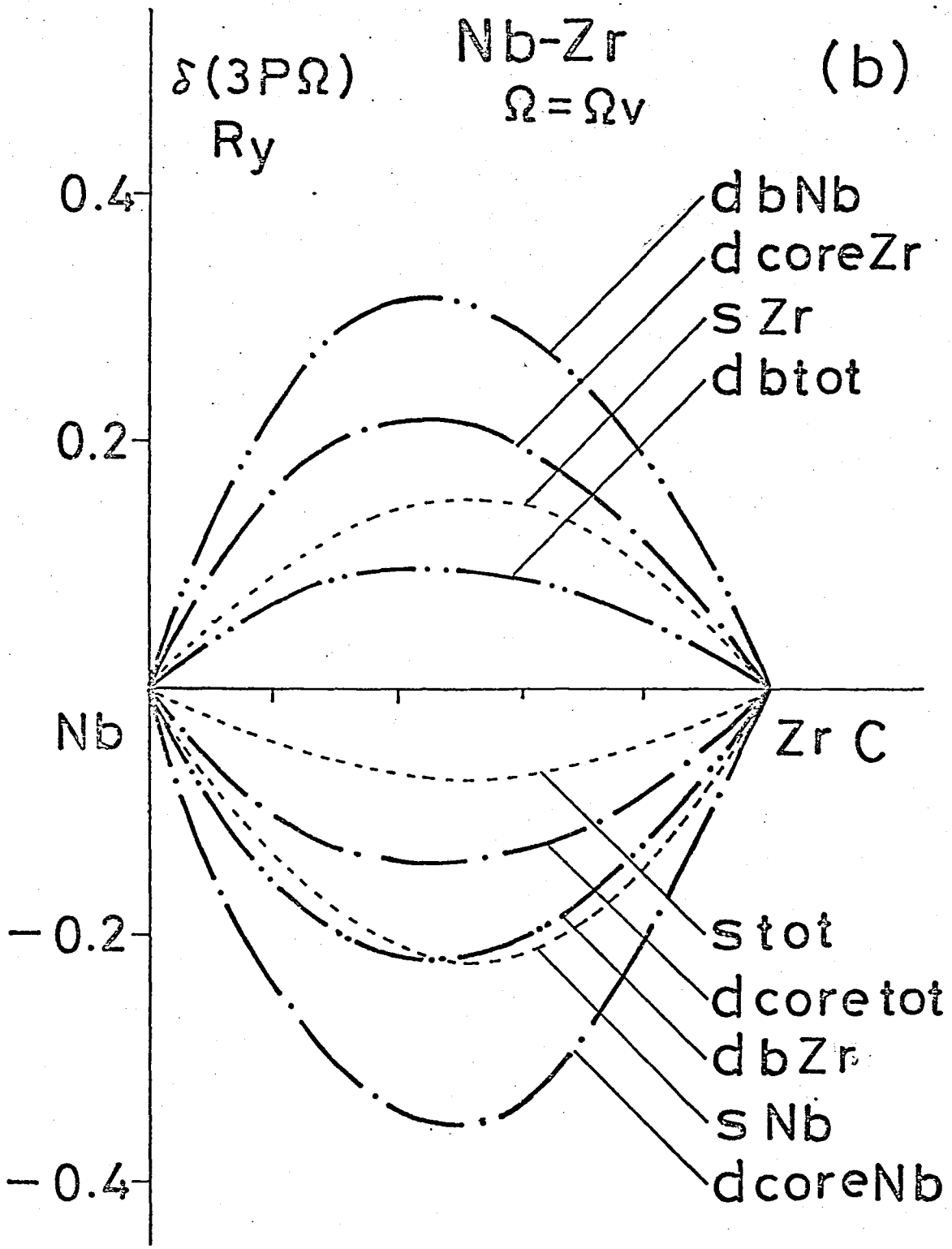
δ(3PΩ)
Ry
Nb-Zr
Ω=Ωv
(b)
0.4
0.2
Nb
−0.2
−0.4
Zr C
d bNb
d coreZr
s Zr
d btot
s tot
d core tot
d bZr
s Nb
d coreNb

Fig.I.4(b)

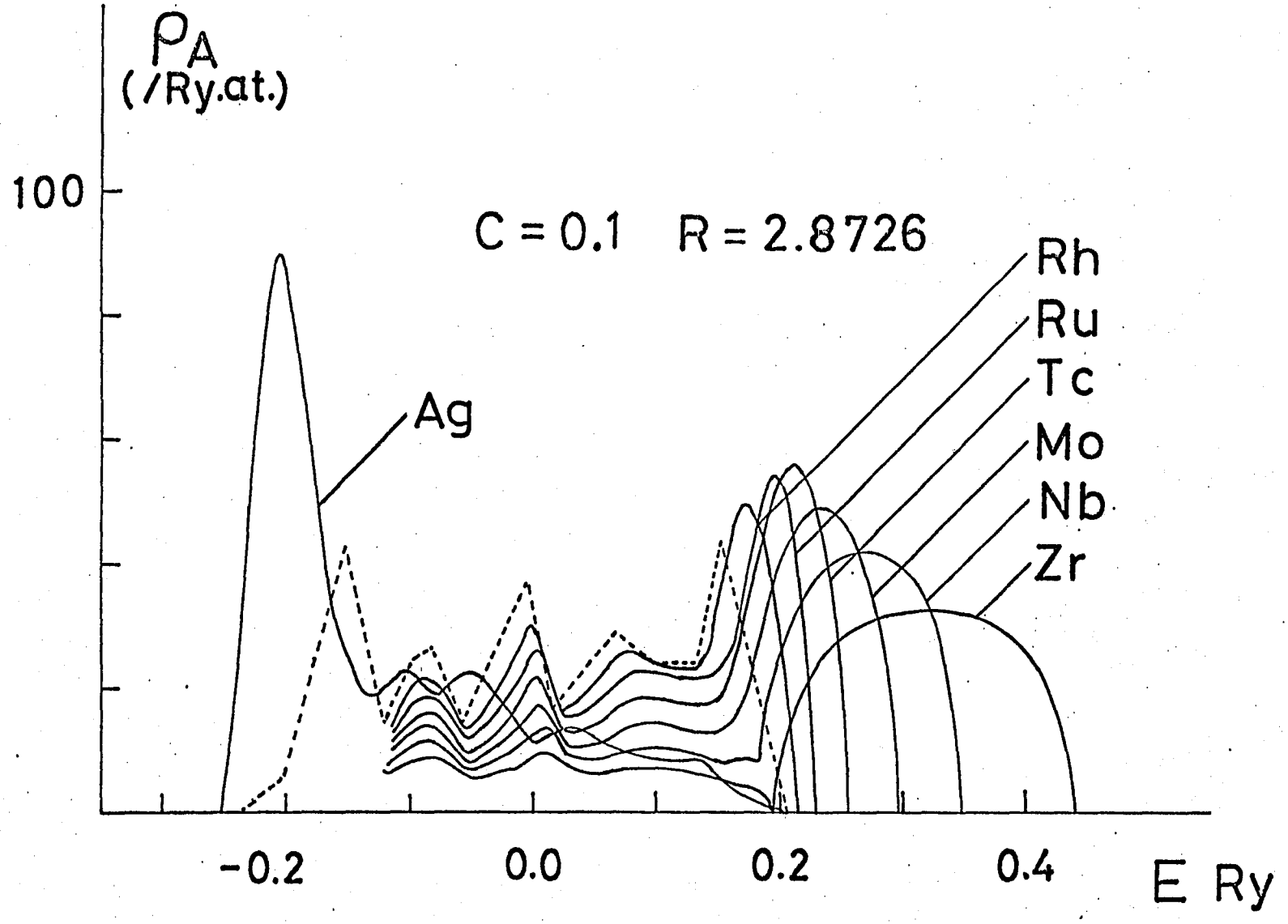

Fig.I.5

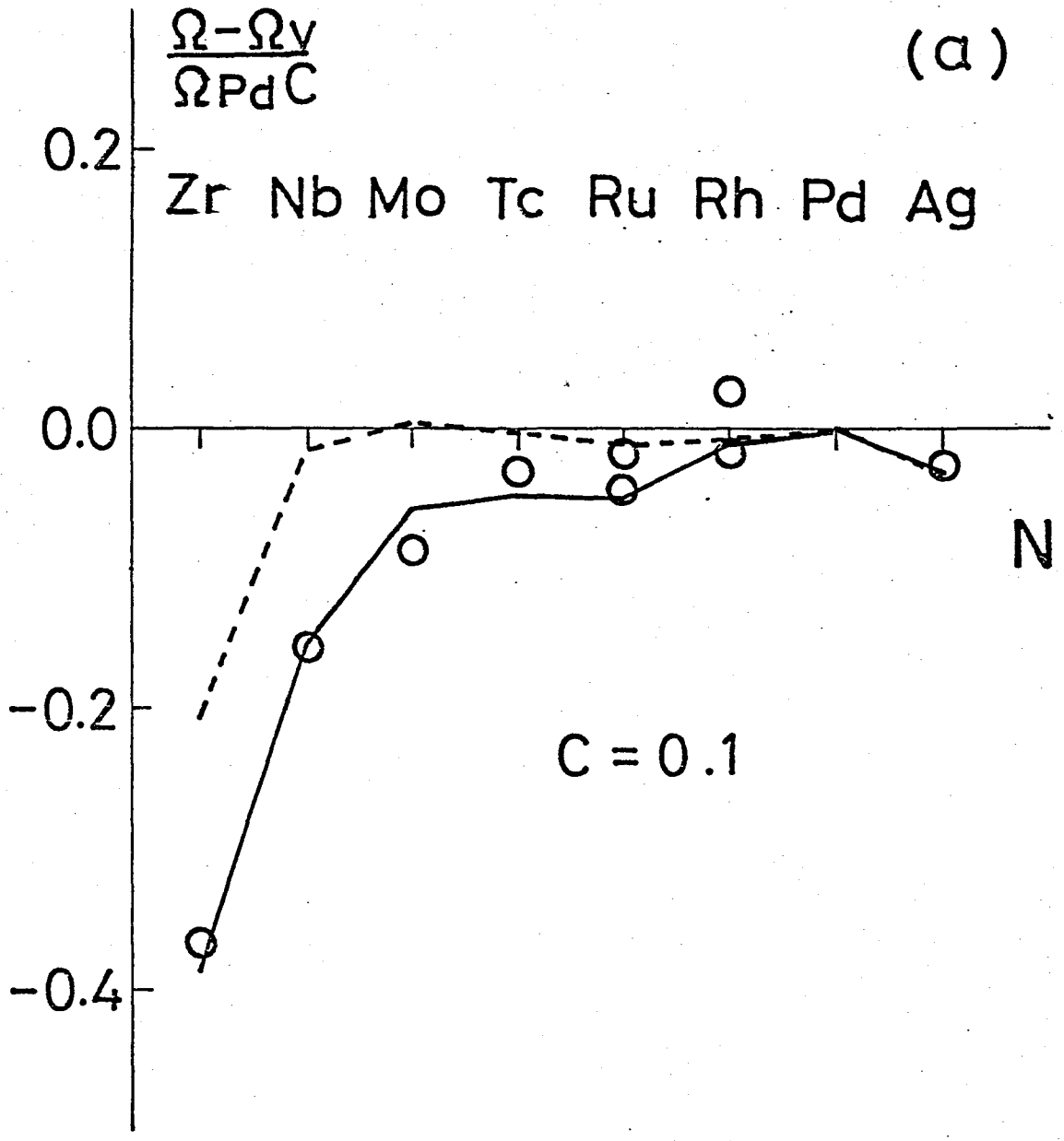

Fig.I.6(a)

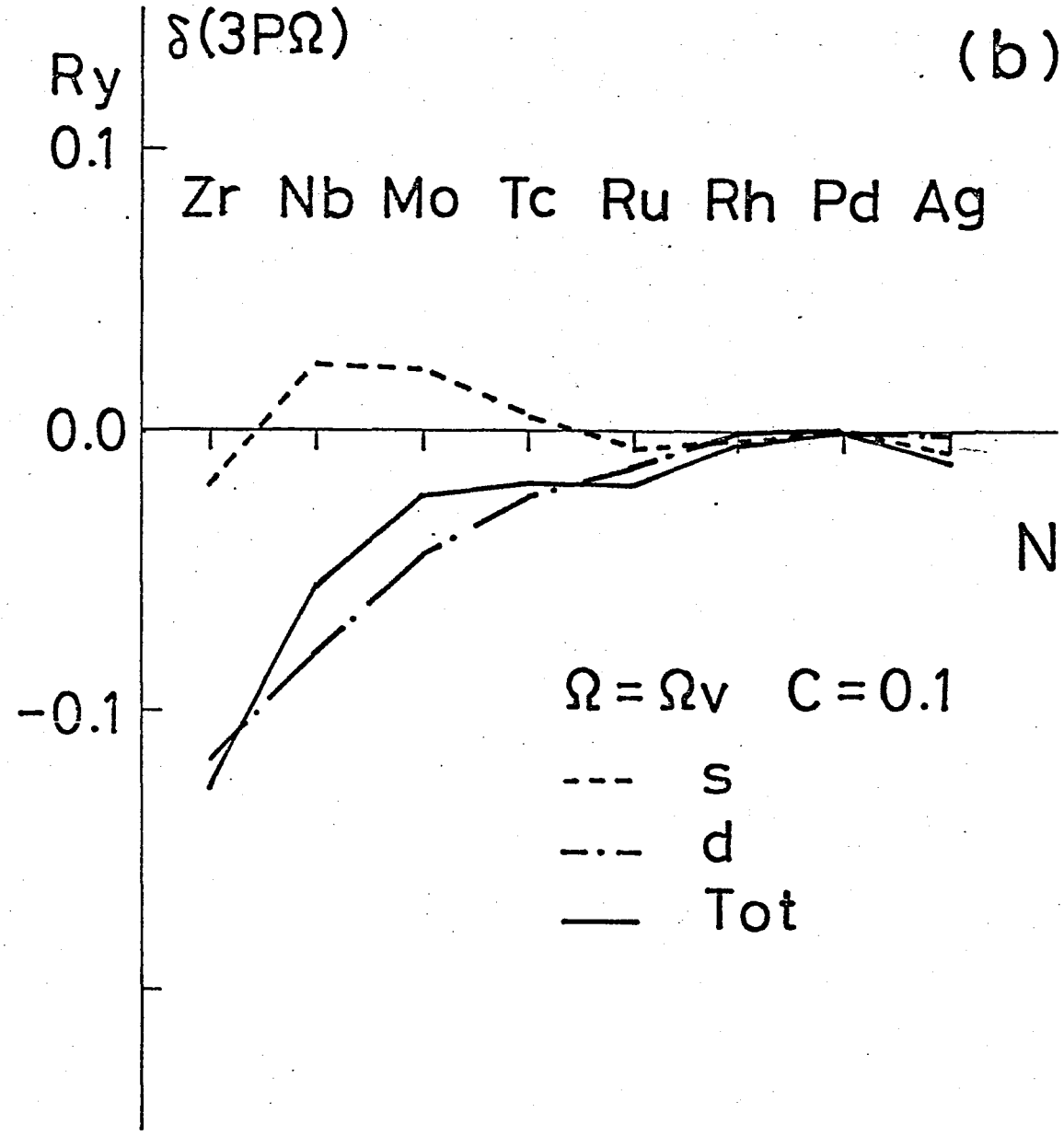

Fig.I.6(b)

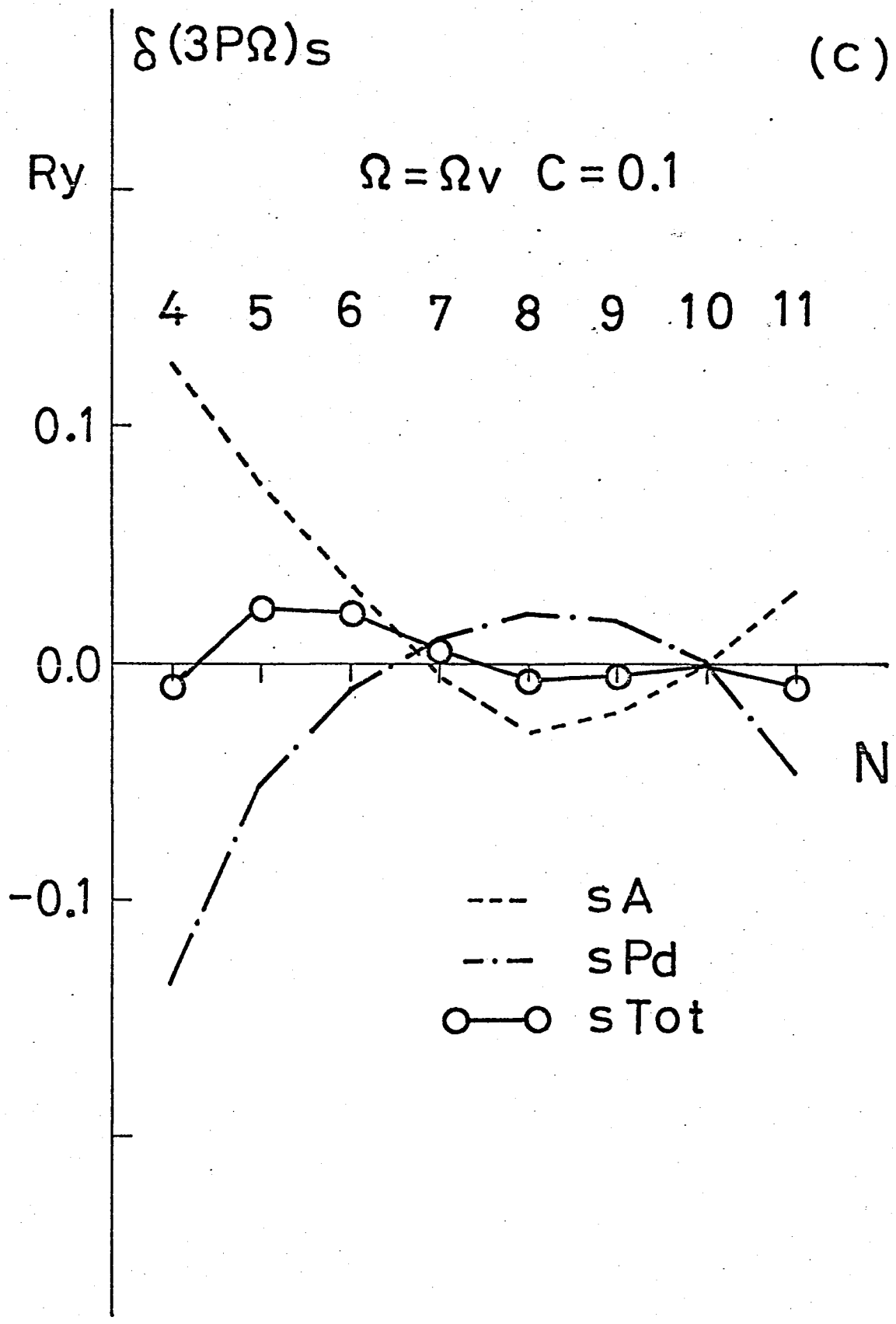

Fig.I.6(c)

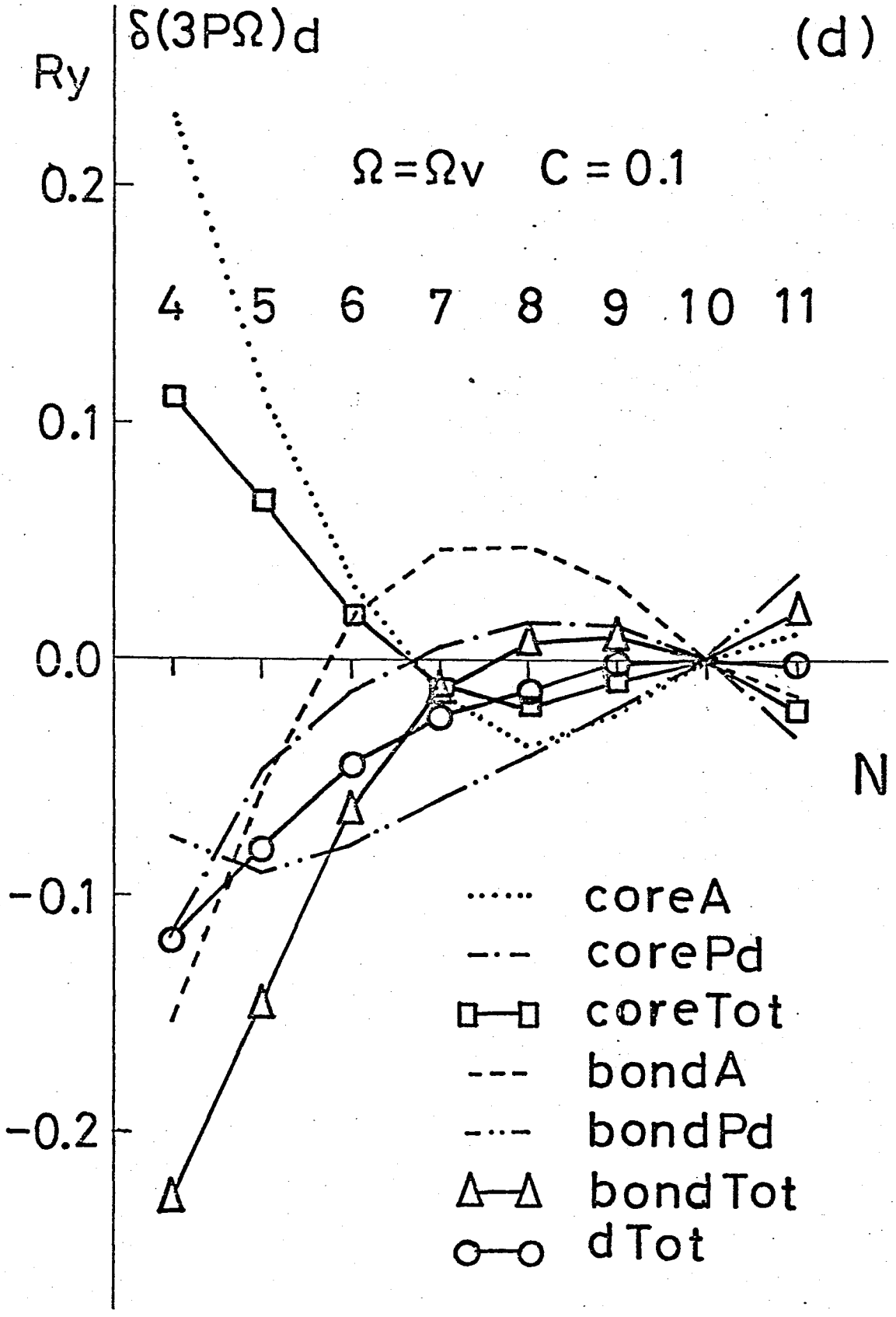
δ(3PΩ)d
(d)
Ry
Ω=Ωv C=0.1
0.2
0.1
0.0
-0.1
-0.2
4 5 6 7 8 9 10 11
N
coreA
corePd
coreTot
bondA
bondPd
bondTot
dTot

Fig.I.6(d)

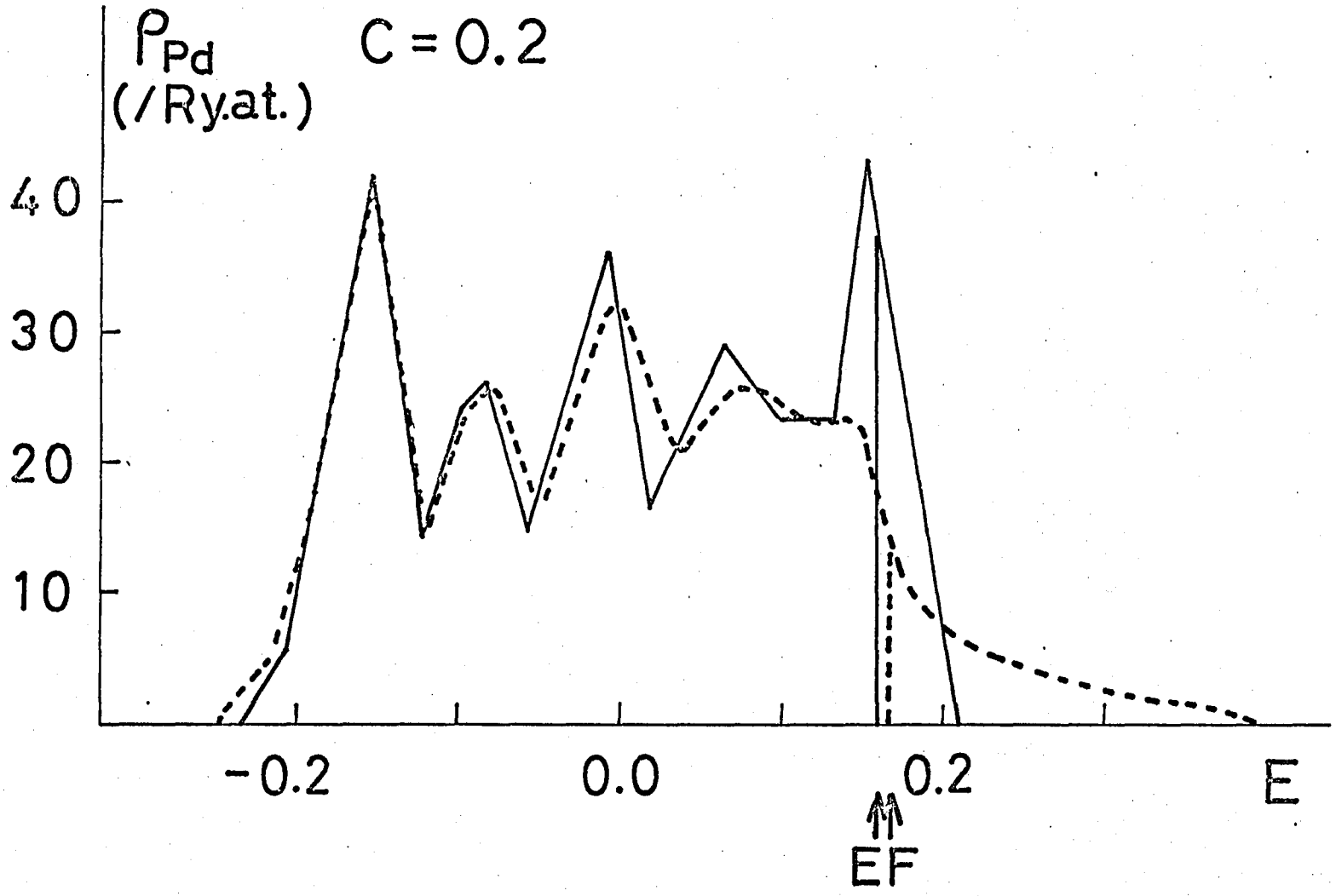

Fig.I.7

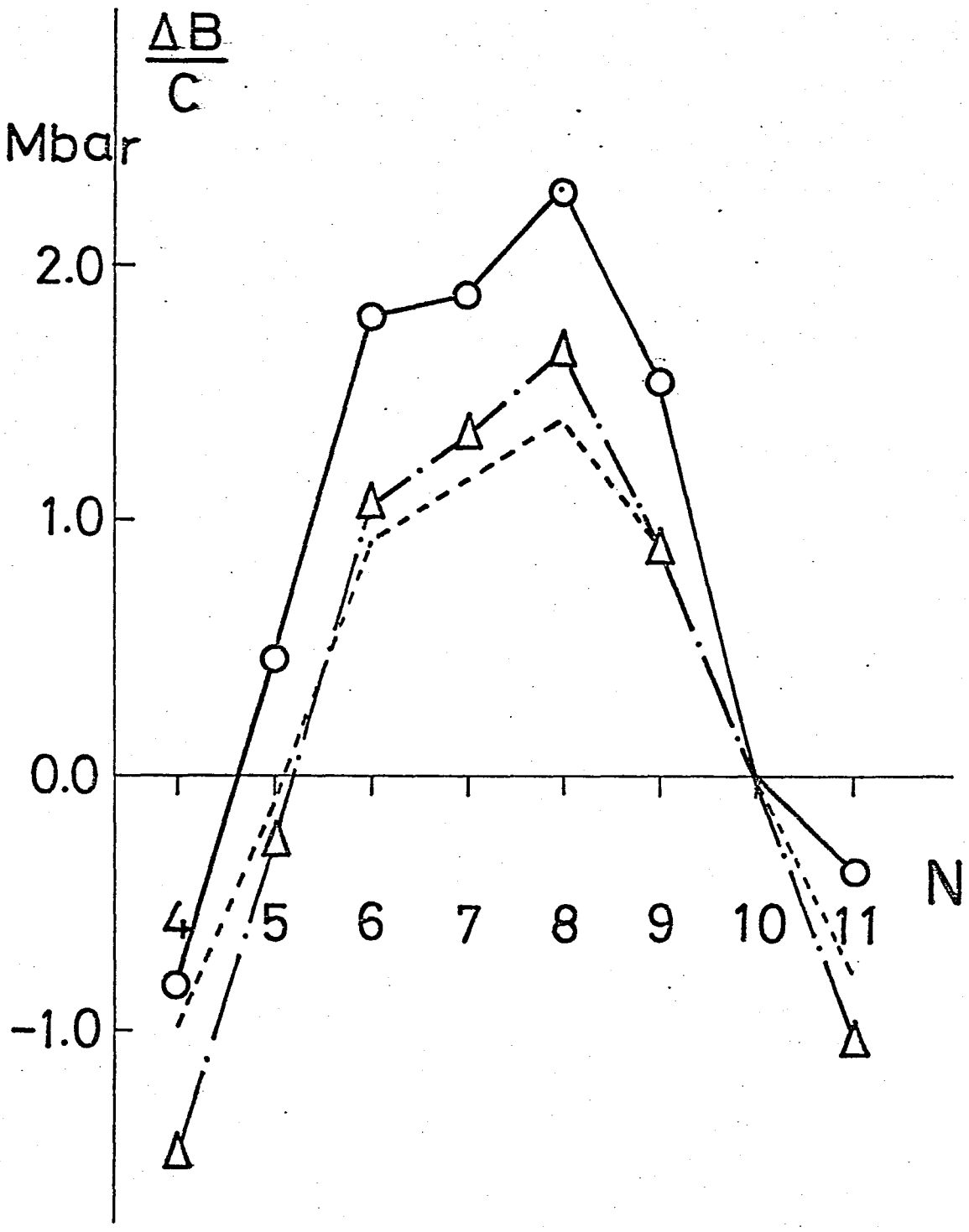

Fig.I.8

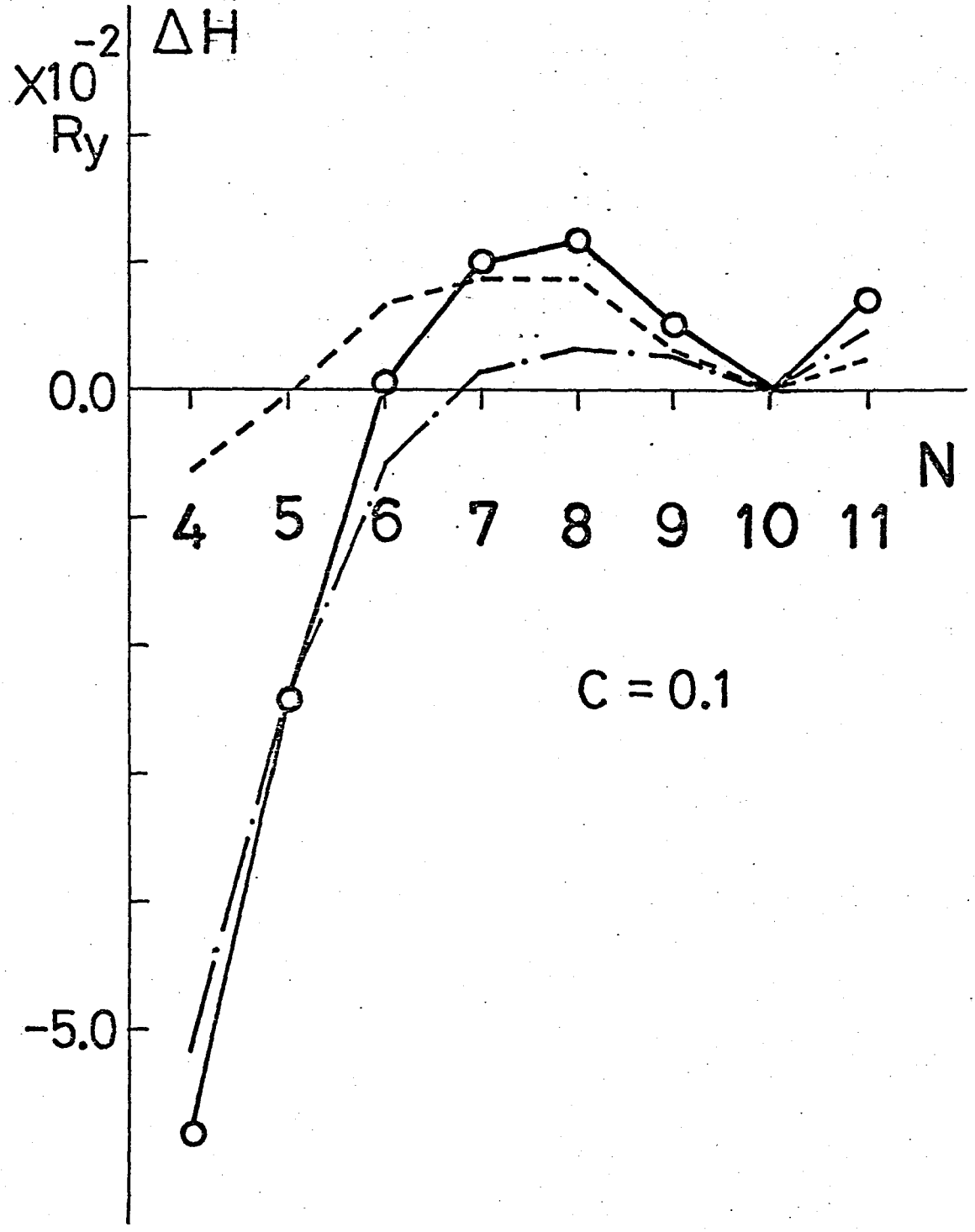

Fig.I.9

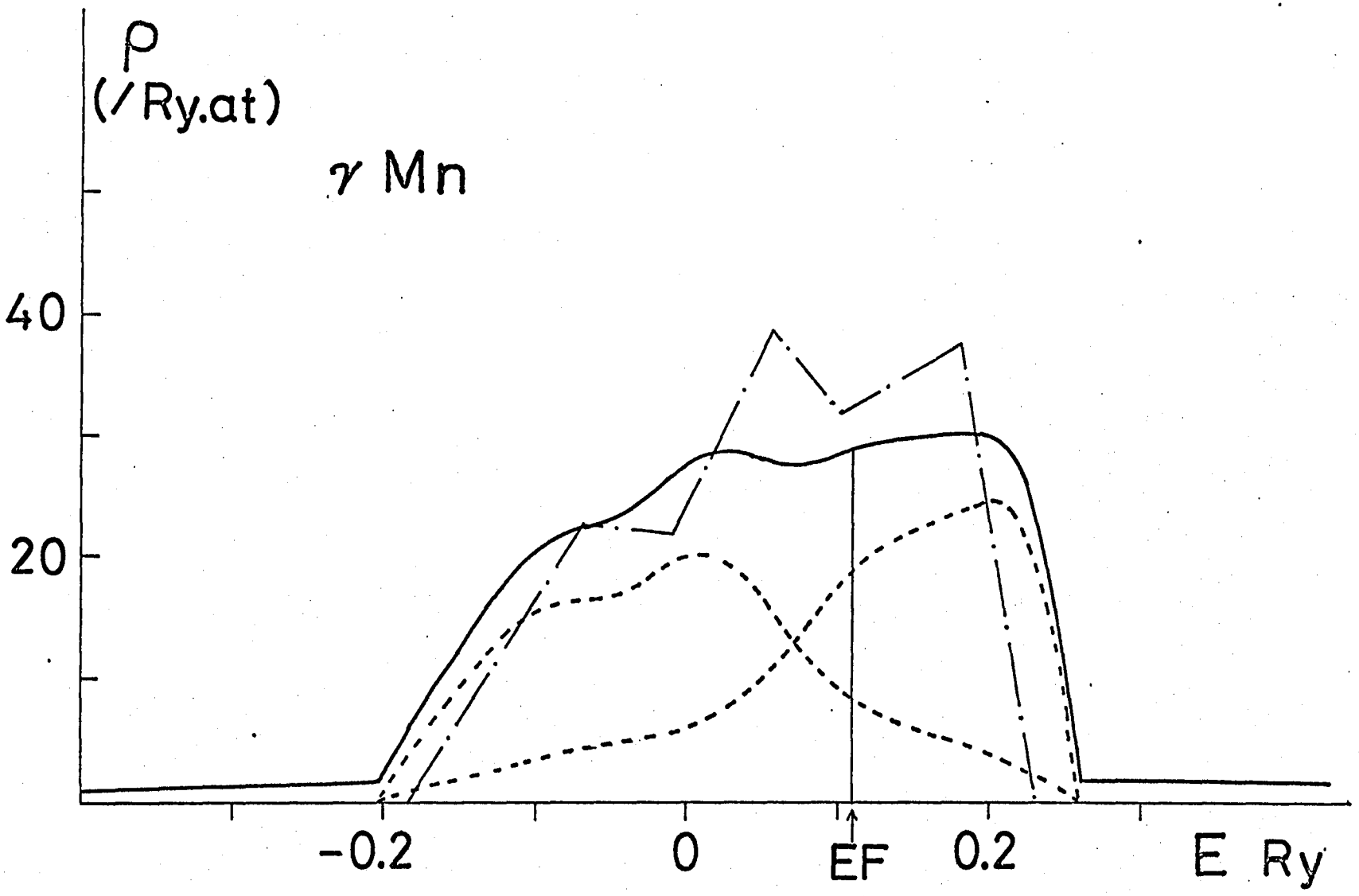

Fig.II.1

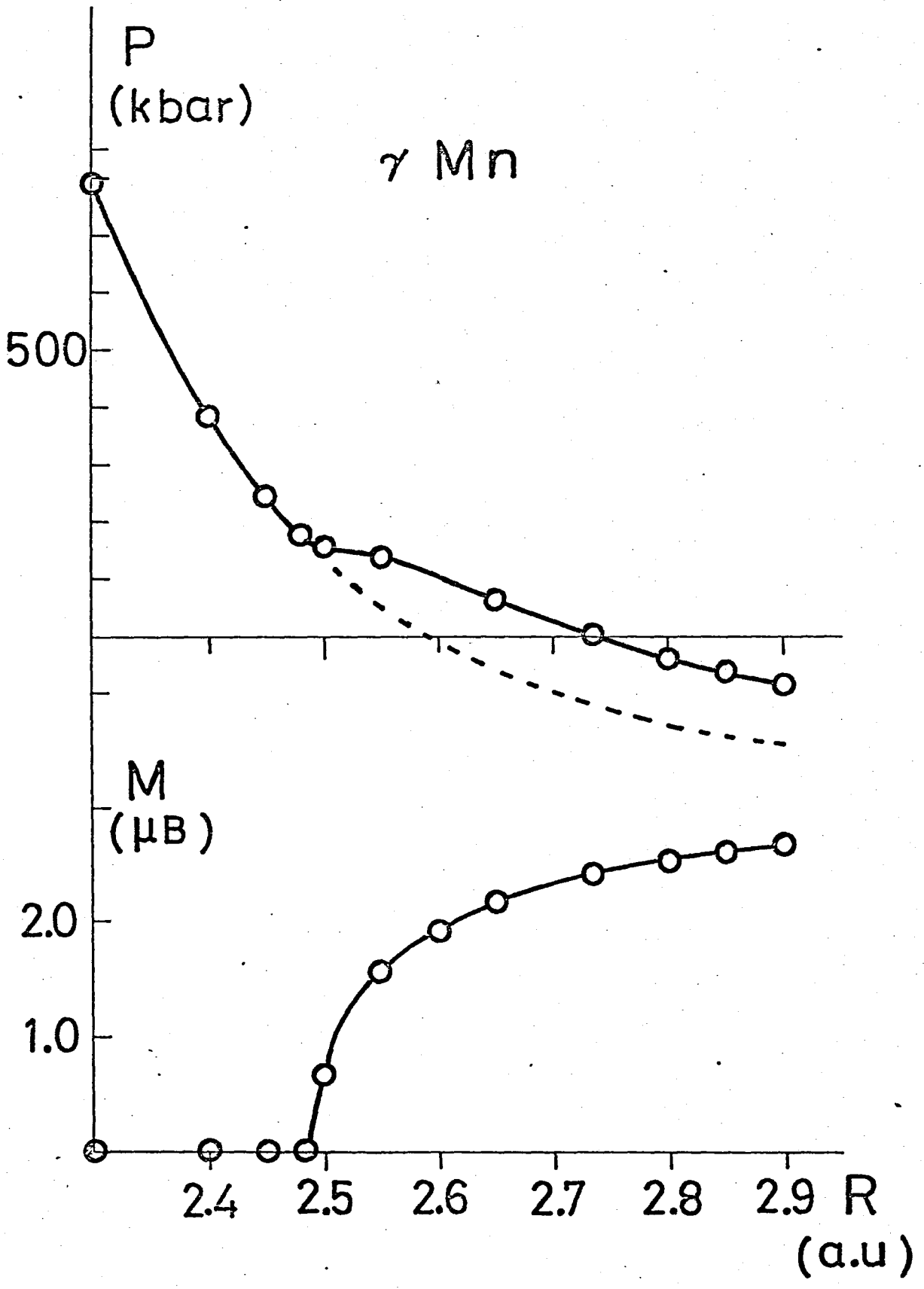

Fig.II.2

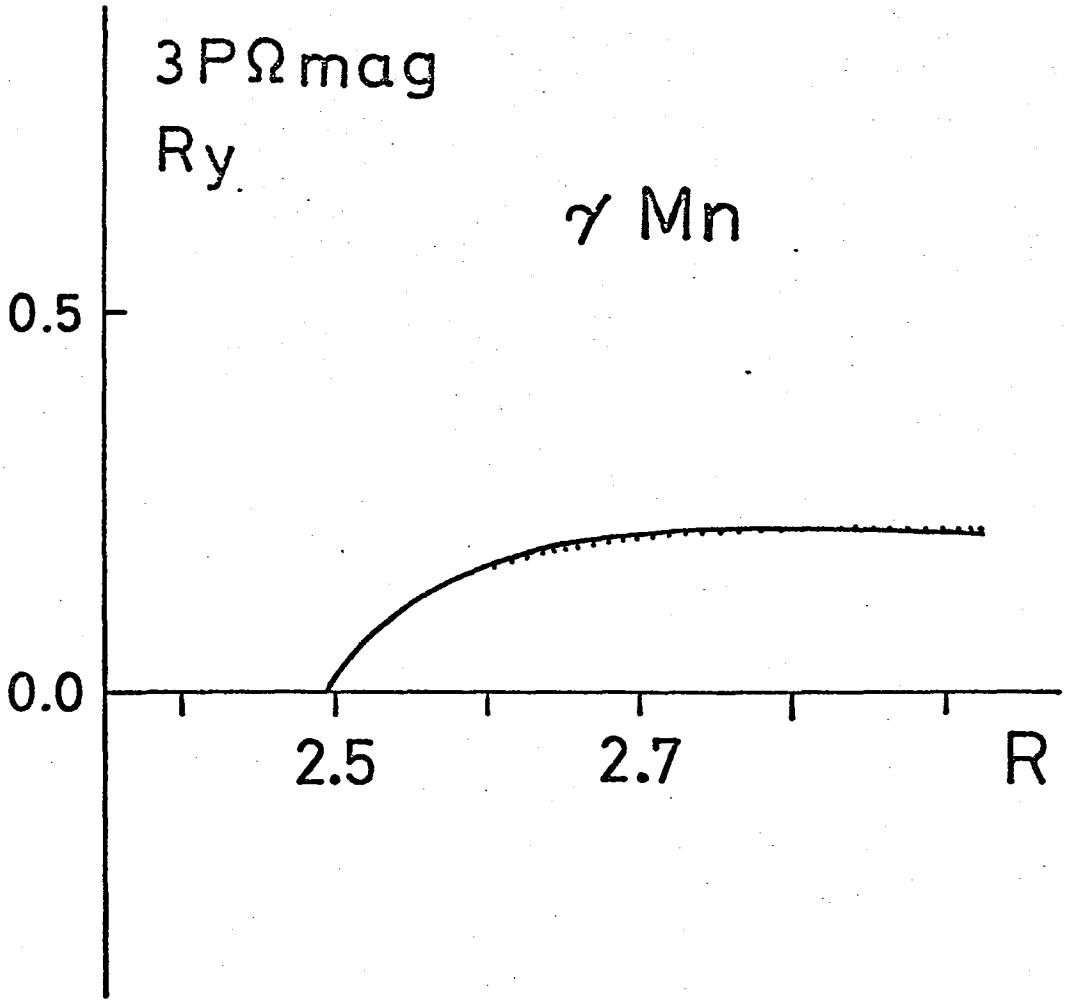

Fig.II.3

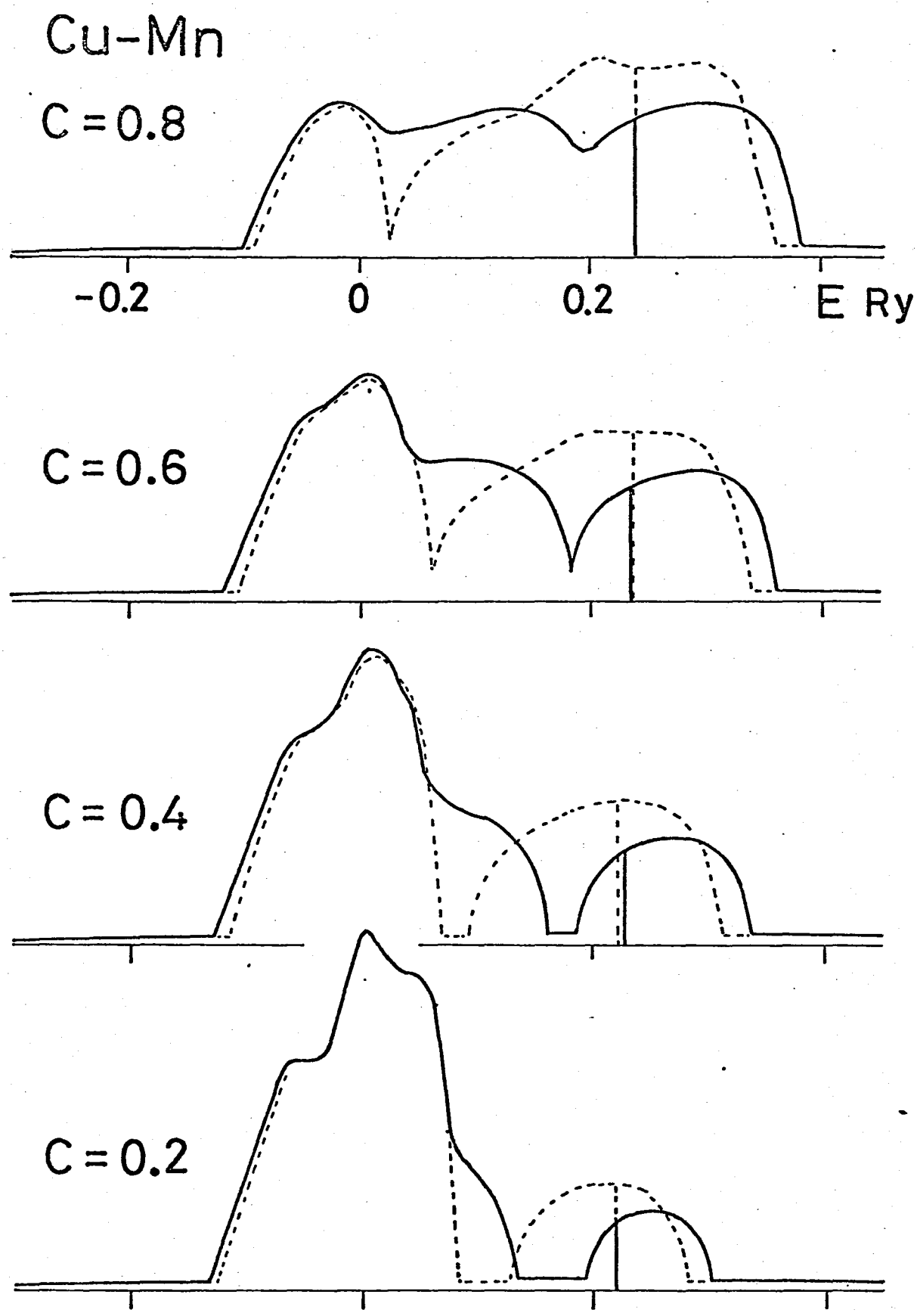

Fig.II.4

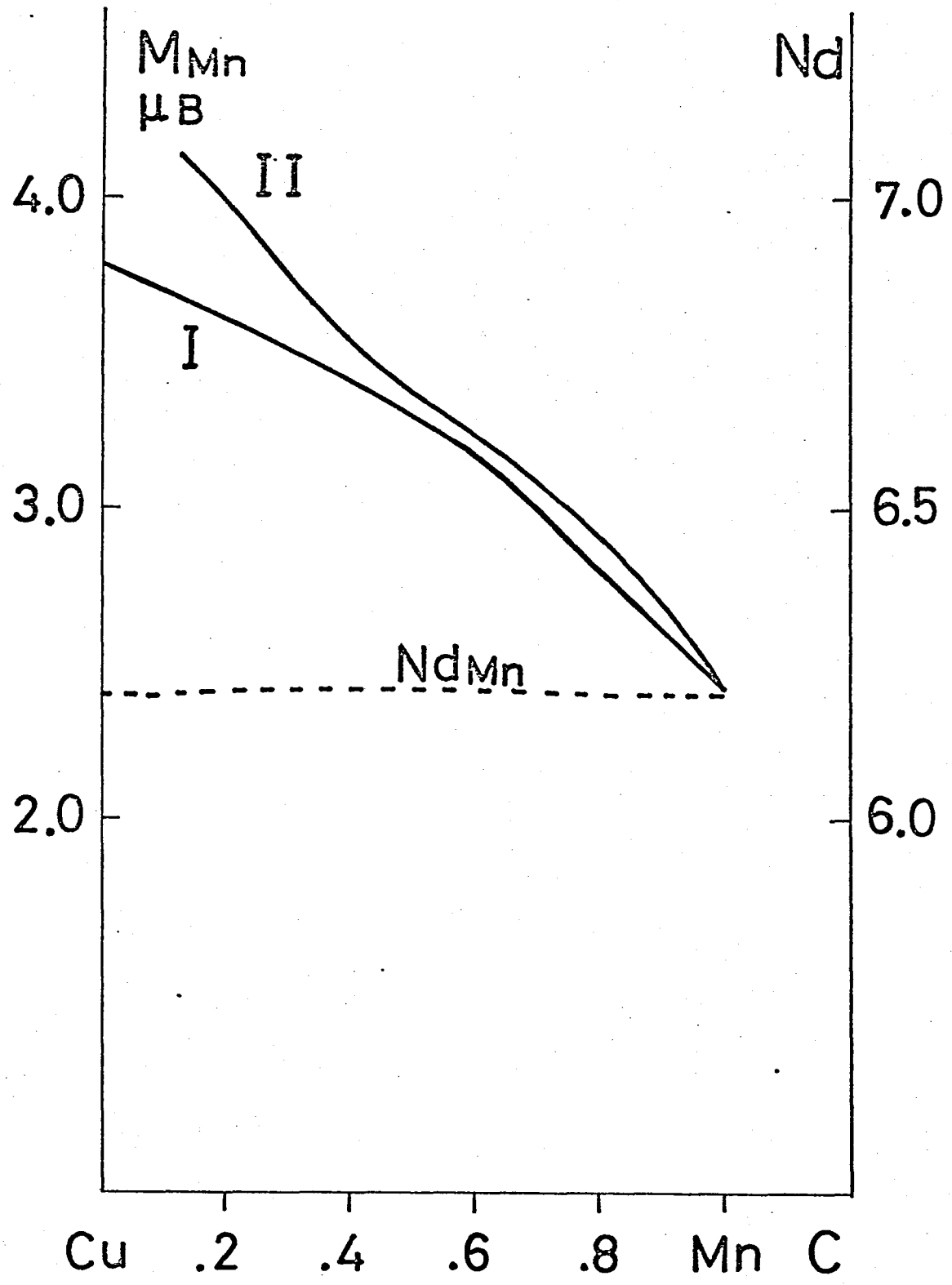

Fig.II.5

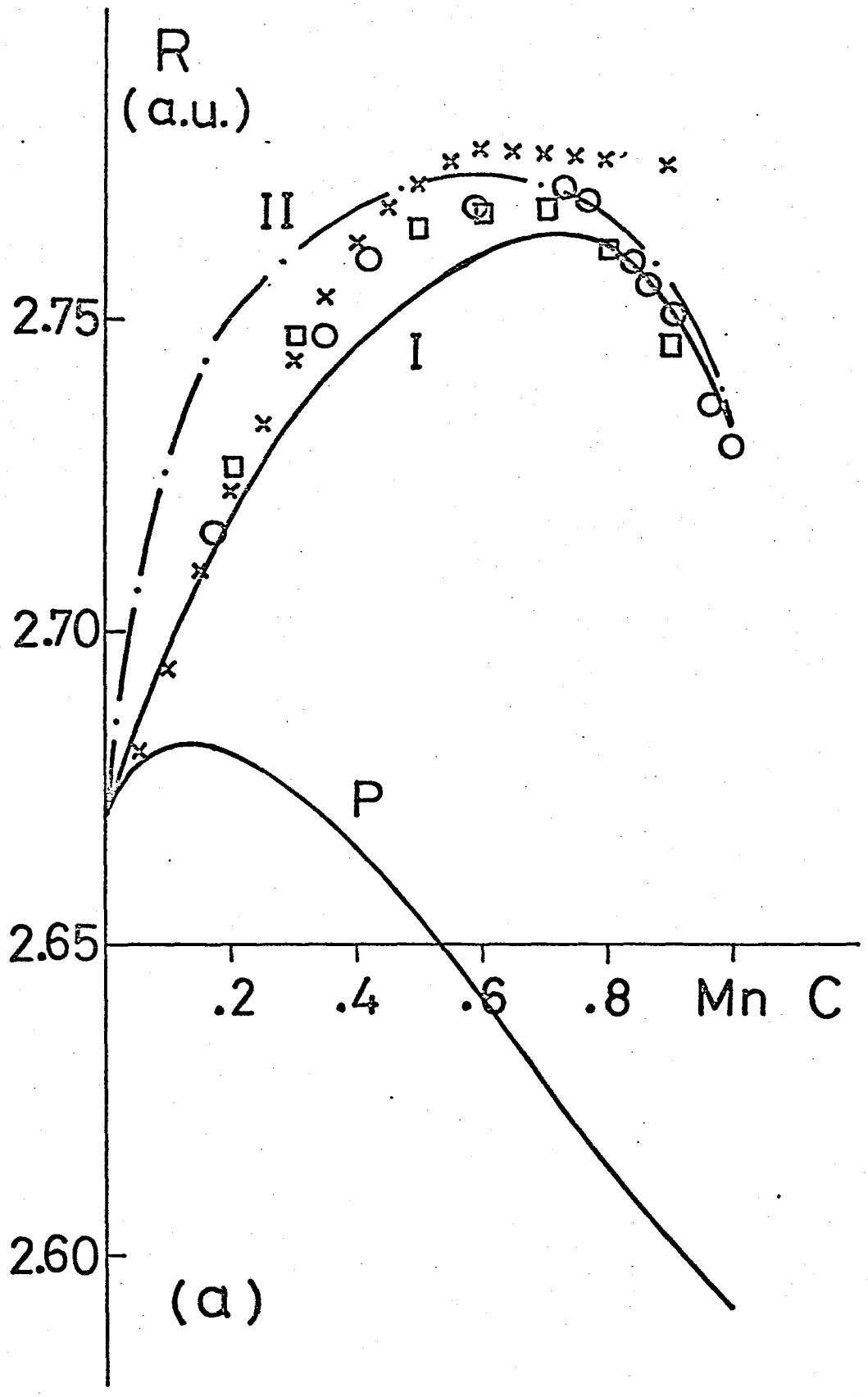

Fig.II.6(a)

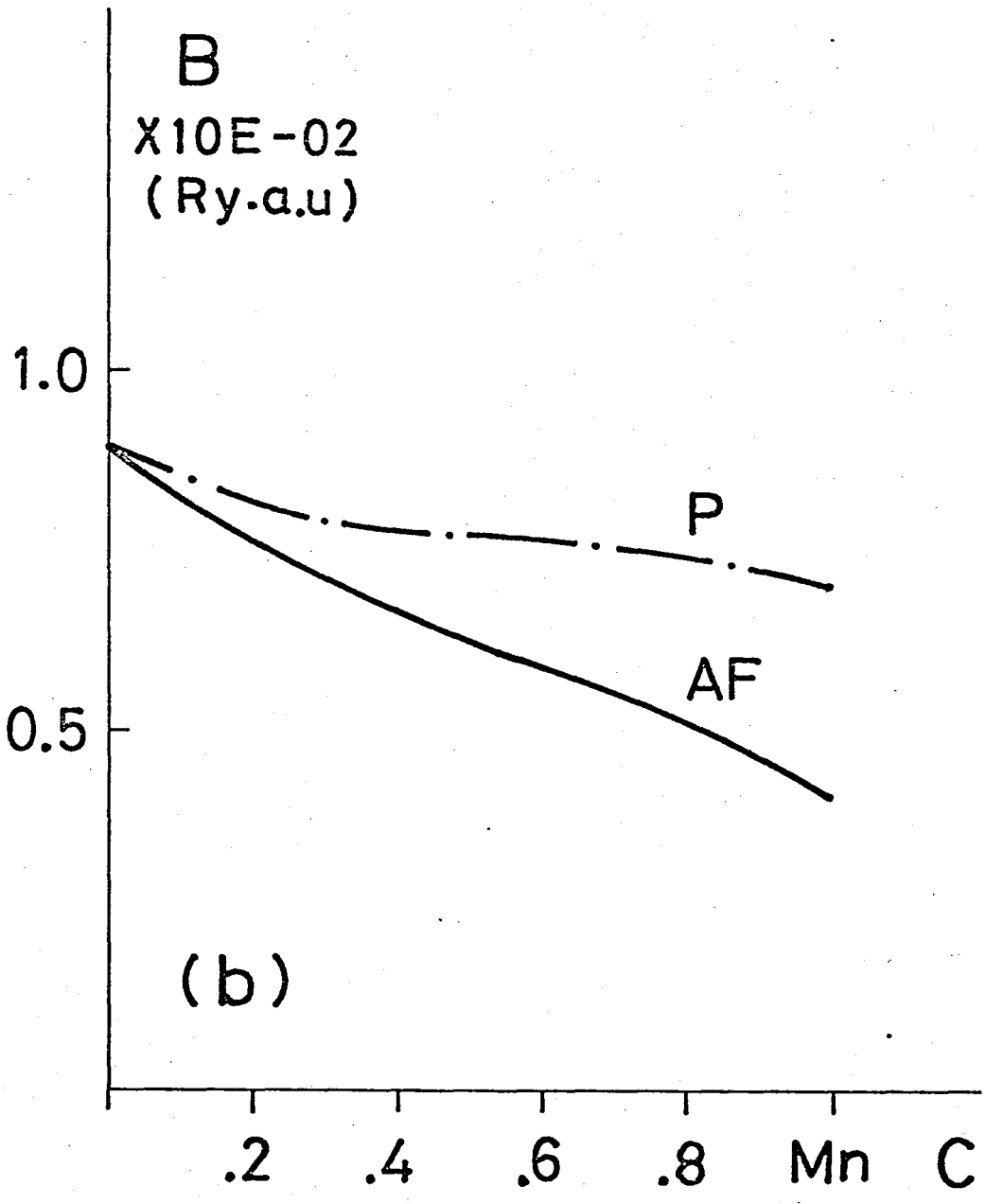

Fig.II.6(b)

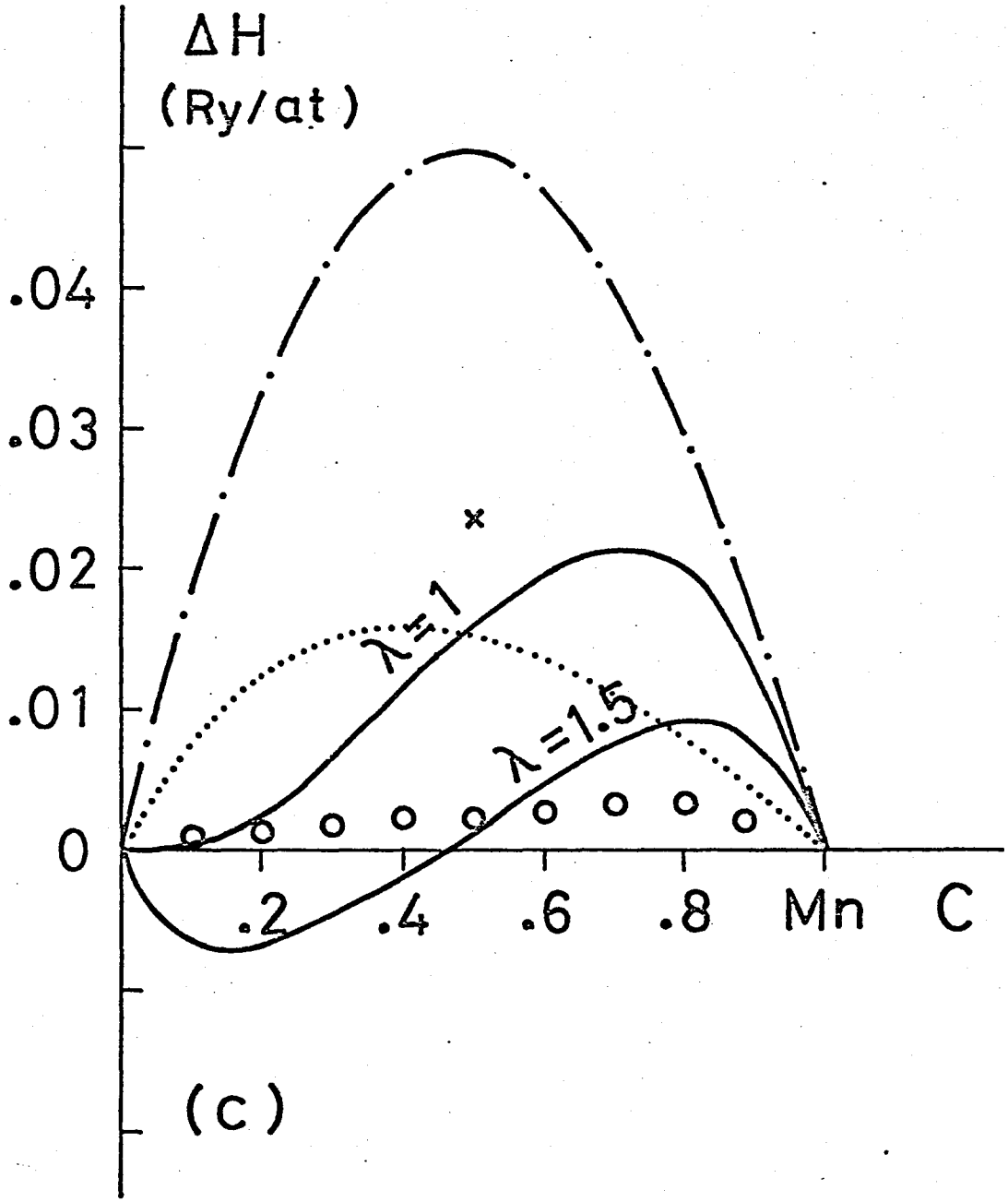

Fig.II.6(c)

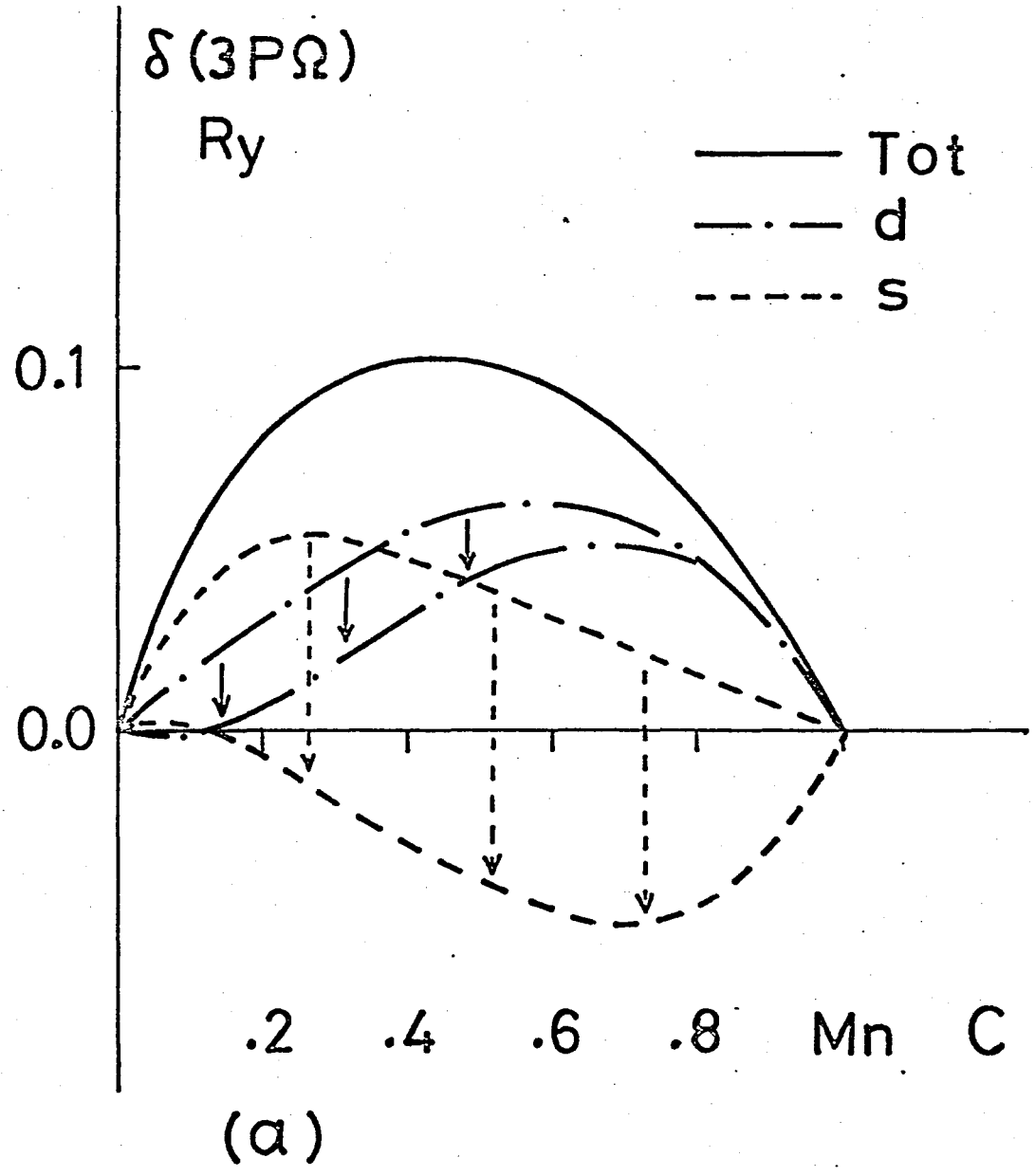

Fig.II.7(a)

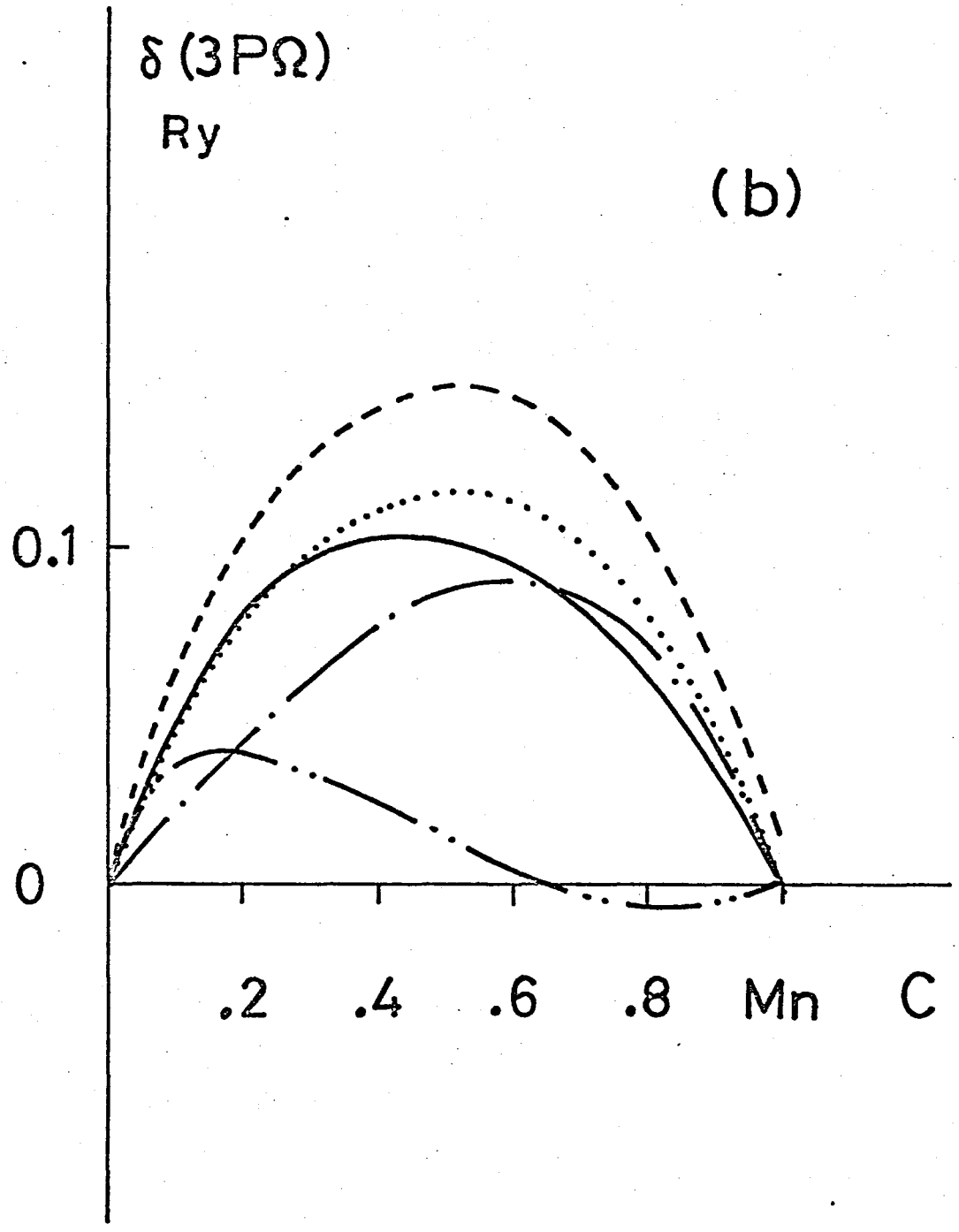

Fig.II.7(b)

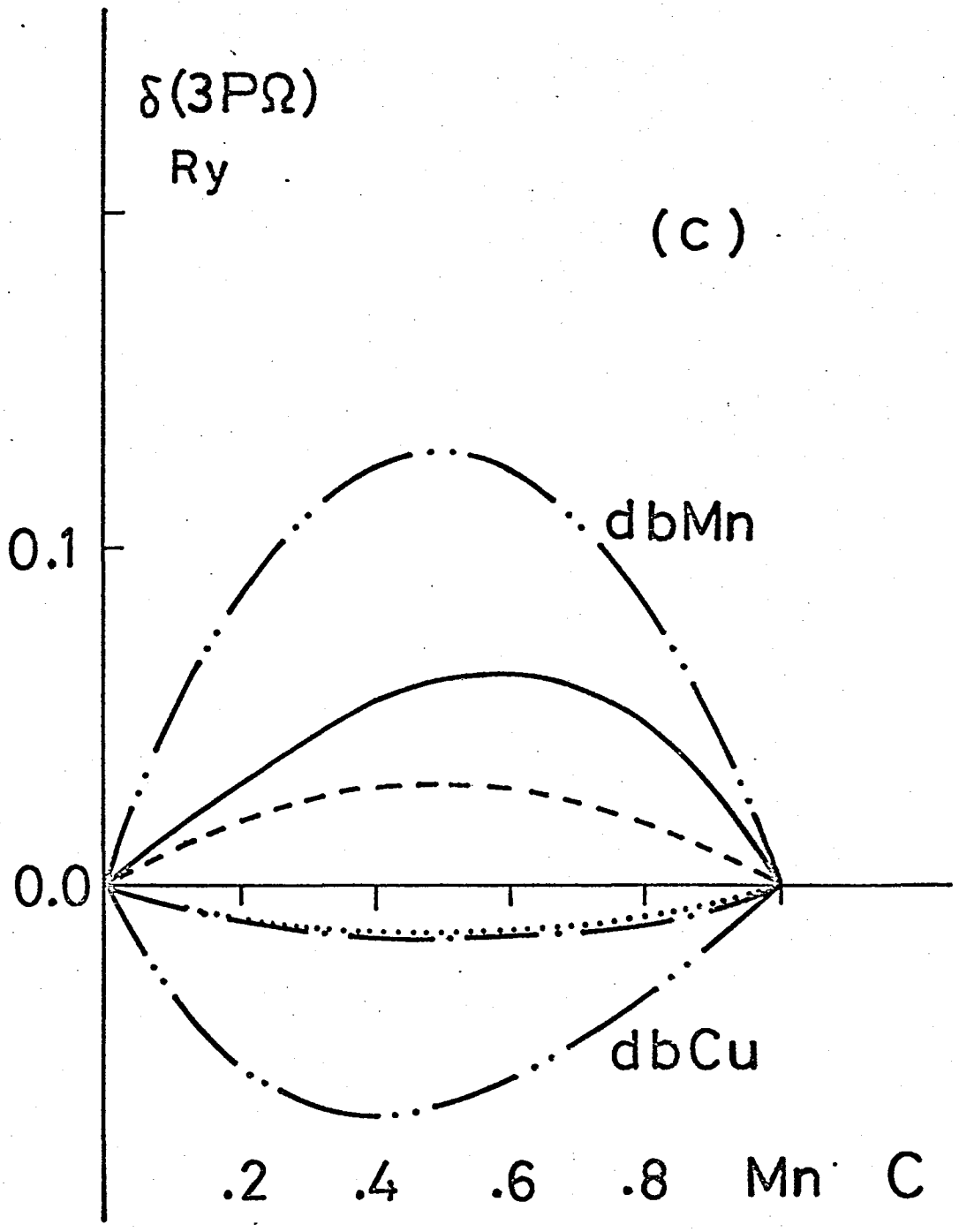

Fig.II.7(c)

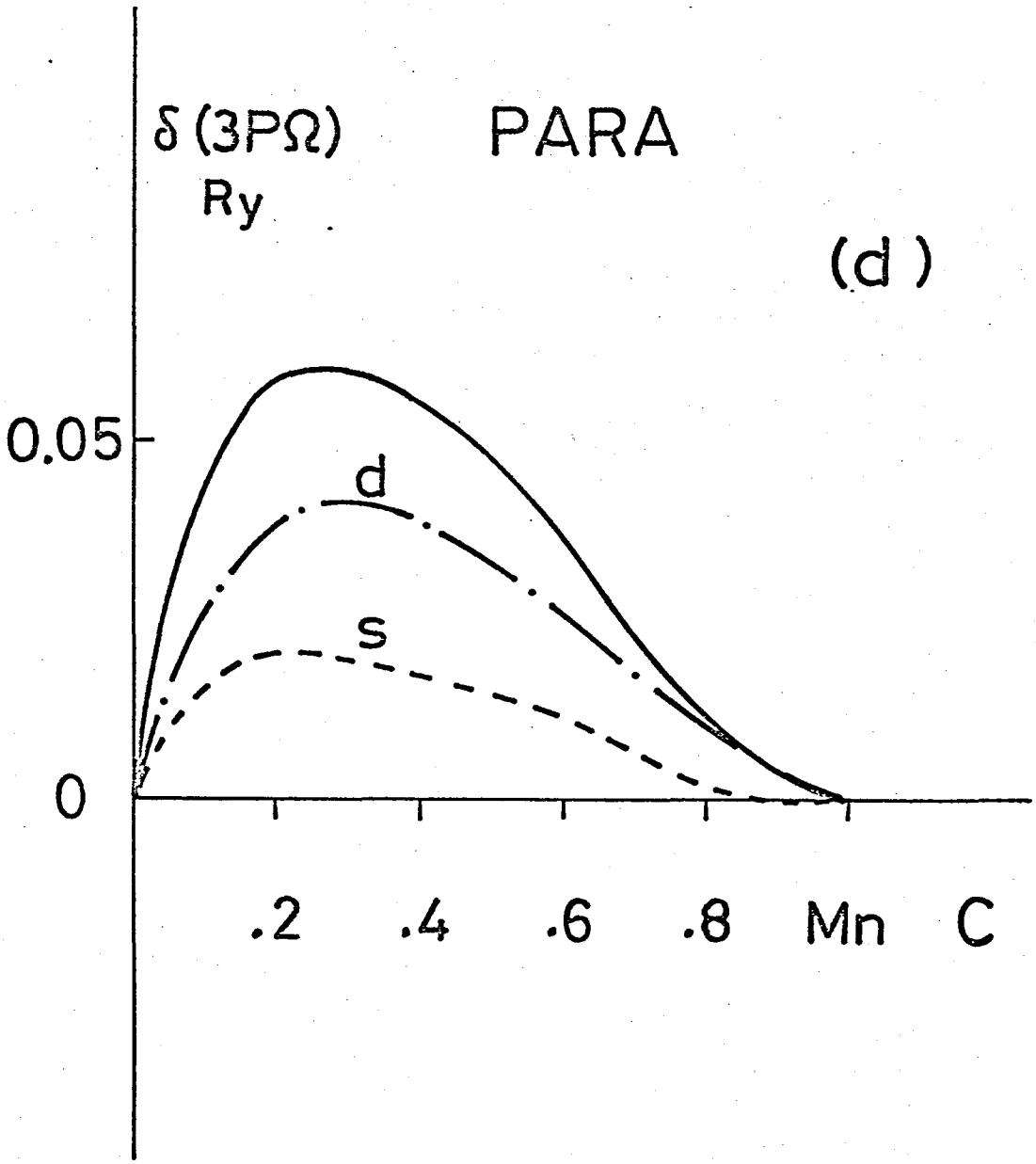

Fig.II.7(d)

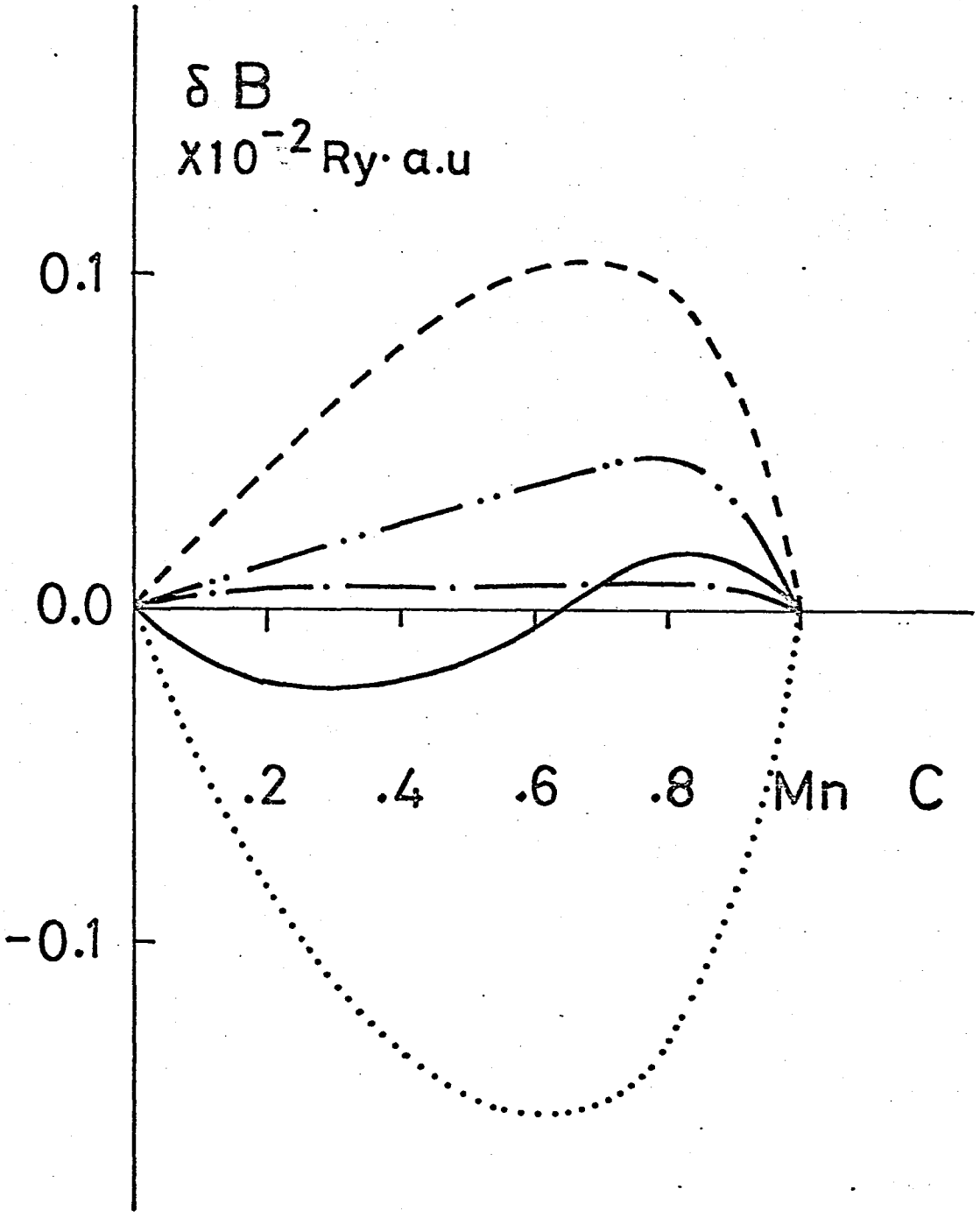

Fig.II.8

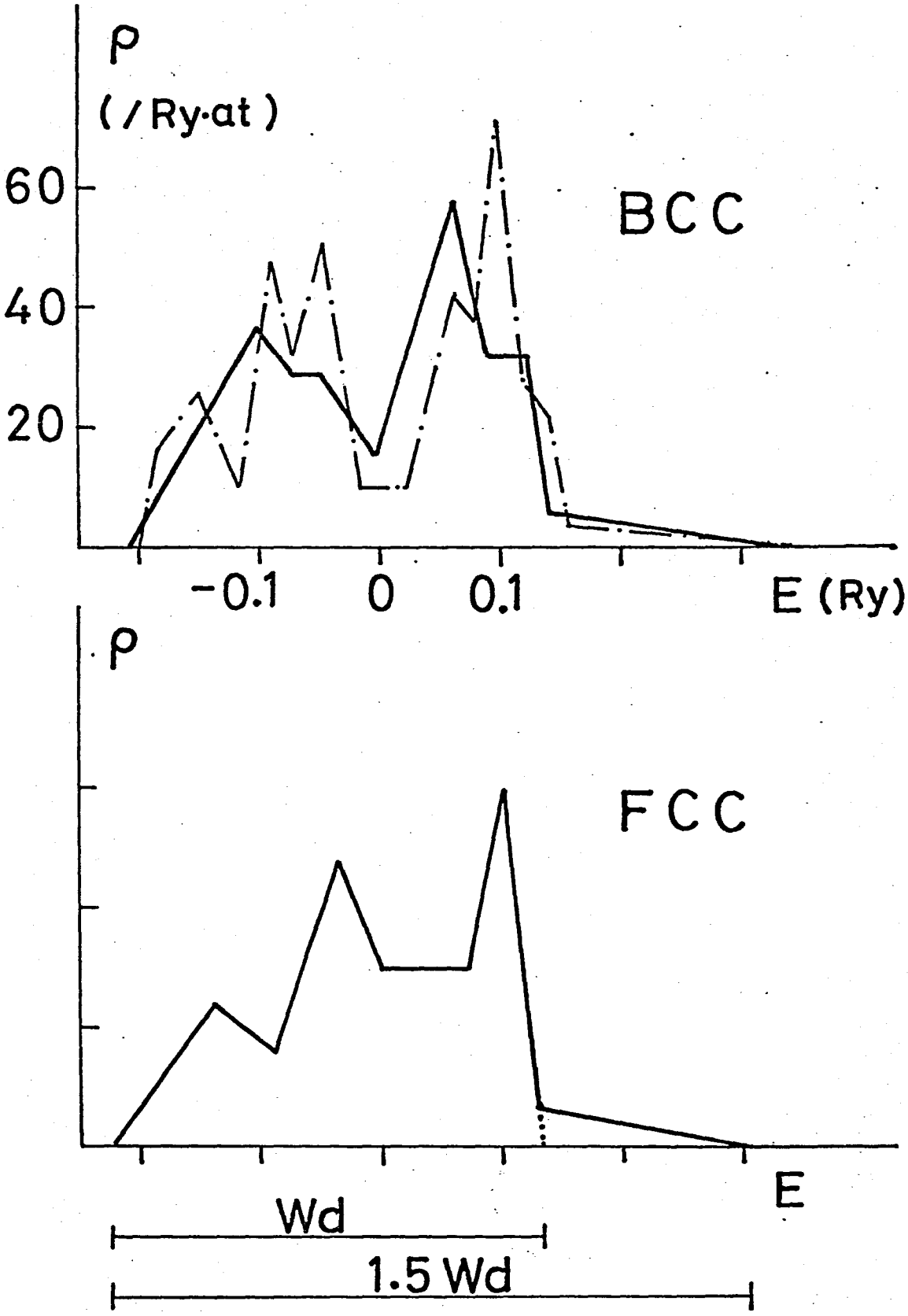

Fig.II.9

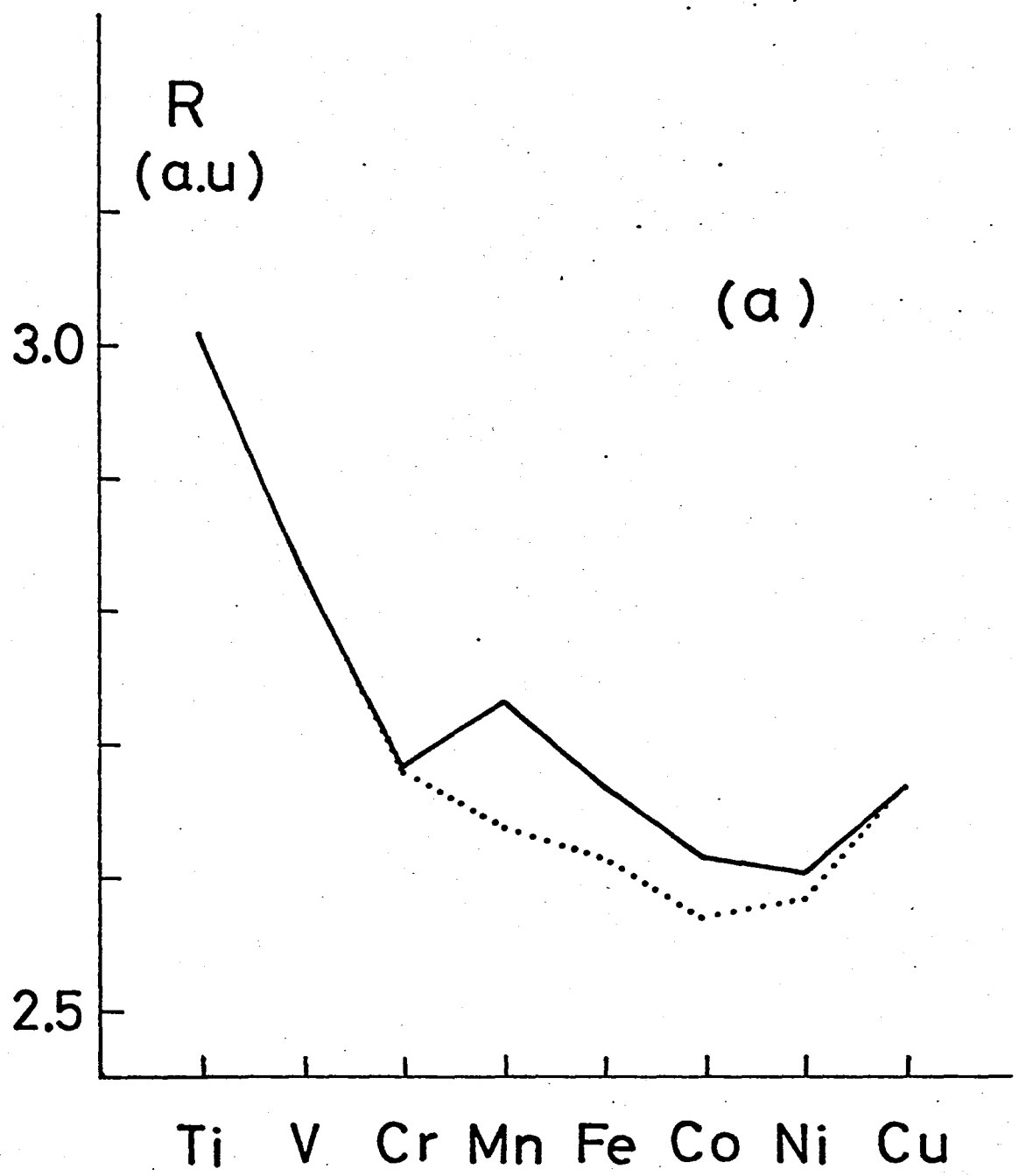

Fig.II.10(a)

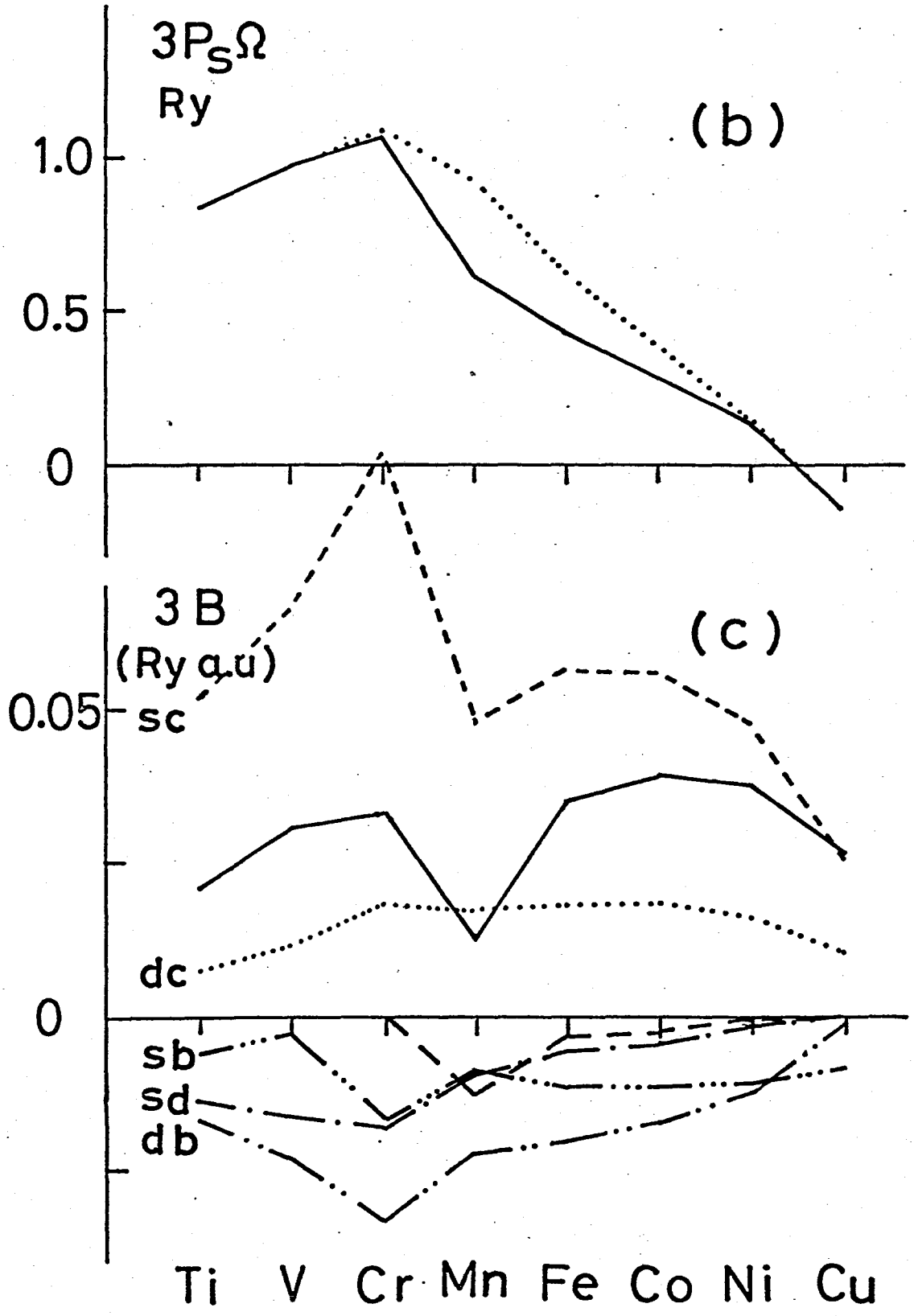

Fig.II.10(b),(c)

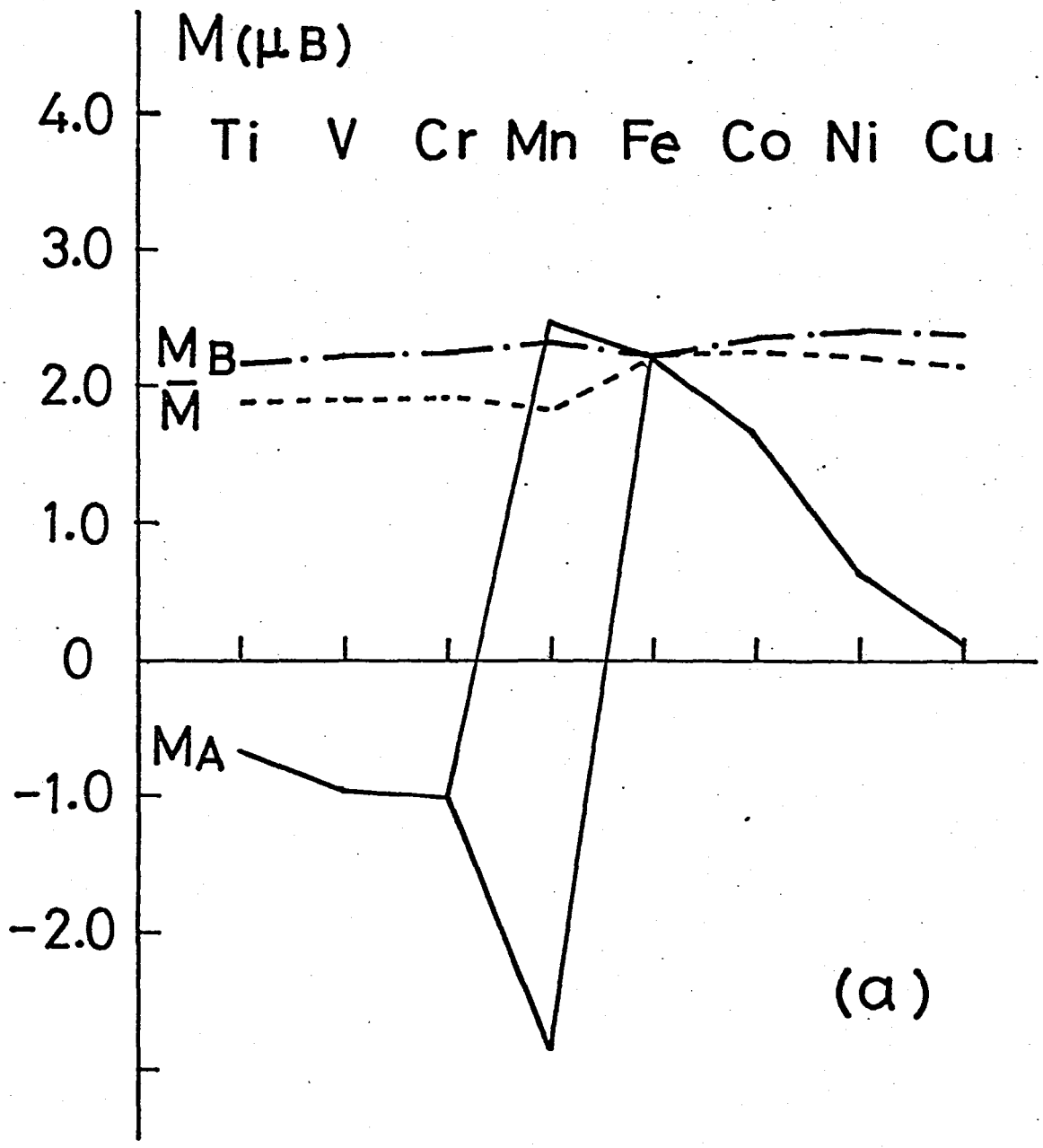

Fig.II.11(a)

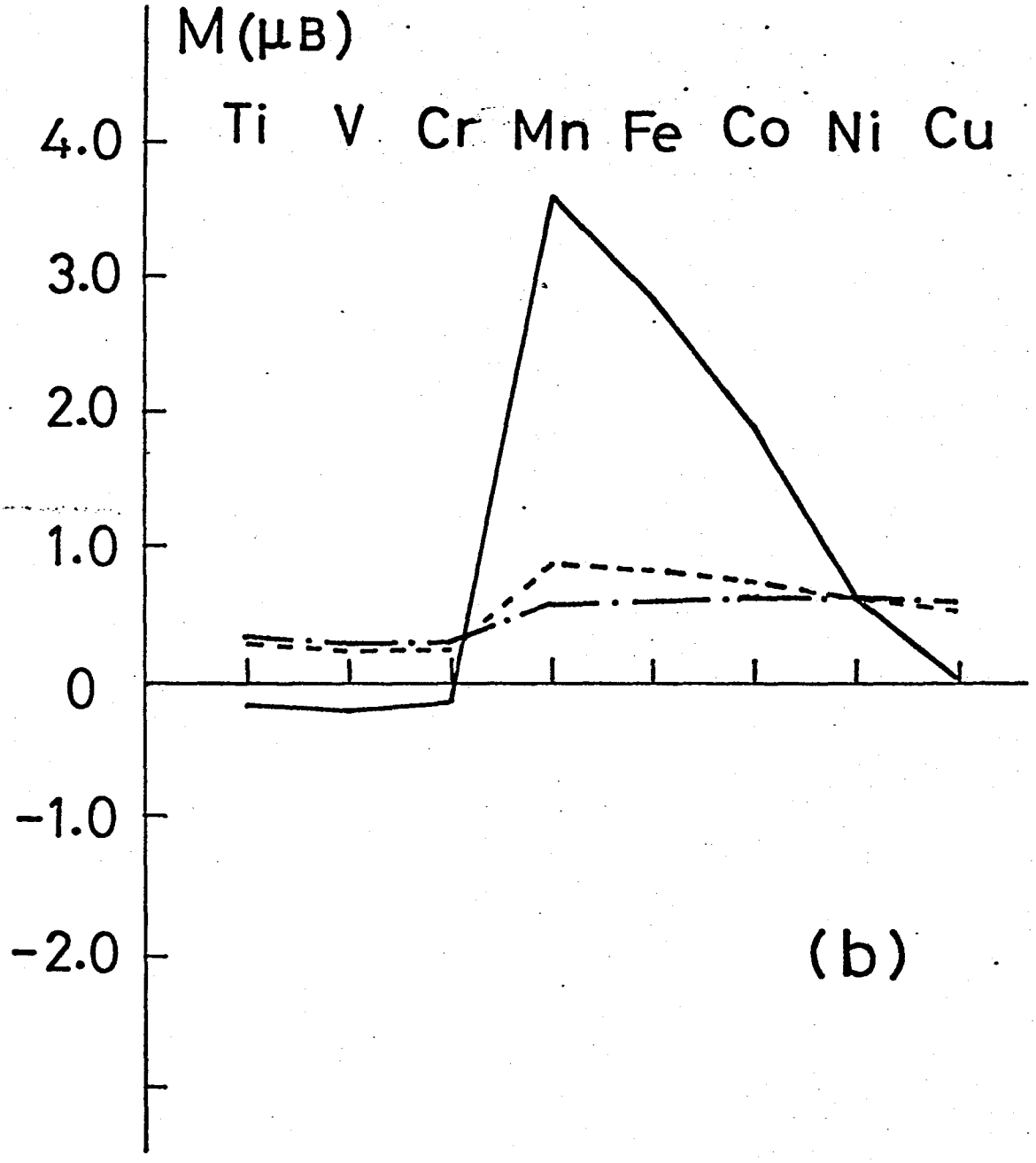

Fig.II.11(b)

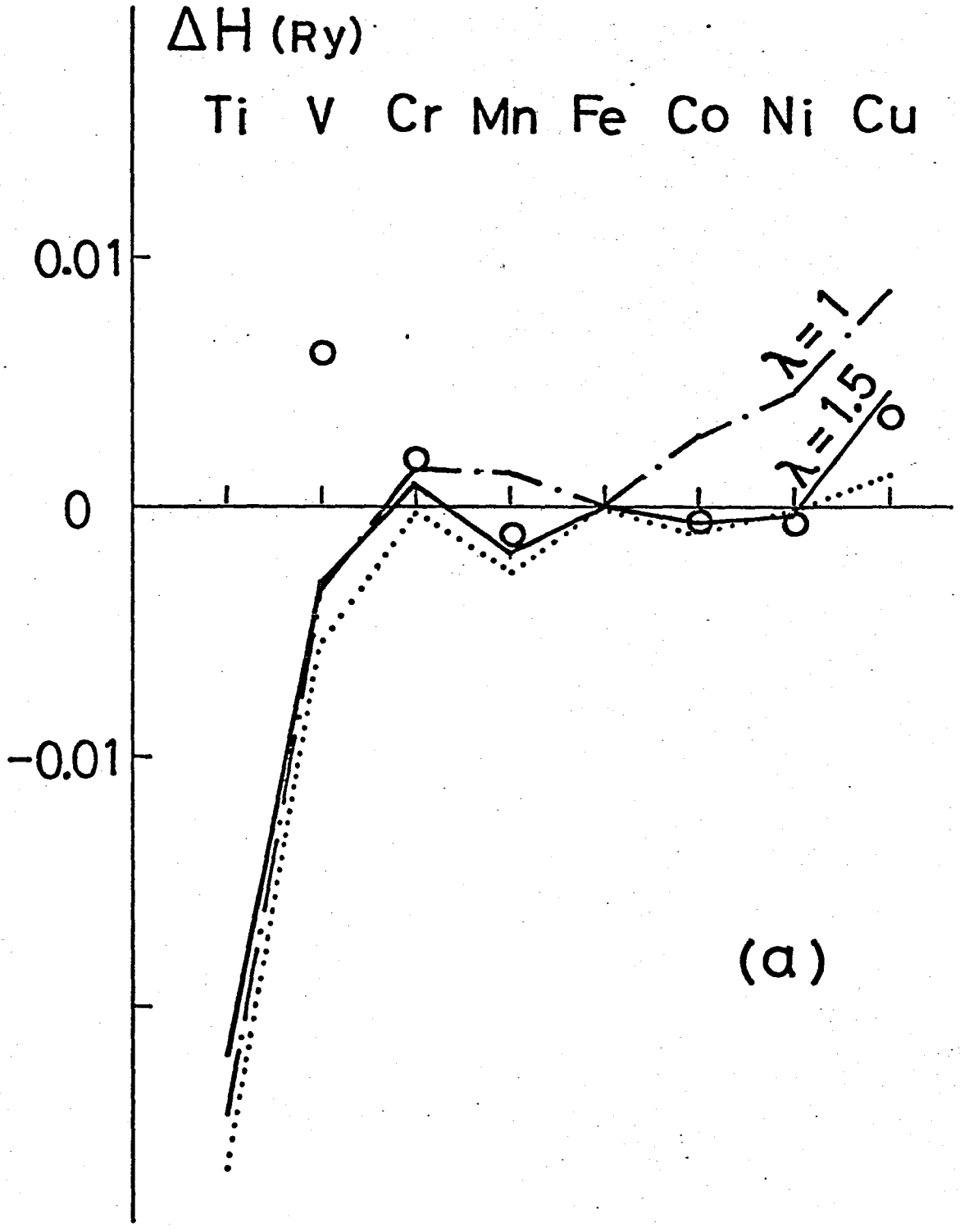

Fig.II.12(a)

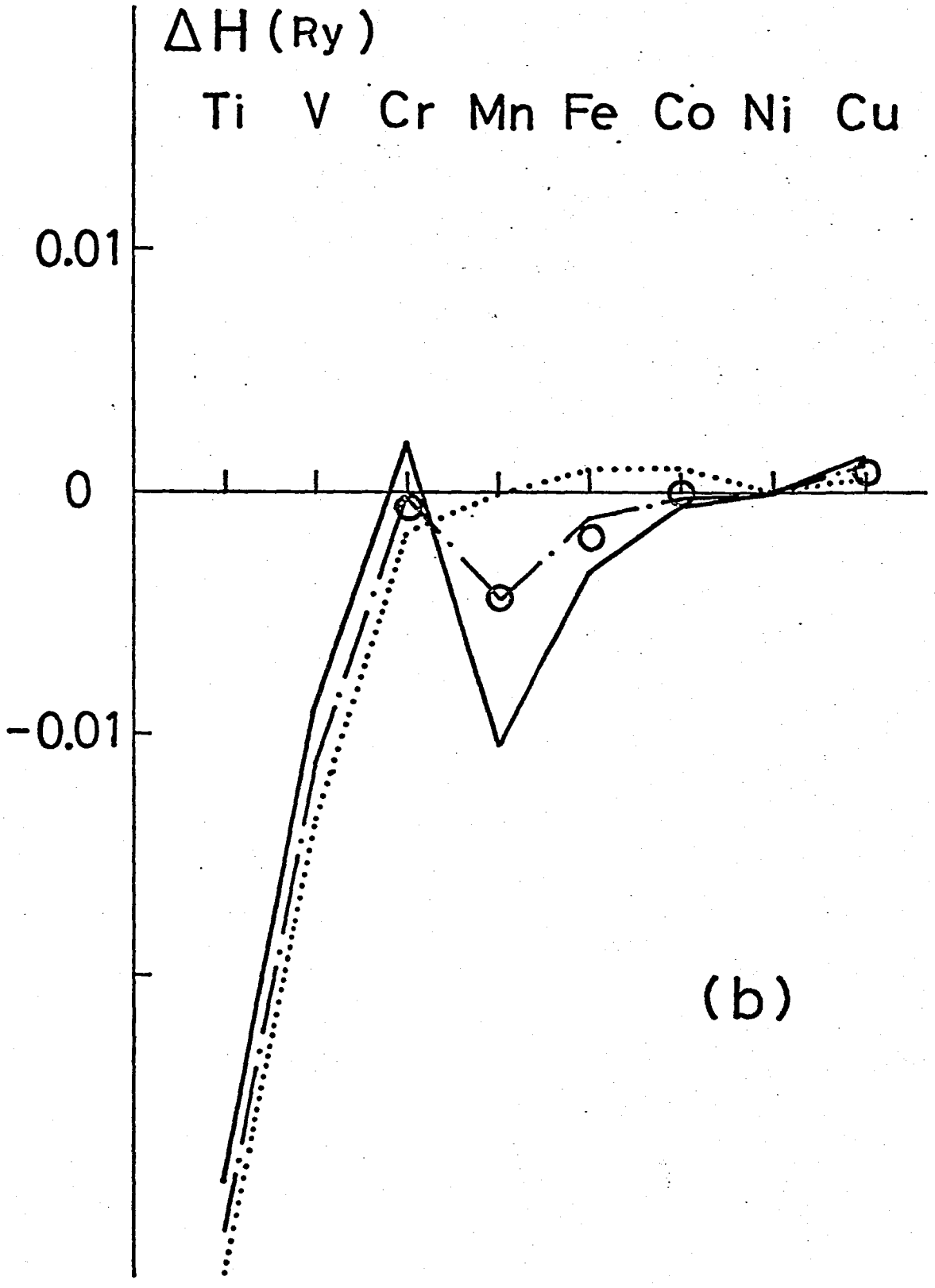

Fig.II.12(b)

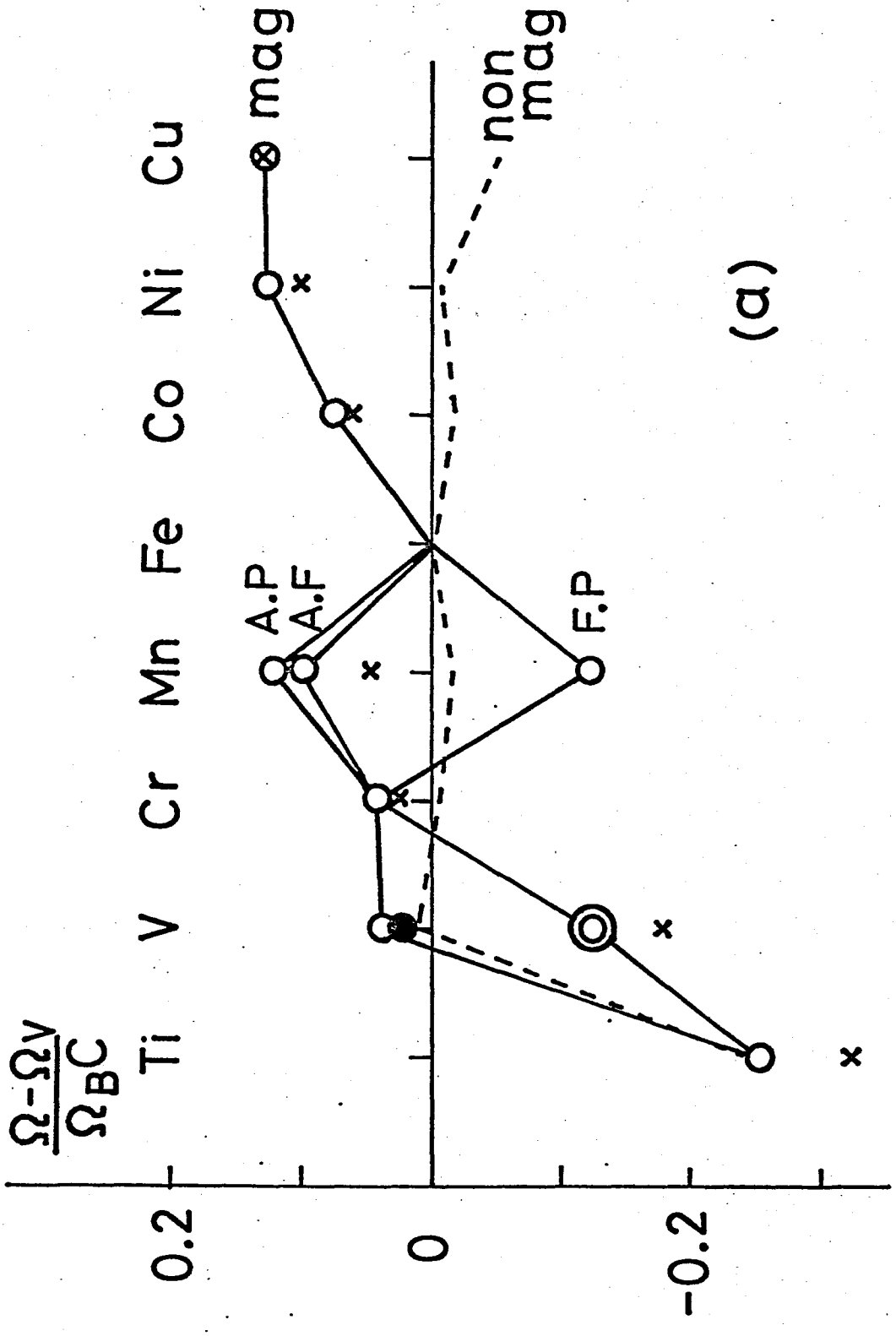
(a)
mag
non mag
A.P
A.F
F.P
Ti V Cr Mn Fe Co Ni Cu
$\frac{\Omega-\Omega_V}{\Omega_B C}$
0.2
0
-0.2

Fig.II.13(a)

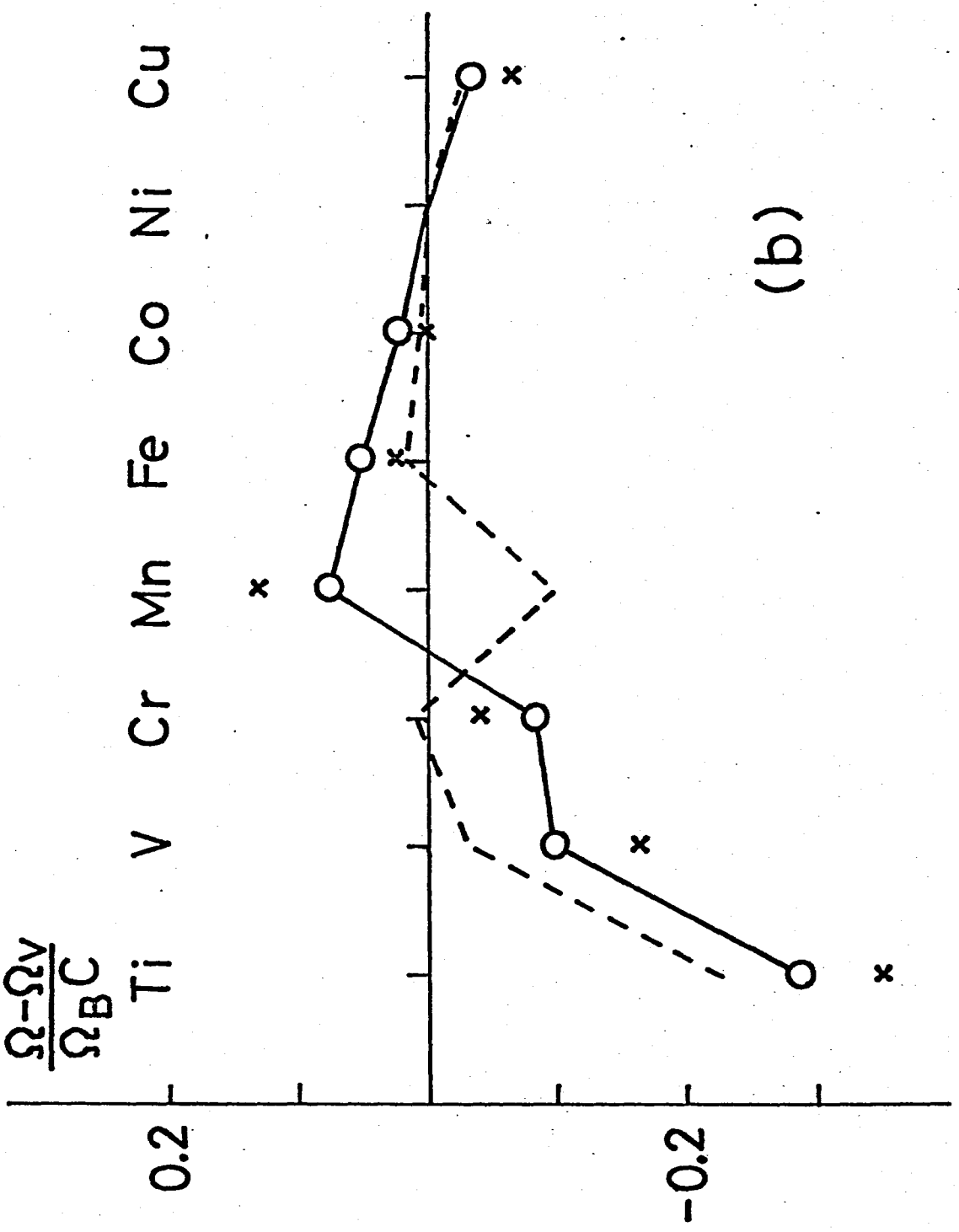

Fig.II.13(b)

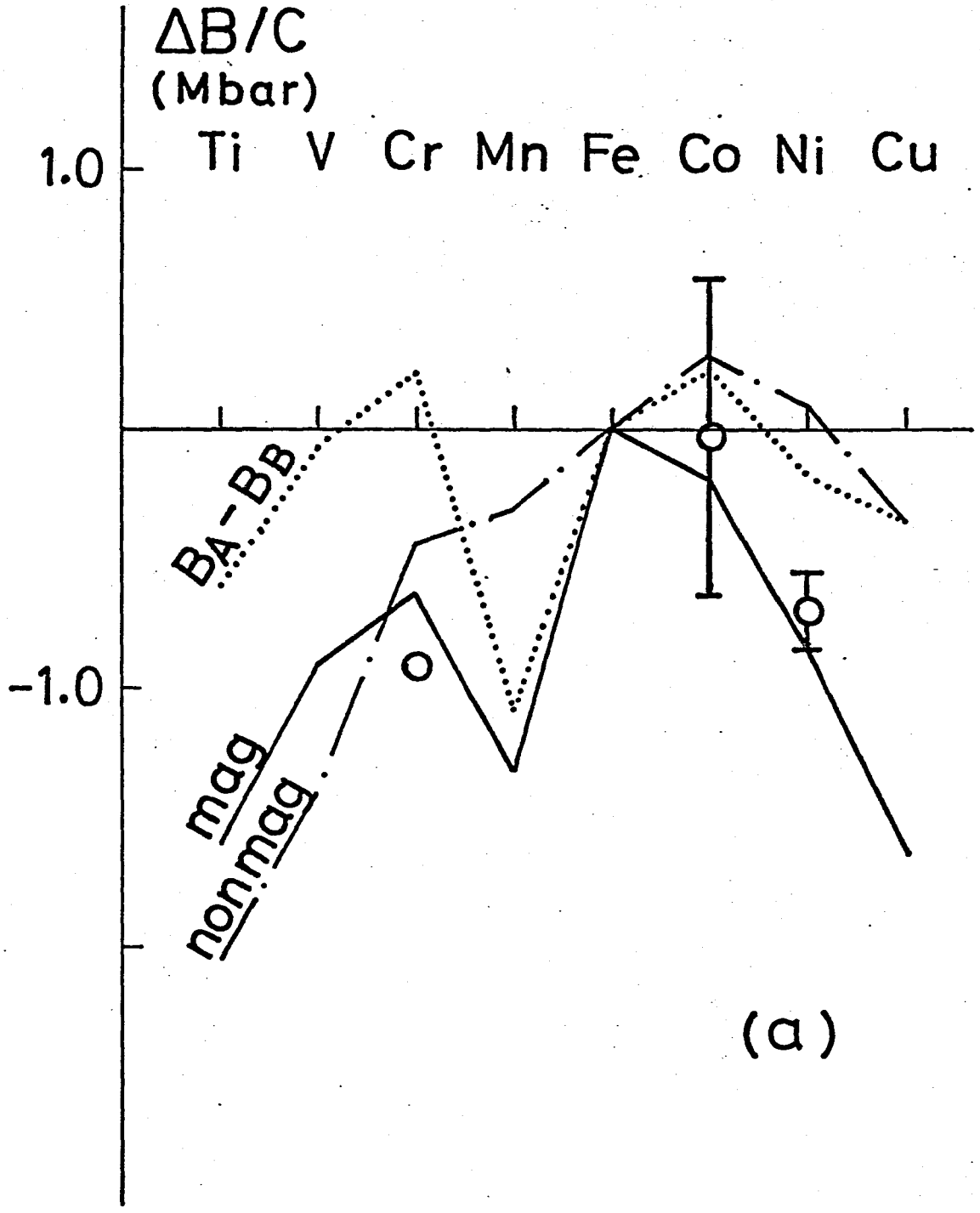

Fig.II.14(a)

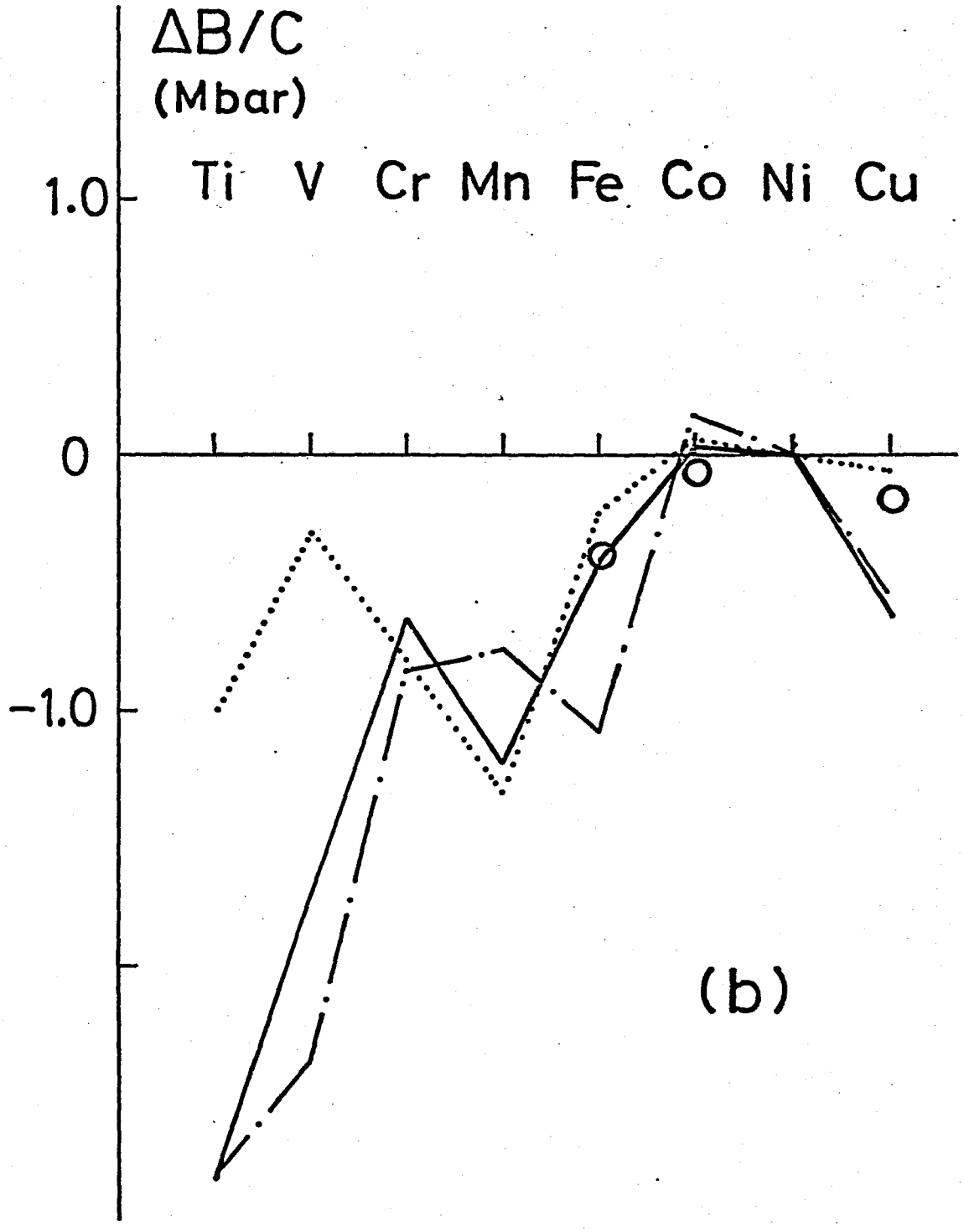

Fig.II.14(b)

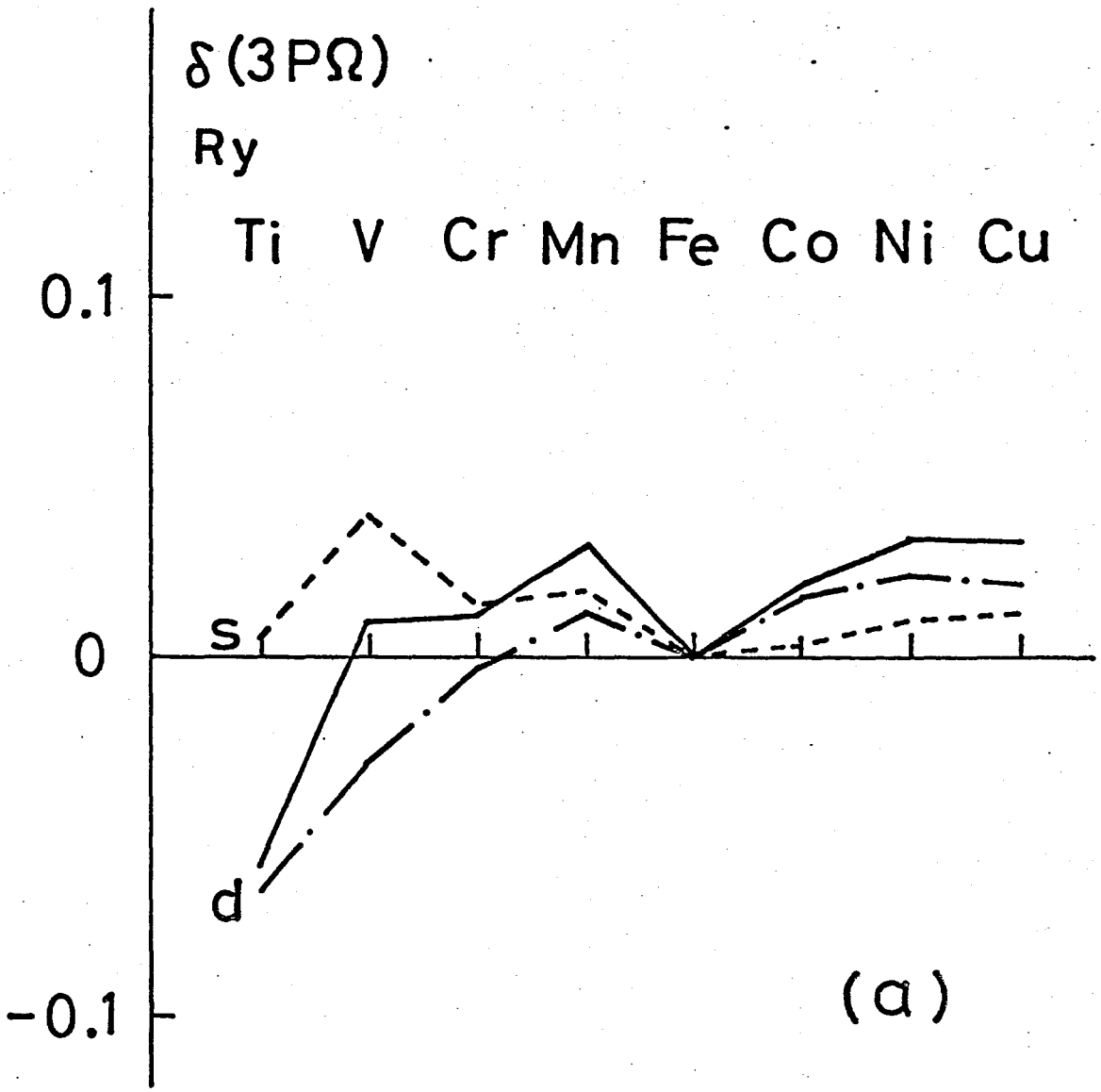

Fig.II.15(a)

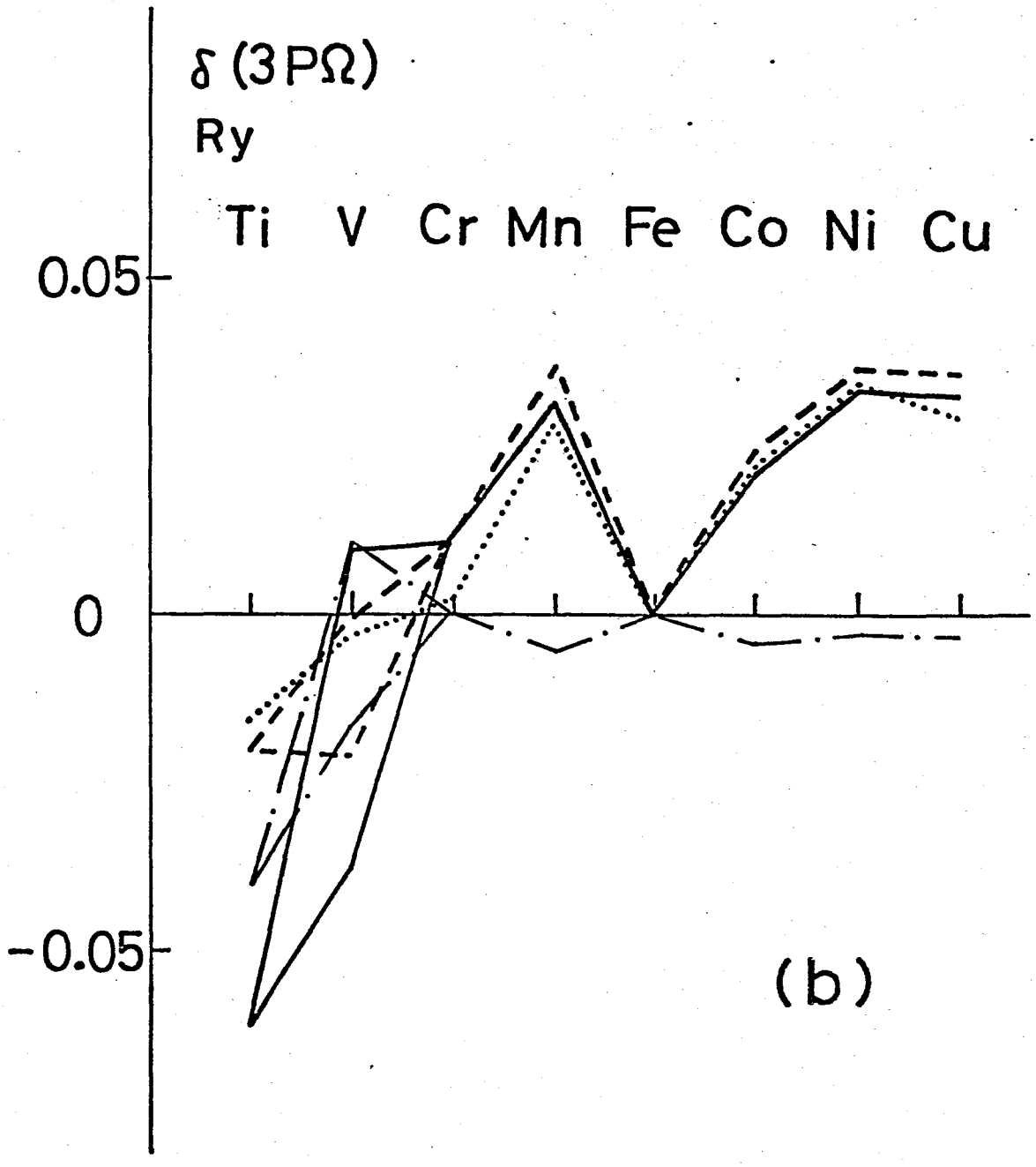

Fig.II.15(b)

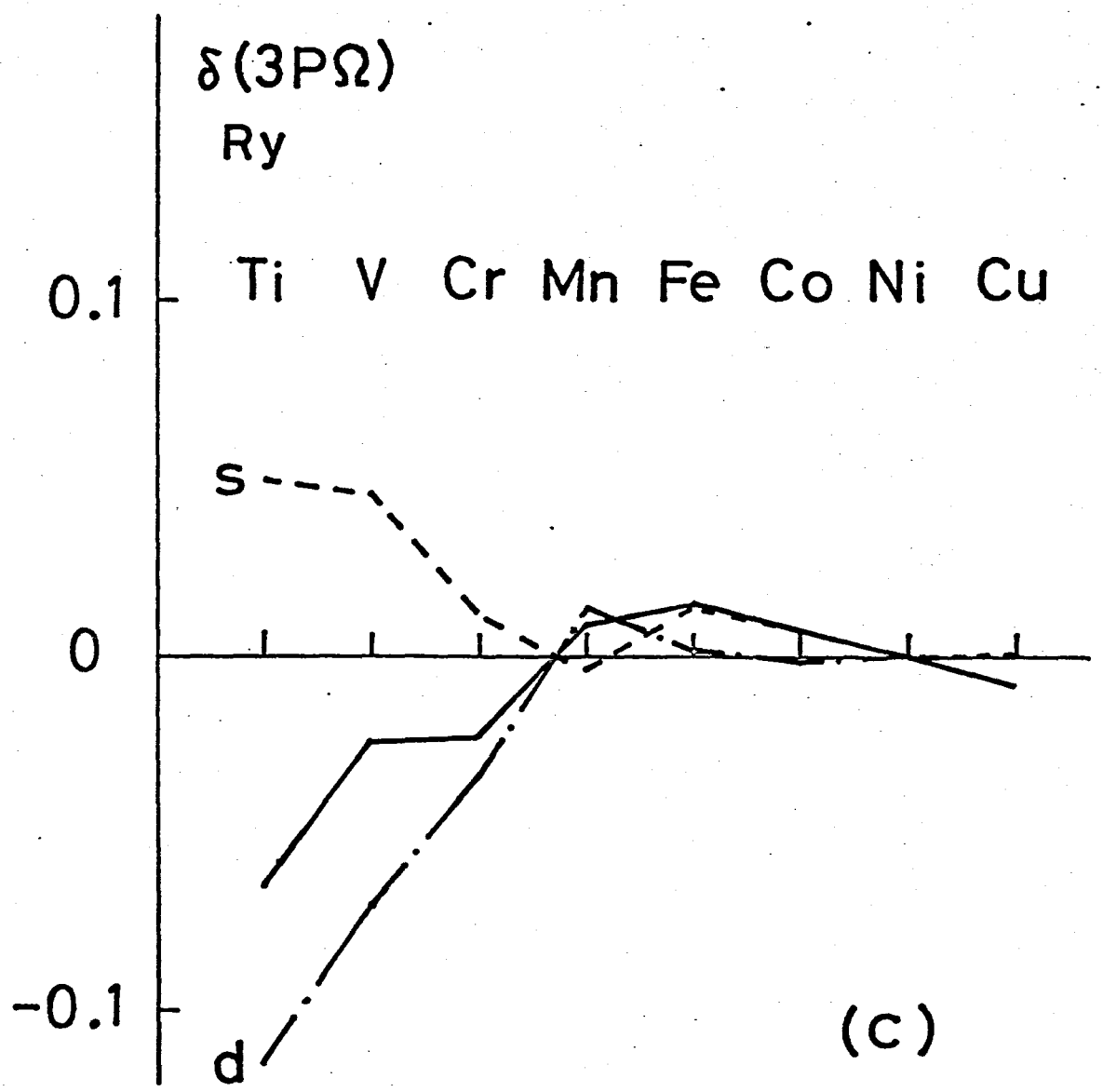

Fig.II.15(c)

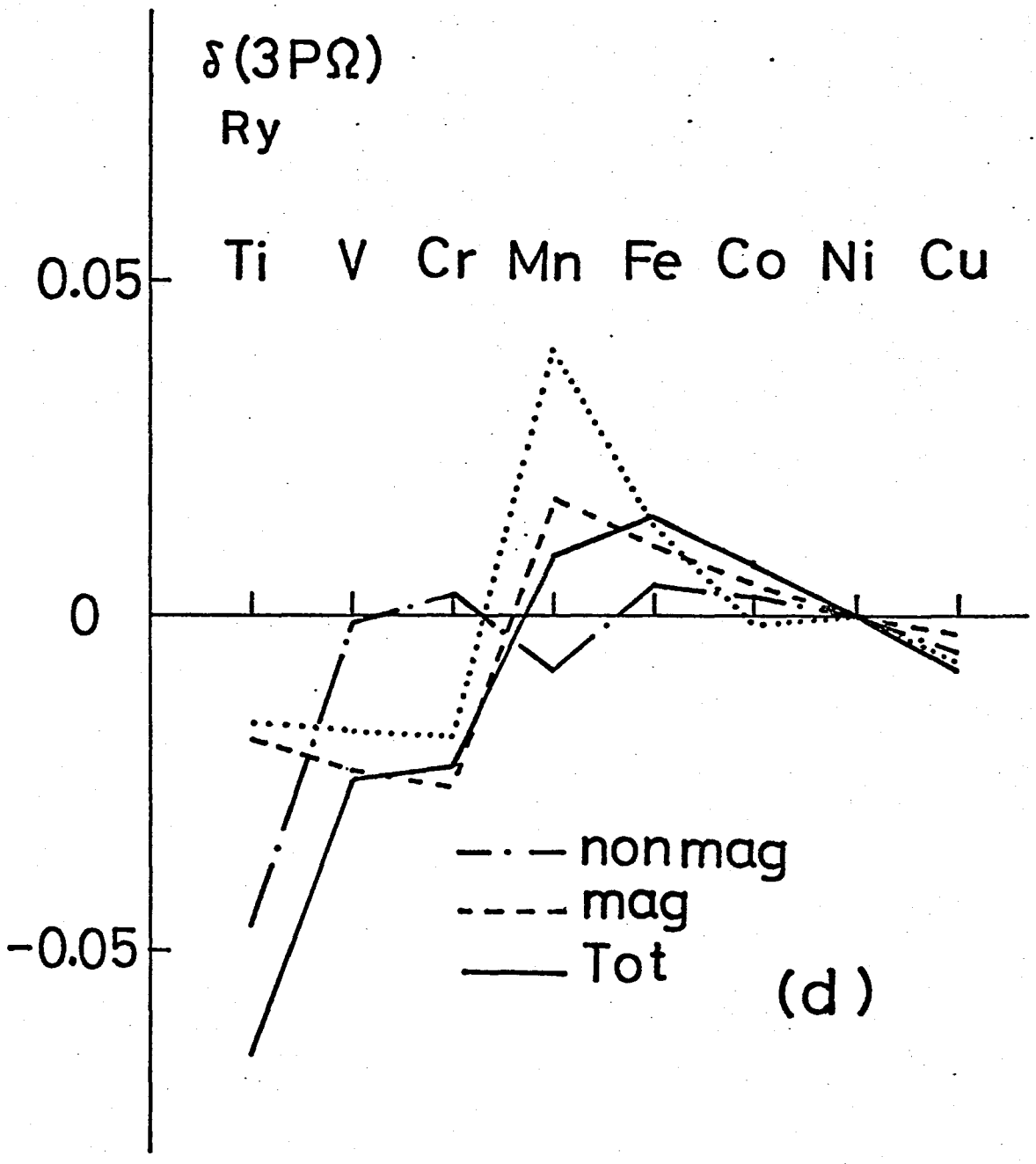

Fig.II.15(d)

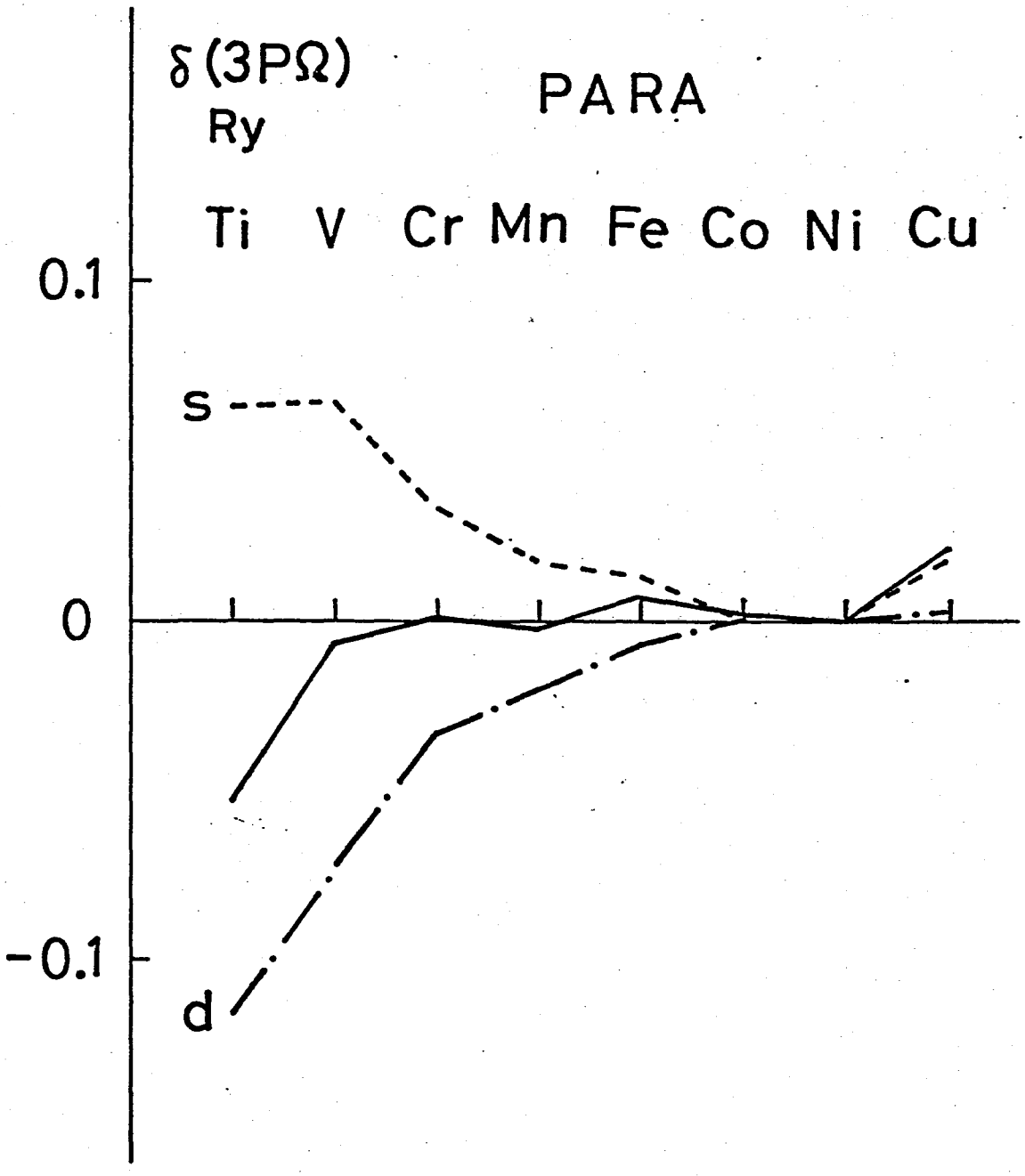

Fig.II.16

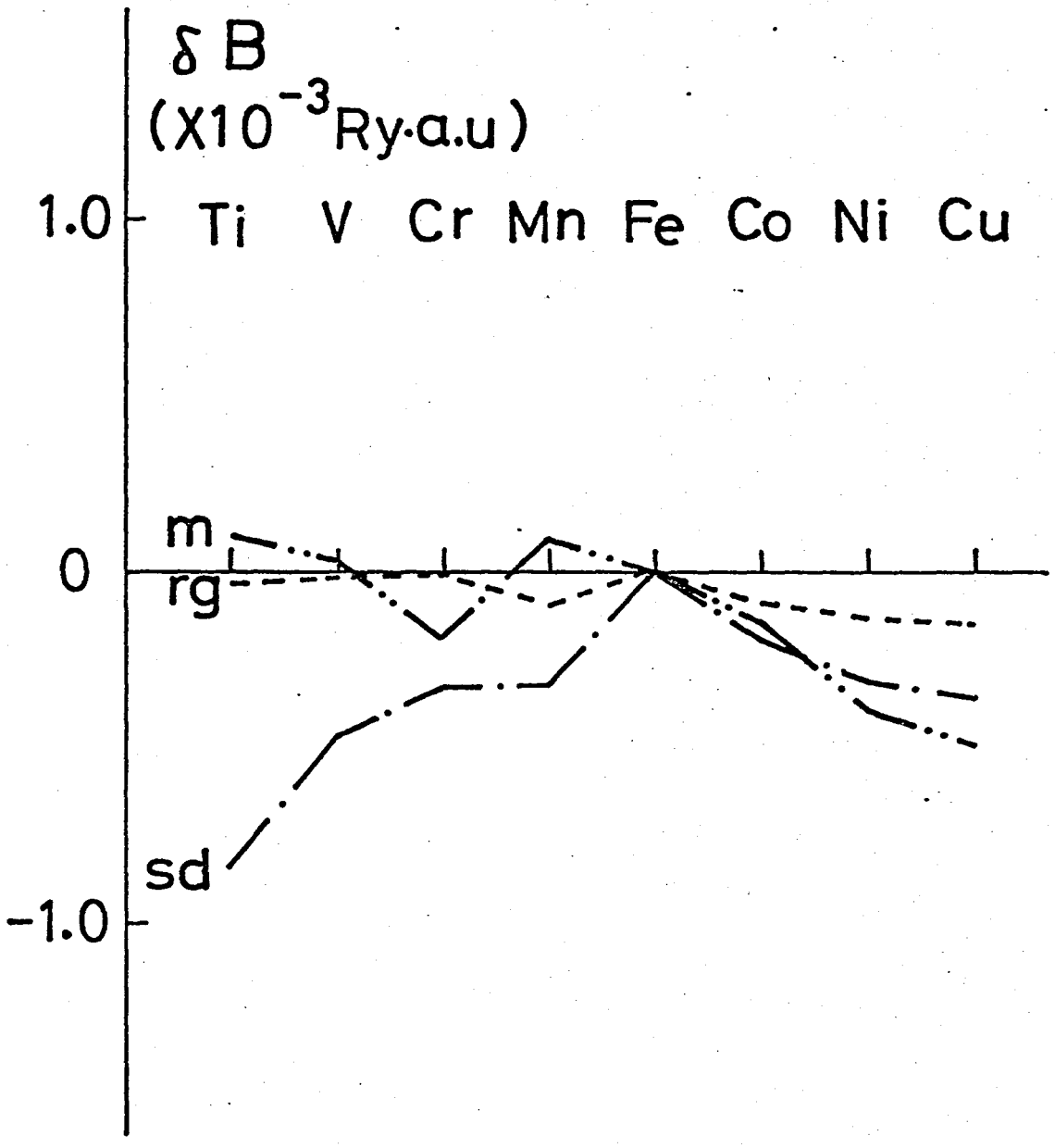

Fig.II.17

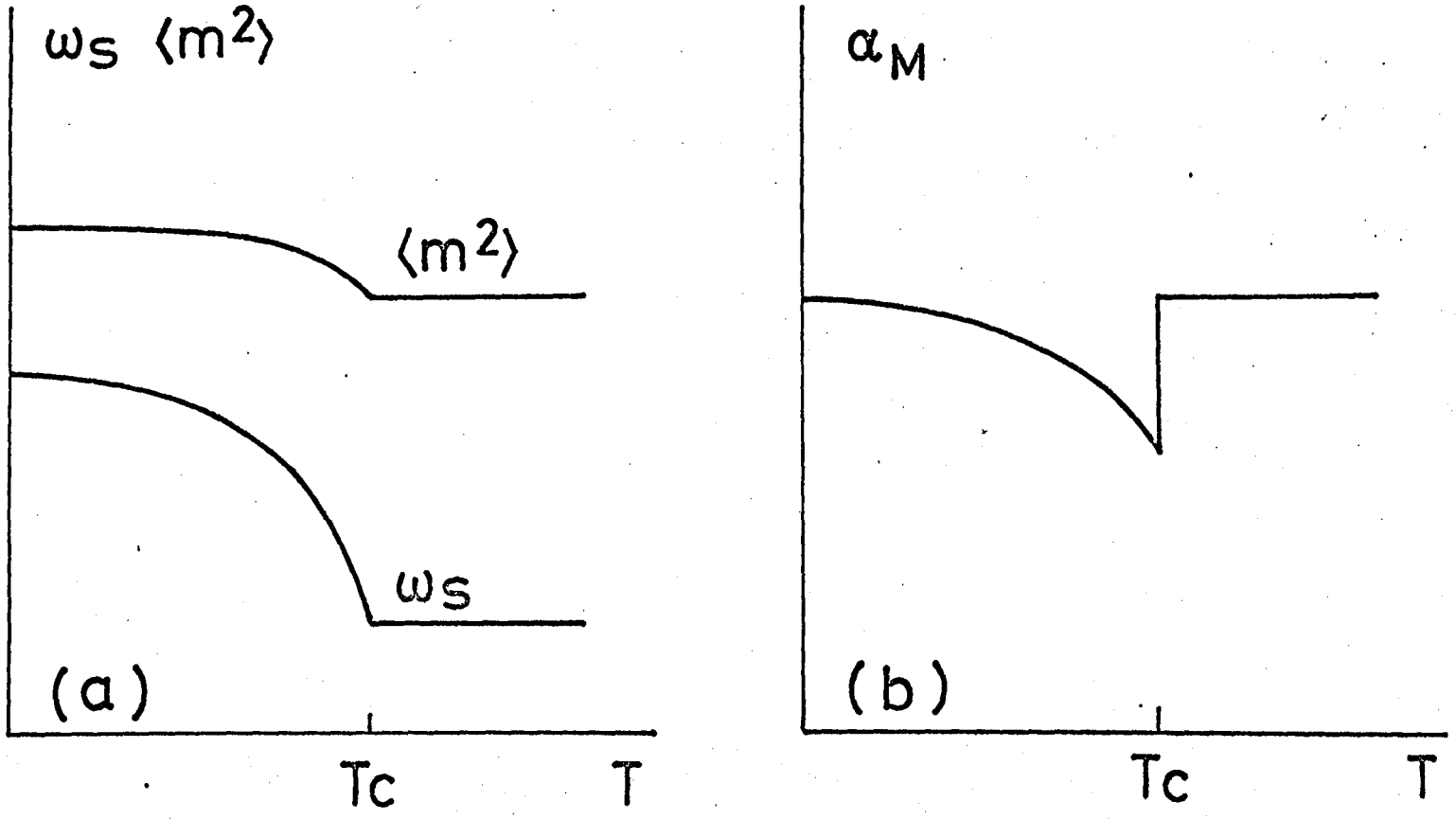
$\omega_S \langle m^2 \rangle$
$\langle m^2 \rangle$
ω_S
(a)
Tc
T
α_M
(b)
Tc
T

Fig.III.1

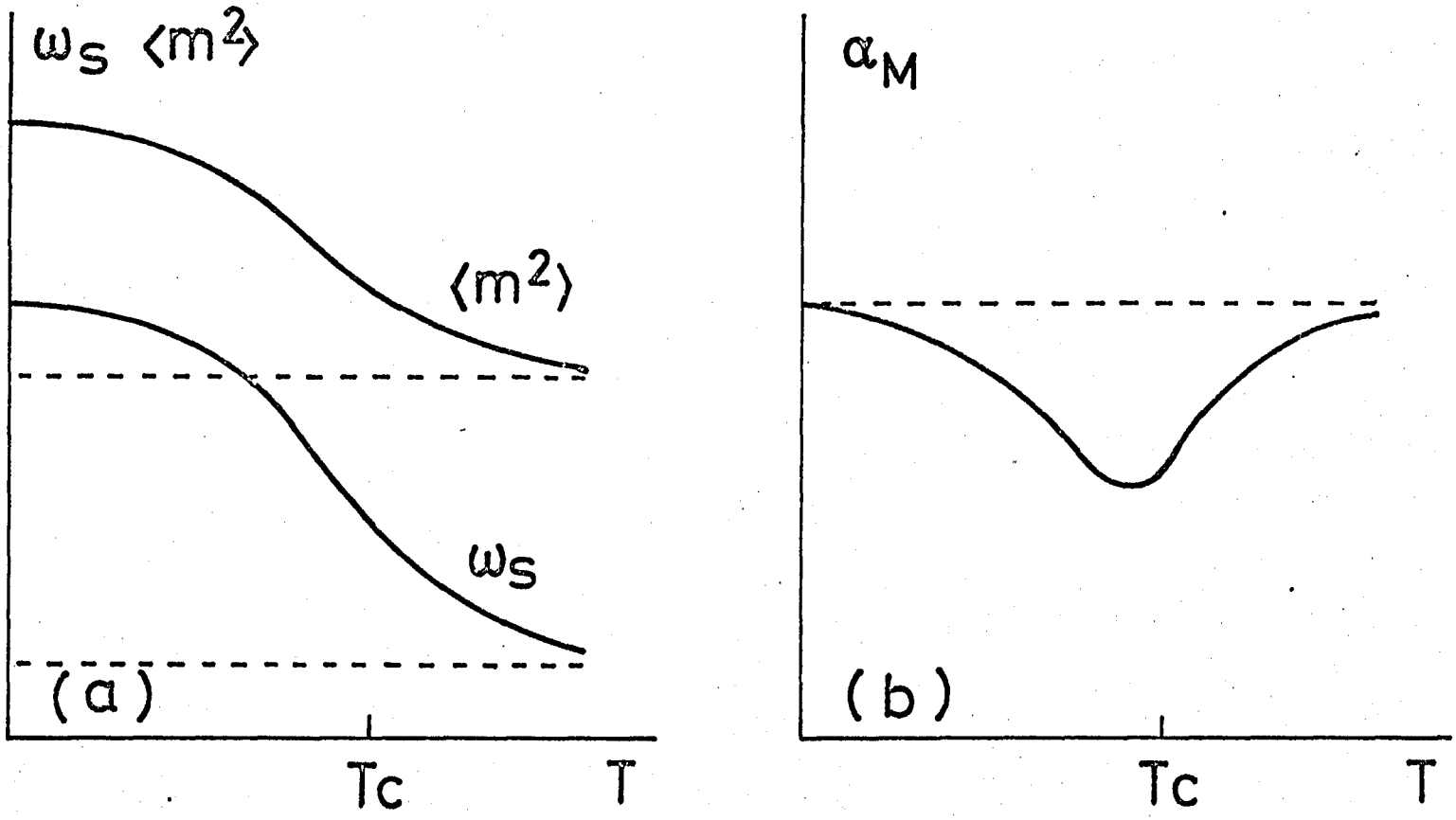
$\omega_S \langle m^2 \rangle$
$\langle m^2 \rangle$
ω_S
(a)
Tc
T
α_M
(b)
Tc
T

Fig.III.2

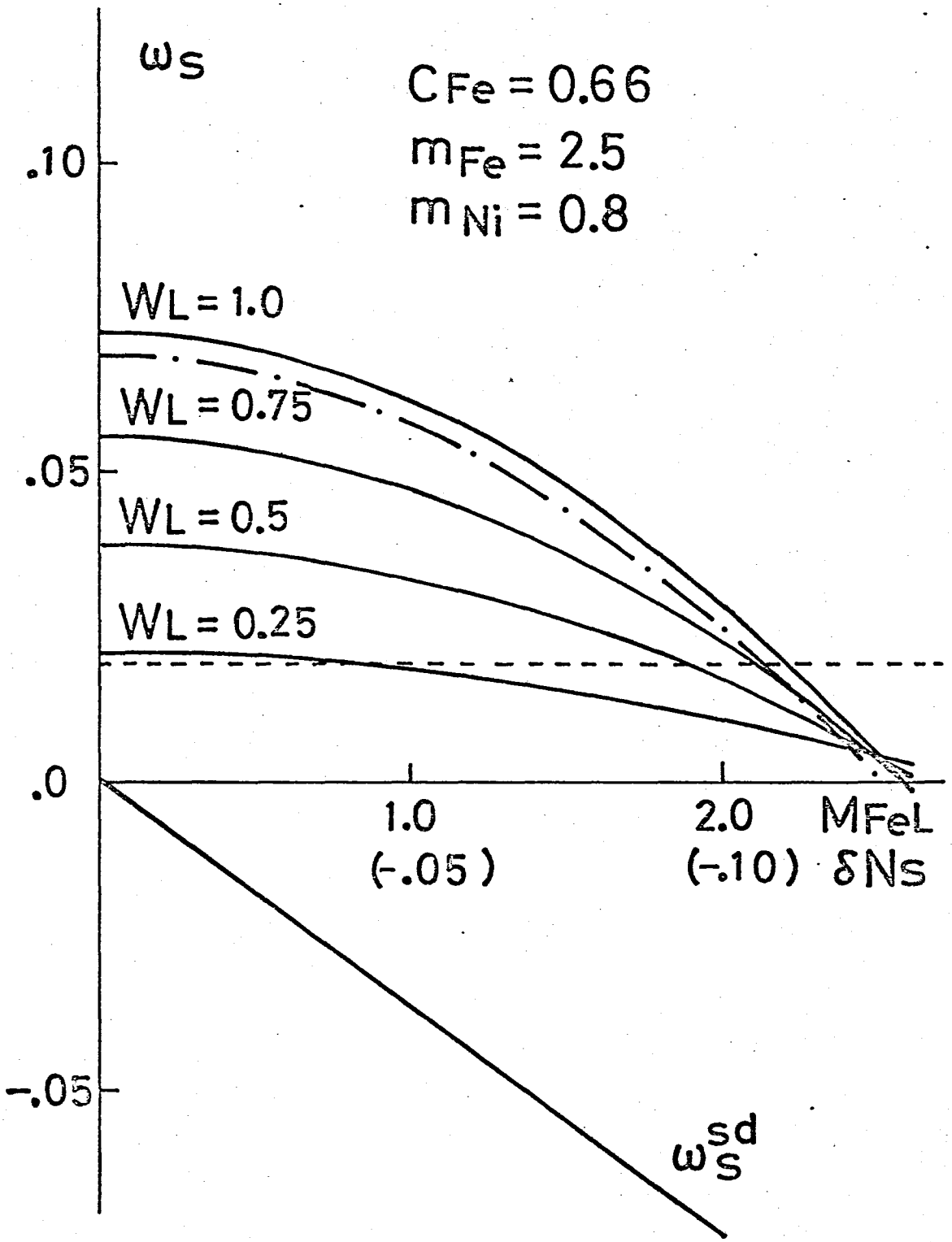
ωs
CFe = 0.66
mFe = 2.5
mNi = 0.8
.10
.05
.0
-.05
WL = 1.0
WL = 0.75
WL = 0.5
WL = 0.25
1.0
(-.05)
2.0
(-.10)
MFeL
δNs
ωsd

Fig.III.3

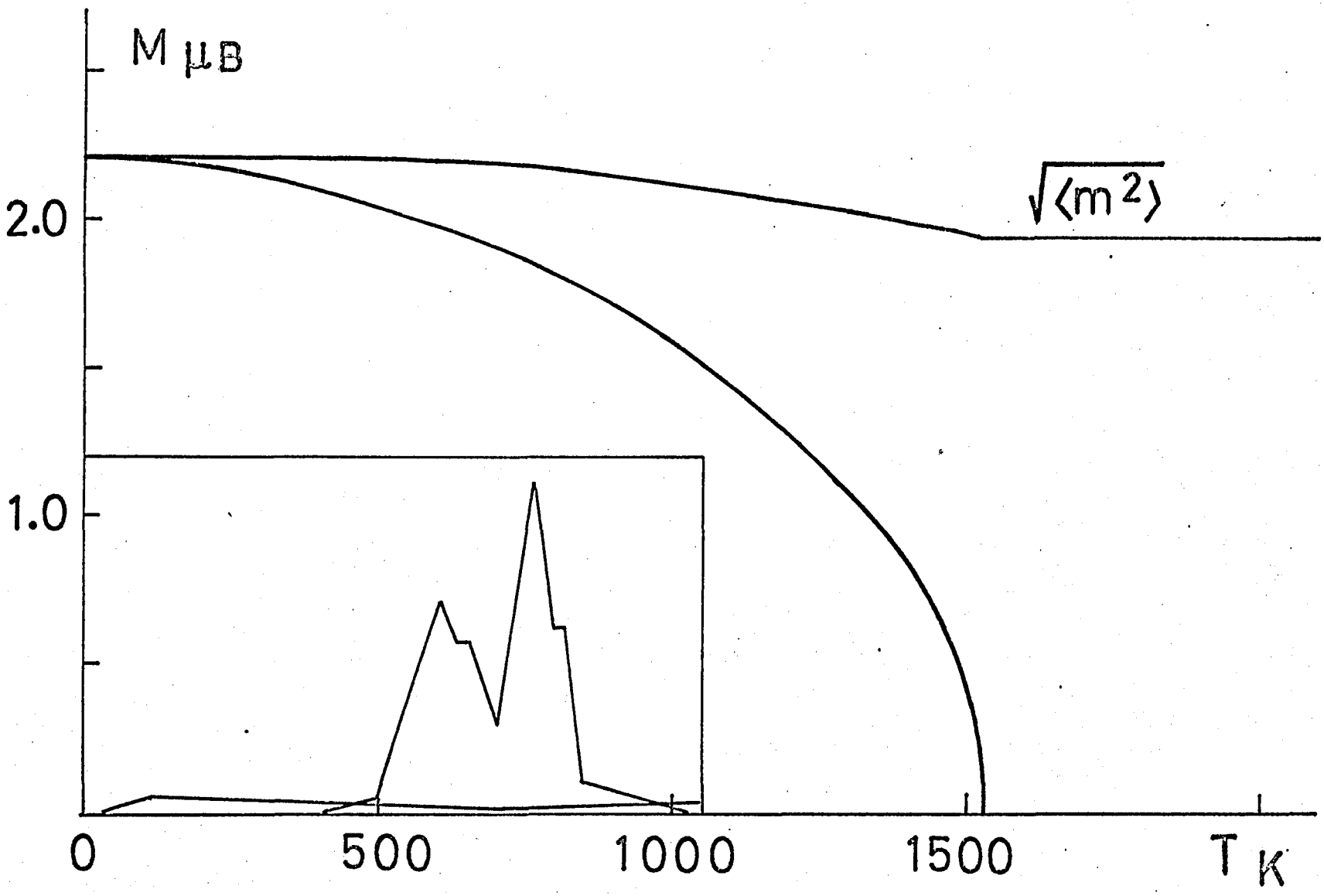

Fig.III.4

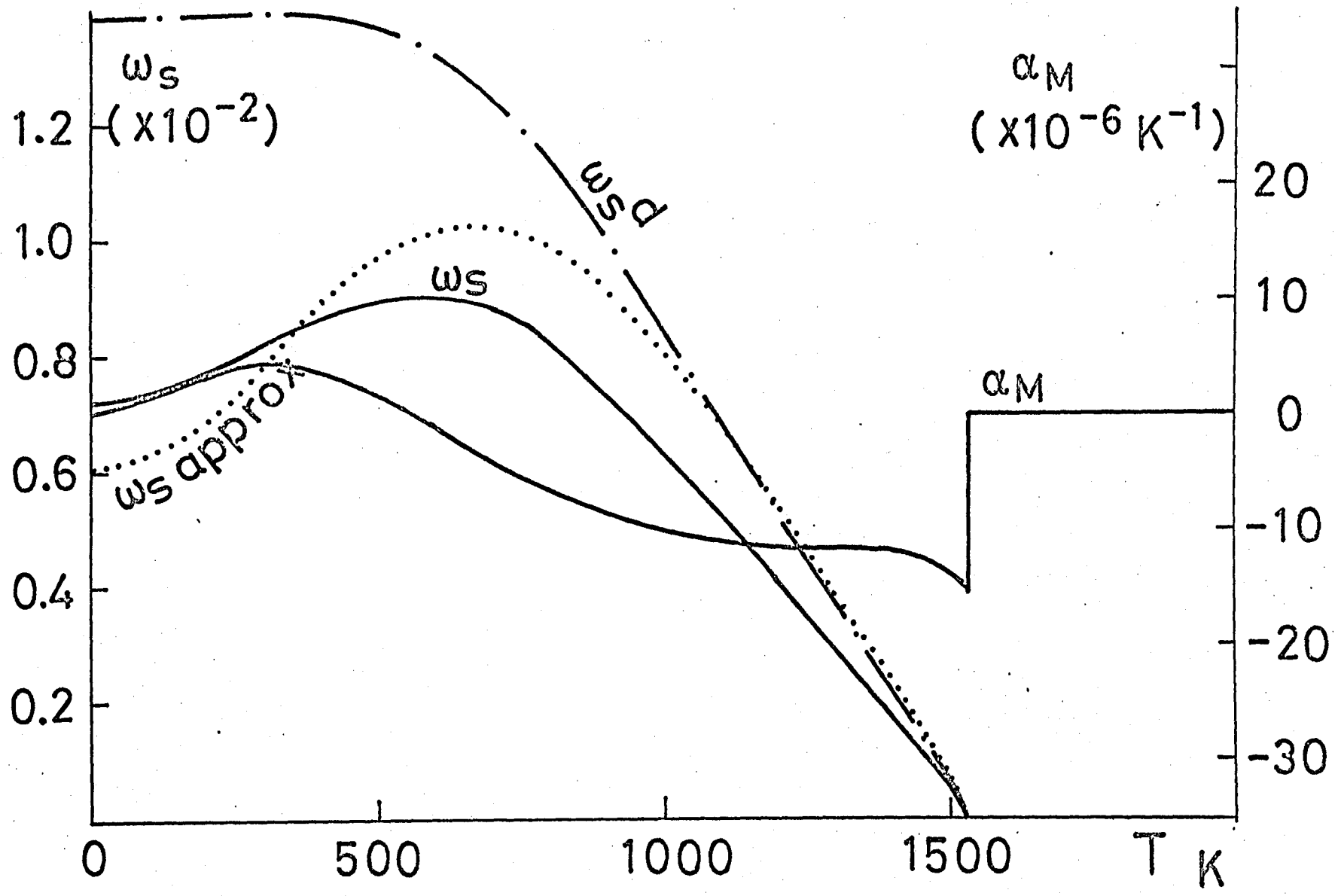
ω_s ($\times 10^{-2}$)
α_M ($\times 10^{-6}\,K^{-1}$)
1.2
1.0
0.8
0.6
0.4
0.2
20
10
0
-10
-20
-30
0
500
1000
1500
T K
ω_{sd}
ω_s
ω_s approx
α_M

Fig.III.5

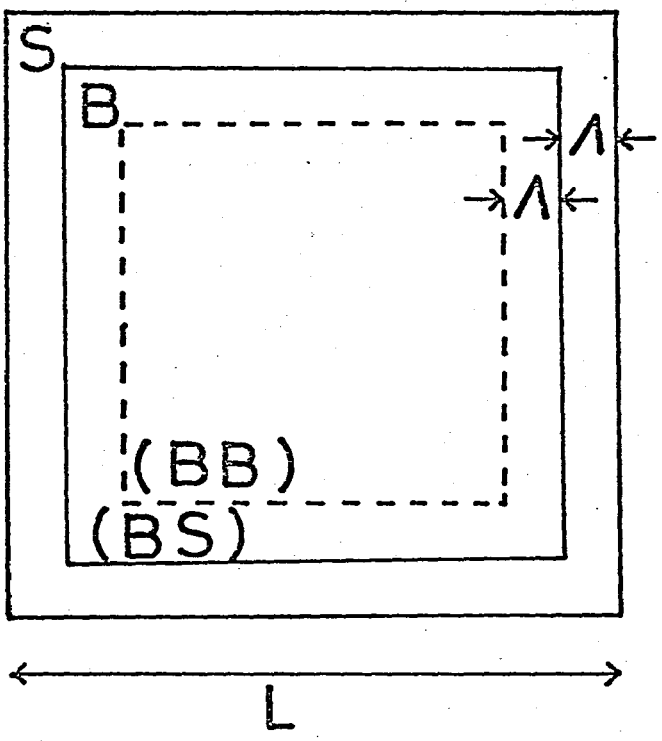

Fig.A.1